



Since January 2020 Elsevier has created a COVID-19 resource centre with free information in English and Mandarin on the novel coronavirus COVID-19. The COVID-19 resource centre is hosted on Elsevier Connect, the company's public news and information website.

Elsevier hereby grants permission to make all its COVID-19-related research that is available on the COVID-19 resource centre - including this research content - immediately available in PubMed Central and other publicly funded repositories, such as the WHO COVID database with rights for unrestricted research re-use and analyses in any form or by any means with acknowledgement of the original source. These permissions are granted for free by Elsevier for as long as the COVID-19 resource centre remains active.



# Combustion in the future: The importance of chemistry<sup>☆</sup>

Katharina Kohse-Höinghaus

*Department of Chemistry, Bielefeld University, Universitätsstraße 25, D-33615 Bielefeld, Germany*

Received 2 November 2019; accepted 28 June 2020

Available online xxx

## Abstract

Combustion involves chemical reactions that are often highly exothermic. Combustion systems utilize the energy of chemical compounds released during this reactive process for transportation, to generate electric power, or to provide heat for various applications. Chemistry and combustion are interlinked in several ways. The outcome of a combustion process in terms of its energy and material balance, regarding the delivery of useful work as well as the generation of harmful emissions, depends sensitively on the molecular nature of the respective fuel. The design of efficient, low-emission combustion processes in compliance with air quality and climate goals suggests a closer inspection of the molecular properties and reactions of conventional, bio-derived, and synthetic fuels. Information about flammability, reaction intensity, and potentially hazardous combustion by-products is important also for safety considerations. Moreover, some of the compounds that serve as fuels can assume important roles in chemical energy storage and conversion. Combustion processes can furthermore be used to synthesize materials with attractive properties.

A systematic understanding of the combustion behavior thus demands chemical knowledge. Desirable information includes properties of the thermodynamic states before and after the combustion reactions and relevant details about the dynamic processes that occur during the reactive transformations from the fuel and oxidizer to the products under the given boundary conditions. Combustion systems can be described, tailored, and improved by taking chemical knowledge into account. Combining theory, experiment, model development, simulation, and a systematic analysis of uncertainties enables qualitative or even quantitative predictions for many combustion situations of practical relevance.

This article can highlight only a few of the numerous investigations on chemical processes for combustion and combustion-related science and applications, with a main focus on gas-phase reaction systems. It attempts to provide a snapshot of recent progress and a guide to exciting opportunities that drive such research beyond fossil combustion.

© 2020 The Combustion Institute. Published by Elsevier Inc. All rights reserved.

**Keywords:** Combustion; Energy; Energy conversion; Combustion chemistry; Combustion kinetics; Combustion diagnostics; Combustion synthesis; Fuels; Biofuels; Synthetic fuels; Emissions; Reaction mechanisms; Combustion modeling

<sup>☆</sup> **Proceedings of the Combustion Institute** Colloquium: “Invited, Hottel paper”.

E-mail address: [kkh@uni-bielefeld.de](mailto:kkh@uni-bielefeld.de)

<https://doi.org/10.1016/j.proci.2020.06.375>

1540-7489 © 2020 The Combustion Institute. Published by Elsevier Inc. All rights reserved.

## 1. Setting the stage: combustion and chemistry in context

Combustion knowledge may be more important for the future than it is currently credited for. This seemingly controversial statement pertains in particular to chemical aspects of combustion. The present article addresses some of these aspects and opportunities with the main focus on gas-phase systems. Several combustion-related areas with strong links to chemistry will be highlighted in some detail in this introduction to provide a broader context. Harmful emissions from fossil combustion will be considered first, to reflect the role of combustion science in understanding the formation mechanisms of combustion emissions and designing cleaner combustion processes. Consequently, with the aim of reducing such harmful emissions, the role of fuels for different modes of transportation, their production, and the joint optimization of fuels, systems, and processes will be briefly addressed next. Chemical storage and conversion processes including combustion fuels will then be introduced briefly, because they are thought to be a valuable part of an energy system based more substantially on renewables. As a last area of combustion that relies substantially on chemical

knowledge, flame synthesis of materials will be considered, where combustion opens up pathways to multiple applications including coatings, ceramics, optics, electronics, catalysis, photovoltaics, electrochemistry, sensing, and medical diagnostics.

### 1.1. Emissions

The use of dominantly fossil resources that still provide by far the largest share of global primary energy, leads to increasing concerns about anthropogenic emissions and their environmental, health, and climate impact [1–10]. To curtail the adverse influences of greenhouse gases (GHGs), it is widely accepted that pathways towards renewable, carbon-reduced energy systems and sustainable industrial production processes should be given urgent attention. However, the time scales on which the infrastructure that generates fossil-fuel emissions could be reduced or phased out, are substantial, and the large-scale transition towards a zero-carbon energy system – if at all technically, economically, and socially feasible – is considered to be challenging within the next 40 years [1].

Regarding the release of carbon dioxide (CO<sub>2</sub>) from fossil-fuel usage, it is currently debated whether or not it seems still possible to meet a

*Abbreviations:* AFM, atomic force microscopy; ALS, Advanced Light Source; APCI, atmospheric pressure chemical ionization; ARAS, atomic resonance absorption spectroscopy; ATcT, Active Thermochemical Tables; BC, black carbon; BEV, battery electric vehicle; BTL, biomass-to-liquid; CA, crank angle; CCS, carbon capture and storage; CEAS, cavity-enhanced absorption spectroscopy; CFD, computational fluid dynamics; CI, compression ignition; CRDS, cavity ring-down spectroscopy; CTL, coal-to-liquid; DBE, di-*n*-butyl ether; DCN, derived cetane number; DEE, diethyl ether; DFT, density functional theory; DFWM, degenerate four-wave mixing; DMC, dimethyl carbonate; DME, dimethyl ether; DMM, dimethoxy methane; DRIFTS, diffuse reflectance infrared Fourier transform spectroscopy; EGR, exhaust gas recirculation; EI, electron ionization; FC, fuel cell; FCEV, fuel cell electric vehicle; FRET, fluorescence resonance energy transfer; FT, Fischer-Tropsch; FTIR, Fourier-transform infrared; GC, gas chromatography; GHG, greenhouse gas; GTL, gas-to-liquid; GW, global warming; HAB, height above the burner; HACA, hydrogen abstraction acetylene addition; HCCI, homogeneous charge compression ignition; HFO, heavy fuel oil; HRTEM, high-resolution transmission electron microscopy; IC, internal combustion; ICEV, internal combustion engine vehicle; IE, ionization energy; IPCC, Intergovernmental Panel on Climate Change; IR, infrared; JSR, jet-stirred reactor; KDE, kernel density estimation; KHP, ketohydroperoxide; LCA, lifecycle analysis; LH<sub>2</sub>, liquid hydrogen; LIF, laser-induced fluorescence; LIGS, laser-induced grating spectroscopy; LII, laser-induced incandescence; TiRe-LII, time-resolved LII; LNG, liquefied natural gas; LOHC, liquid organic hydrogen carrier; LT, low-temperature; LTC, low-temperature combustion; MDO, marine diesel oil; MS, mass spectrometry; TOF-MS, time-of-flight MS; MBMS, molecular-beam MS; OTMS, Orbitrap MS; MTO, methanol-to-olefins; MVK, methyl vinyl ketone; NO<sub>x</sub>, nitrogen oxides; NTC, negative temperature coefficient; OME, oxymethylene ether; PACT, predictive automated computational thermochemistry; PAH, polycyclic aromatic hydrocarbon; PDF, probability density function; PEM, polymer electrolyte membrane; PEPICO, photoelectron photoion coincidence; PES, photoelectron spectrum/spectra; PFR, plug-flow reactor; PI, photoionization; PIE, photoionization efficiency; PIV, particle imaging velocimetry; PLIF, planar laser-induced fluorescence; PM, particulate matter; PM<sub>10</sub> PM<sub>2.5</sub>, sampled fractions with sizes up to ~10 and ~2.5 μm; PRF, primary reference fuel; QCL, quantum cascade laser; RCCI, reactivity-controlled compression ignition; RCM, rapid compression machine; REMPI, resonance-enhanced multi-photon ionization; RMG, reaction mechanism generator; RON, research octane number; SI, spark ignition; SIMS, secondary ion mass spectrometry; SNG, synthetic natural gas; SNR, signal-to-noise ratio; SOA, secondary organic aerosol; SOEC, solid-oxide electrolysis cell; SOFC, solid-oxide fuel cell; SO<sub>x</sub>, sulfur oxides; STM, scanning tunneling microscopy; SVO, straight vegetable oil; TDLAS, tunable diode laser absorption spectroscopy; TPES, threshold photoelectron spectrum/spectra; TPRF, toluene primary reference fuel; TSI, threshold sooting index; UFP, ultrafine particle; VOC, volatile organic compound; VUV, vacuum ultraviolet; WLTP, Worldwide Harmonized Light Vehicle Test Procedure; XAS, X-ray absorption spectroscopy; YSI, yield sooting index; 2M2B, 2-methyl-2-butene.

global warming target of 1.5 °C [1–3], assuming a forceful commitment to replace the relevant infrastructure including fossil-fuel power plants [1,2]. Such estimates with different assumptions about parameters such as marine uptake of CO<sub>2</sub> and radiative forcing [1] have not included possible feedback from permafrost melting [10]. Sensitivity is noted to the climate effect of aerosols that are associated in part with combustion emissions [1,3], with forcing effects not known accurately enough, however [1]. Mitigation scenarios leading to GHG reduction include the transition to low-carbon energy systems, increase in energy efficiency, use of carbon capture and storage (CCS) strategies, reduction of the emissions of other GHGs, as well as limiting current transformations of land use [2]. Net CO<sub>2</sub> removal is thought to be possible in the second half of the 21st century with bioenergy usage coupled with CCS, potentially complemented with reforestation [2]. However, their influences on food production and biodiversity, among others, as well as the realistic geological storage capacity for CO<sub>2</sub> remain unclear, and technically possible options might not be implemented because of lacking societal support [2]. Alternative factors and assumptions are being discussed, including the impact of rapid and continuing introduction of the most energy- and material-efficient technology in all sectors, increased renewably-based electrification, carbon taxes, changes in agricultural production, changes in consumer habits and lifestyle, less rapid population growth, and combinations of the above factors [2]. Regarding the technological aspects considered in these projections, CO<sub>2</sub> reductions depend significantly on efficiency increases in transport, industrial production, and heat usage as well as limited use of energy-intensive materials such as steel, while increased electrification will need technical advances in storage and load management [2].

Numerous effects are associated with increasing GHG load and increasing temperature. Anderson and Clapp [10] describe, as one area of concern, a cascade of feedbacks that can be driven by the loss of ice volume in the Arctic region. This loss can affect the heat transport systems of the atmosphere and the ocean and may be accompanied by increased absorption of solar radiation by land and ocean surfaces and resultant release of carbon from soil-based reservoirs [10]. Fig. 1 demonstrates the potential contribution of permafrost-melting-induced emissions of CO<sub>2</sub> and methane (CH<sub>4</sub>) from methane clathrates, as depicted in the insert, to the total GHG budget (given in gigatons of carbon per year, GtC y<sup>-1</sup>) [10]. The values and scenarios in Fig. 1 follow the analysis of the Intergovernmental Panel on Climate Change (IPCC) [11]. Several aspects of the information in this graphic are worth of consideration: First, for each year since 2007, the carbon added from fossil-fuel use to the atmosphere has surpassed the max-

imum release rate projected by the IPCC [10]. Second, the remarkable magnitude of the Arctic soil carbon reservoirs points towards the importance and urgency of quantifying their impact. Compared to the present amount of 10 GtC y<sup>-1</sup> released to the atmosphere from human activity, the Arctic soil reservoir is estimated at 1400–1850 GtC in the upper 3 m of the soil, and if only 0.5% of the trapped CO<sub>2</sub> and CH<sub>4</sub> would be released annually, it would almost double the amount of carbon in the atmosphere by adding another 8 GtC y<sup>-1</sup> [10].

Emissions from fossil-fuel combustion are known to have adverse effects on air quality and health, especially because of particulate matter (PM) [3–10]. Lelieveld et al. [3] have recently discussed that such combustion emissions may be globally responsible for up to about 65% of excess mortality. The COVID-19 pandemic may, however, impact such evaluations. The combustion-related air pollution associated with transportation, often in densely populated areas [4,6], with power generation, and with industrial processes, may significantly increase the hazards for mortality from cardiovascular, respiratory, and other diseases [3,4]. Lelieveld et al. [3] have thus removed all fossil-fuel-related emissions in their recent model to estimate avoidable mortality and found the attributable effect of anthropogenic pollution to be a factor of 3 stronger than the influence of other avoidable environmental risks such as unsafe water or poor sanitation. The occurrence of large wildfires in various parts of the world, potentially related to changing climate conditions, contributes significantly to emissions, not only of carbon dioxide, but also of particulate matter.

With regard to their importance to climate, air quality, and health, in-depth information on the chemical composition and characteristics of particulates and their interaction with different environments is needed, including their accurate monitoring and improved mechanistic understanding of their effects. The particular influences of ultrafine particles (UFPs) with aerodynamic diameters below 100 nm, their reactivity and their oxidative and toxic potential remain to be explored in more detail [4], especially since present knowledge is largely based on laboratory-generated soot particles. Although a small fraction by mass, UFPs can make up more than 90% of urban PM by particle number concentration, and their high surface-to-volume ratio can favor the accumulation of further toxic air pollutants [4]. The knowledge of kinetics and formation mechanisms for these particles, their interaction with reactive species, and the development of predictive models are thus important, with the aim to understand the relation between chemical characteristics and health effects [4]. The interaction of emissions in the biosphere with those from combustion is another area of concern [5], especially regarding the formation of secondary or-

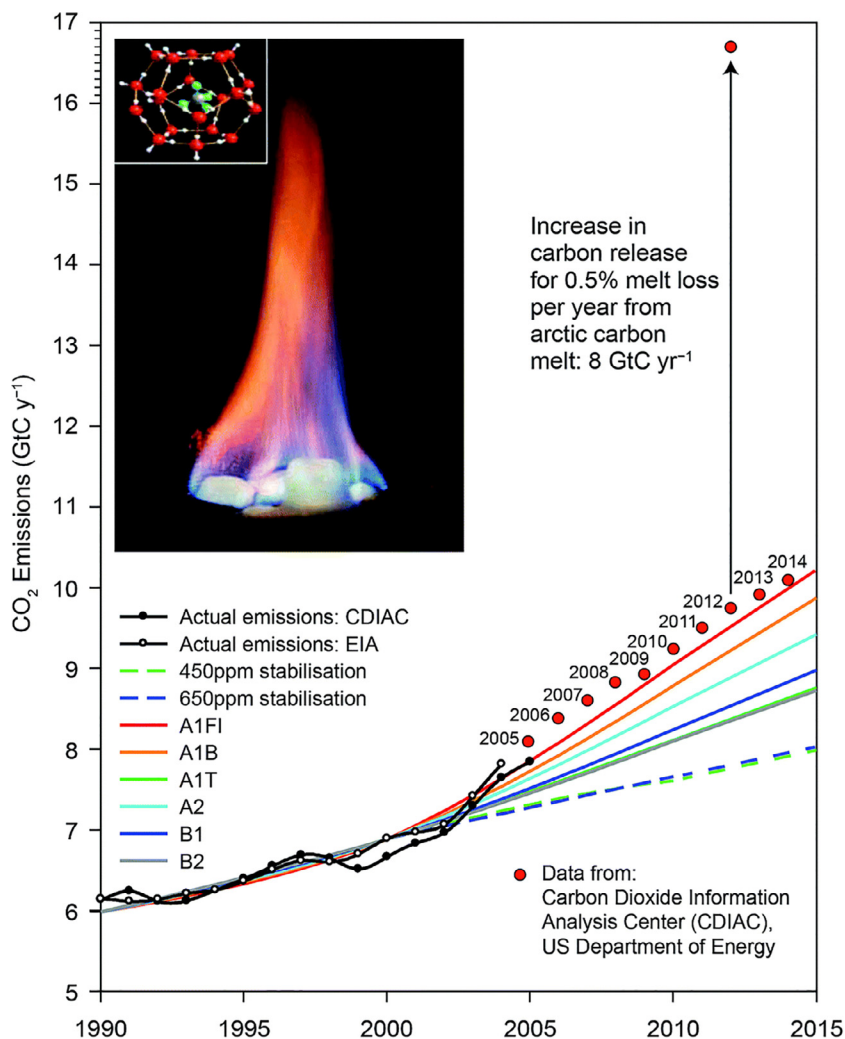


Fig. 1. Just 0.5% of the labile carbon contained in the upper 3 m of the soils in Northern Siberia and the North Slope of Alaska equals the total mass of carbon released worldwide to the atmosphere as CO<sub>2</sub> by the extraction, distribution, and combustion of fossil fuels. *Insert*: structure of methane clathrate and its combustion. CDIAC: Carbon Dioxide Information Analysis Center (US Department of Energy); EIA: US Energy Information Administration; scenarios A1–B2 according to [11]. Reprinted from [10], Open Access Article licensed under a Creative Commons Attribution 3.0 Unported Licence, DOI: 10.1039/C7CP08331A.

ganic aerosol (SOA) and reactions between volatile organic compounds (VOCs) and nitrogen oxides (NO<sub>x</sub>) from anthropogenic sources such as traffic, biomass burning, wood heating, agricultural fertilization, and those of natural origin. *In-situ* formation of particles, especially in the UFP range, from various precursors, including traffic-related and agricultural emissions, is a process that needs further mechanistic understanding [6,7], again in view of consequences for environment and health. More information is needed for such purposes, especially acknowledging the inhomogeneous nature of such particles and their associated physicochem-

ical behavior, including reactive radical reactions in the gas phase and heterogeneous reactions [4,5].

To address globally important, emission-related questions, combustion science, and especially, combustion chemistry and diagnostics, can contribute valuable knowledge and methods including, but not limited to, the physico-chemical analysis, characterization, and monitoring of combustion-generated pollutants and aerosols, development of

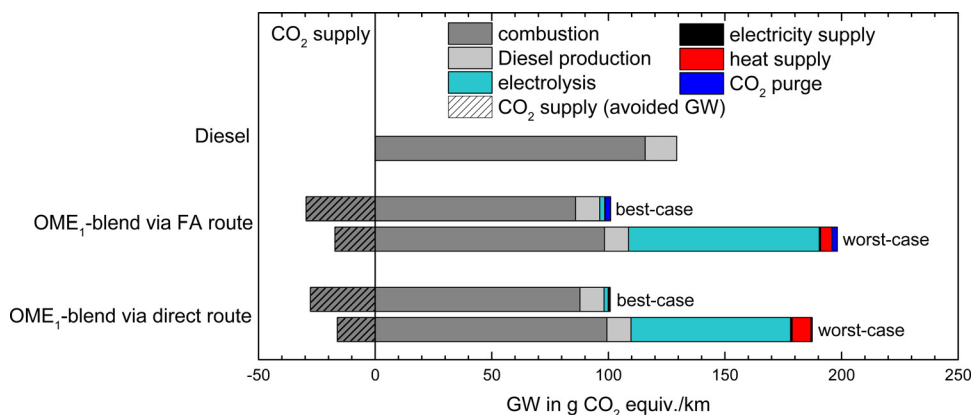


Fig. 2. Cradle-to-grave analysis of the global warming (GW) impact of an OME<sub>1</sub>-blend and fossil diesel fuel for the best- and worst-case scenarios discussed in the text and the original paper. Reprinted from [23], Open Access Article licensed under a Creative Commons Attribution 3.0 Unported Licence, DOI: 10.1039/C7EE01657C.

homogeneous and heterogeneous reaction mechanisms for their formation and further reaction, as well as reaction and transport models that can be critically inspected for different boundary conditions and examined against experimental observations.

## 1.2. Fuels

Colossal numbers of combustion-powered units around the globe – light- and heavy-duty cars, aircrafts, ships, power plants, heaters, industrial furnaces, and so on – are not readily replaced, much less within short time scales, by non-combustion systems, nor is the associated infrastructure. While introducing renewable technology, efficient and clean combustion may contribute to a faster transformation towards reducing GHG and air pollutant emissions. The transportation sector, despite increasing electrification in some areas, is largely powered by combustion. High-energy-density energy carriers such as today's liquid fuels are advantageous especially for long-distance and heavy-duty transportation, in marine applications, and in aviation. Combustion systems for these purposes are harder to replace than in passenger cars [12]. However, fuels are not fossil-only. The joint optimization of fuel and propulsion systems can exploit the potential of efficient, ultra-low-emission combustion, using renewably made fuels or fuel additives. Chemistry knowledge is needed to tailor their combustion properties and understand the influence of their molecular structure on their reaction mechanisms [13–18] for current and advanced combustion conditions, as well as to determine efficient pathways to make such fuels sustainably and in large scale [17,18].

As discussed by Dryer [14], a rapid change to less net carbon emissions from the transport sector can be facilitated by integrating sustainably made alternative fuels into the current liquid petroleum-derived fuel streams, using existing infrastructure. Beyond ethanol and biodiesel with their known properties, advantages, and problems [19,20], different chemical classes of compounds (mainly oxygenates such as ethers, alcohols, ketones, esters, etc.) have received attention as liquid fuel alternatives for road transportation. The relationship between their molecular structure, reaction mechanism, and combustion behavior is an intense area of research, particularly for the development of predictive combustion models. Proposed fuel classes include, among others, cellulosic biofuels such as the furanic family [17,18] and synthetic fuels such as oxymethylene ethers (OMEs, CH<sub>3</sub>O(CH<sub>2</sub>O)<sub>n</sub>CH<sub>3</sub>). The latter, attractive diesel replacement fuels, offer large pollutant reduction potential owing to their molecular structure featuring only C<sub>1</sub> units [21,22]. These oligomeric ether compounds can be synthesized through different steps from hydrogen (H<sub>2</sub>) and CO<sub>2</sub>, best using electricity from renewables for hydrogen production. In their recent lifecycle analysis (LCA), Deutz et al. [23] discussed several production routes for OMEs and the associated GHG reduction potential. The LCA followed standardized procedures to assess all associated energy and material flows. An overview of some of their results is given in Fig. 2 that shows the global warming impact of a blend of 35vol% OME<sub>1</sub> (dimethoxy methane (DMM) or methylal, CH<sub>3</sub>OCH<sub>2</sub>OCH<sub>3</sub>) with 65vol% fossil diesel fuel, compared with neat diesel, in a single-cylinder research engine. Speed and load variations were conducted according to the Worldwide Harmonized Light Vehicle Test Procedure (WLTP) cycle, and reductions of the global warming (GW) potential of 22%, and of

emissions of  $\text{NO}_x$  and soot of 43% and 75%, respectively, were demonstrated [23].

For pure diesel fuel as a reference, GW (in g  $\text{CO}_2$  equivalent per kilometer driven by a passenger vehicle) is mainly from combustion with a smaller part for diesel production. The GW impact of the  $\text{OME}_1$ -diesel mixture is evaluated with four different scenarios. Two synthesis routes for  $\text{OME}_1$  are assumed, one *via* formaldehyde (FA in Fig. 2), the other in a direct process using methanol ( $\text{CH}_3\text{OH}$ ),  $\text{CO}_2$ , and  $\text{H}_2$ ; for both, best-case and worst-case situations are analyzed [23]. GW contributions from combustion are lowered in each case because of the replacement of 35vol% of fossil diesel with  $\text{OME}_1$ . GHG savings of different magnitude are possible regarding the  $\text{CO}_2$  source for the synthesis; these are more substantial when  $\text{CO}_2$  is separated from biogas (best case) where it is co-produced with methane ( $\text{CH}_4$ ) than when it is obtained by the more energy-demanding process of direct capture from the air (worst case). The major difference between best- and worst-case scenarios, however, arises for  $\text{H}_2$  production, assumed *via* polymer electrolyte membrane (PEM) electrolysis at 75 bar, depending on the source of electricity. A factor of 38 difference in GW impact is noted between the best case using electricity from wind and the worst case with an assumed 2020 EU grid mix [23]. Slight differences are also seen depending on the choice of heat supply (with a higher demand for the direct synthesis route) either from natural gas or through electricity from wind. Best and worst cases show substantial difference in GW impact by about a factor of two, and depending on the assumed supply and production scenario for  $\text{OME}_1$ , neat diesel might even be superior regarding total GHG emissions [23].

For maritime applications, alternative fuel-propulsion concepts [24–27] are important in view of the enormous volume of long-range cargo transport and the comparatively low attention that had been paid until quite recently to the GHG and pollutant emissions of this sector. According to Thomson et al. [24], international shipping is responsible for 2–3% of global  $\text{CO}_2$  emissions. The need to comply with stricter emission regulations for  $\text{SO}_2$  and  $\text{NO}_x$  in coastal ranges and near ports has facilitated changes, especially for new vessels, towards better exhaust aftertreatment and dual-fuel operation. Marine engines equipped for combinations of conventional diesel fuel and liquefied natural gas (LNG) and a growing infrastructure make natural gas a potentially attractive marine fuel that could reduce local air pollutant emissions (especially  $\text{SO}_2$  and PM) [24]. Methane as a key component of LNG is a potent GHG, however, and methane leakage must be prevented, both regarding infrastructure and engine combustion. From their "well-to-wake" evaluation of emissions (including  $\text{NO}_x$ ,  $\text{PM}_{10}$ ,  $\text{CO}_2$ ,  $\text{CH}_4$ , and  $\text{N}_2\text{O}$ ) for three typical mar-

itime transport cases using LNG, Thomson et al. [24] conclude that a switch to LNG could contribute immediately to reducing air pollutant levels substantially below those of conventionally fueled marine diesel engines. Compared with low-grade fuels and associated sulfur oxide ( $\text{SO}_x$ ) emissions, this would be particularly valuable; net GHG emissions could potentially also be reduced, provided appropriate measures against  $\text{CH}_4$  leakage would be taken [24].

Similarly, Gilbert et al. [25] have recently evaluated conventional marine fuels, namely heavy fuel oil (HFO) and marine diesel oil (MDO), *versus* six alternatives including LNG, methanol, liquid hydrogen ( $\text{LH}_2$ ), biodiesel, straight vegetable oil (SVO), and bio-LNG. GHG emissions of  $\text{CO}_2$ ,  $\text{CH}_4$ , and  $\text{N}_2\text{O}$  were calculated for these fuels per unit power for upstream processes and for the combustion in the respective main engine. Their LCA includes multiple factors, such as the regional origin of the fuel, its production (extraction, cultivation, synthesis, etc.) and pretreatment (refining, liquefaction, drying, anaerobic digestion, etc.), the associated feedstock transport and conversion processes, and the engine, *i.e.* compression ignition (CI), spark ignition (SI), or fuel cell (FC). With most alternatives to HFO and MDO, local pollutant emissions can be reduced, particularly  $\text{SO}_x$  and PM; regarding GHG performance, however, total emissions from upstream processing and operation differ considerably for the chosen options [25]. While LNG combusted in SI engines is evaluated as promising for meeting air quality regulations, it is not a low GHG emission fuel, and for bio-derived fuels, GHGs from different land use and fertilization must be accounted for [25]. The suitability of  $\text{LH}_2$  depends crucially on the upstream processes and differs notably for pathways through LNG and steam reforming *versus* electrolysis with electricity from existing grids, with or without assumed CCS, or from wind power [25].

While fuel selection is important, increasing the combustion efficiency and minimizing the substantial heat losses for marine diesel engines that power 90% of commercial shipping is another pathway that can contribute to reducing pollutant and GHG emissions [26,27]. Beyond such factors as engine operation, optimized thermodynamic cycles, and waste heat recovery, innovative hybrid technologies can combine different power units, including combinations from diesel engines, solid oxide FCs, gas turbines, batteries, towing kites, or the use of alternative power sources in port [27]. As a reference case, a combination of several diesel engines with auxiliary photovoltaic modules and lithium ion batteries was analyzed for its emission performance to demonstrate that such hybrid systems, especially in new vessels, could potentially contribute to reductions of combustion emissions [27].

Air transportation is another area where conventional liquid fuels are not easily replaced. Aviation is considered to be responsible for almost 6% of global oil consumption, with a projected increase of jet fuel demand of about 1.9% per year until 2025 [28]. Approximately 3% of the anthropogenic CO<sub>2</sub> emissions are reported to be caused by aviation [29]. Zhang et al. [28], in their review, focus on drop-in alternative aviation fuels that are compatible with present engines and infrastructure and can be blended with conventional fuels. Such fuels can either be provided through synthetic processing of natural gas or coal or by hydrotreatment of bio-oils and fats. For several bio-derived, renewable jet fuels and respective conversion technologies, a recent LCA is given in [30]. Here, well-to-wake GHG emissions were assessed from feedstock cultivation (including fertilizer, but not land use changes), upstream transport and processing, and fuel distribution, while combustion itself was treated as carbon-neutral. Most considered pathways, e.g., hydrothermal liquefaction or pyrolysis providing bio-crude or bio-oil, respectively, need hydrogen for hydrodeoxygenation which was assumed to be produced through steam reforming of natural gas [30]. This was not the case for Fischer Tropsch (FT) synthesis from gasification of cellulosic biomass. Valuable co-products such as electricity from the excess steam in the gasification FT process were assigned GHG credits. Overall, sensitive contributions to GHG emissions were noted from fertilizers in feedstock cultivation, hydrogen consumption, and the conversion process itself. With the given analysis conditions, most pathways suggest potential GHG savings near 60% compared to fossil jet fuel; processes based on residues and FT conversion seem favorable, and renewably provided H<sub>2</sub> could improve the outcome in some cases [30]. It should be noted in addition that most GHG analyses consider CO<sub>2</sub>, CH<sub>4</sub>, and N<sub>2</sub>O emissions, but neglect black carbon (BC) emitted from aircraft, although it can differ between conventional or alternative jet fuels depending on aromatic content [29].

With all suggested alternative fuels, fundamental knowledge on their combustion properties is needed, including ignition and extinction characteristics, flame development, combustion speciation, and emissions, most of which may depend sensitively on the fuel's chemical composition and the molecular nature of its compounds. One aspect of concern for future aero-engines with high compression ratios is the low-to-intermediate temperature chemistry and the potential negative temperature coefficient (NTC) behavior, for which studies under real engine conditions are still largely lacking [28]. Also, the development of surrogates and respective fuel models deserves attention to improve the predictability of the combustion performance. Won et al. [31] have proposed a procedure to screen the suitability of emerging non-fossil jet fuels and their blends with petroleum-derived conventional

jet fuel. They analyzed fuel surrogate parameters, namely H/C ratio, mean molecular weight, derived cetane number (DCN), and threshold sooting index (TSI), and correlations with the combustion behavior including laminar flame speed, extinction limit, and global reactivity profile [31]. Examined fuels included petroleum-derived jet fuel as a reference and synthetic as well as bio-derived alternatives, using e.g., fuels from FT gas-to-liquid (GTL) and coal-to-liquid (CTL) processes or from different animal fats or plant oils [31]. While such analyses can prove useful in experimental screening procedures, understanding the chemical-kinetic reaction behavior of the compounds of a real fuel in applications involving turbulent multi-phase environments will need to build on substantial fundamental knowledge.

Regarding transportation and other fuels, fuel blends, and fuel-engine combinations, combustion science is needed for their critical evaluation. For pathways towards large-scale environmentally friendly fuels for future transportation, it is useful to consider the full picture, as illustrated by the few examples of lifecycle analyses above. Chemistry is not only needed to understand the combustion process in the engine itself, but chemical knowledge is indispensable for upstream processing steps. Innovative pathways improving their environmental and greenhouse gas balance can make a substantial difference for the complete process and could be of similar or larger impact than optimizing the combustion system alone. To avoid systemic roadblocks regarding fuels, propulsion concepts, and infrastructure, the combustion community should also feel answerable in view of the larger context and bring in their chemical and engineering expertise.

### 1.3. Fuels, energy storage, and conversion

The fuel spectrum that may contribute to CO<sub>2</sub> reduction can also provide interesting solutions for chemical energy storage and conversion between heat, power, transportation fuels, and other chemicals [32–34]. Proposed options include methane and other compounds with C<sub>1</sub> building blocks such as methanol, dimethyl ether (DME, CH<sub>3</sub>OCH<sub>3</sub>), OMEs, methyl formate (HCOOCH<sub>3</sub>), and dimethyl carbonate (DMC, CH<sub>3</sub>OCOOCH<sub>3</sub>) [32–35] as well as hydrogen [36–38] and ammonia (NH<sub>3</sub>) [39–42]. As a chemical building block for the C<sub>1</sub> compound syntheses, CO<sub>2</sub> might be captured preferentially from point sources, potentially from combustion systems [34].

Koj et al. [33] have recently evaluated a number of power-to-X options, which they defined as



process chains for the conversion of electricity into various products or applications and their associated technological components. They have identified about 30 LCA literature studies for respective systems (described as power-to-X, power-to-fuel, power-to-gas, power-to-liquids, power-to-mobility, power-to-transport, power-to-chemicals, and power-to-heat) and analyzed those in terms of potential GHG reduction and other environmental effects. Different conversion technologies from electricity to products with their relevant process steps are illustrated in Fig. 3 [33], which also shows some relevant inputs, infrastructures, and applications. Power should preferentially be renewable but depends on the source, the integration into the system, and the full load operation hours [33]. Other inputs such as CO<sub>2</sub> and H<sub>2</sub>O and technologies for their supply, transport, and treatment (separation, purification, etc.) must be considered, with potential integration of systems emitting CO<sub>2</sub> such as e.g., fossil power plants, waste incinerators, cement plants, and other industrial sources [33]. Transport, distribution, infrastructure, and storage options will also have an impact for the respective process chain.

It is obvious from Fig. 3 that a huge variety of concepts and routes exist that depend on a multiplicity of factors, even if only technological aspects are considered. Choices of targets for the assessment, e.g., a focus solely on GHG emissions or consideration of further environmental aspects, will lead to different results. Nevertheless, power-to-X concepts that use available renewable or surplus electricity and available CO<sub>2</sub> captured from industrial processes may seem promising and deserve further attention. Much work and creativity is needed towards viable process chains and efficient conversion steps, regarding also useful, environmentally friendly transportation fuel choices. Koj et al. [33] have considered some power-to-transport options based on results from four different studies. These include four vehicle-fuel types, namely internal combustion engine vehicles (ICEVs) with gasoline, ICEVs using synthetic natural gas (SNG), fuel cell electric vehicles (FCEVs) using hydrogen, and battery electric vehicles (BEVs) using electricity stored in chemical compounds such as hydrogen. The evaluation of their climate change impact (in g CO<sub>2</sub>-equivalent per km) considers direct emissions and those from fuel production, distribution, and other factors as well as different characteristics for the sources of electricity. As expected, the outcome depends to a large extent on the choice of such boundary conditions, showing, however, that power-to-transport concepts using SNG-fueled ICEVs could be competitive with FCEVs or BEVs in terms of GHG emissions [33]. Realistic choice and transparent description of conditions, regarding infrastructure as well as energy and material streams, and knowl-

edge of the respective technological potential in the different fields – including combustion – will matter for a fair assessment of future directions.

The conversion steps, fuels, and products briefly discussed above are not exhaustive. Further options of interest for combustion applications are being proposed, e.g., those derived from energy vectors such as NH<sub>3</sub>. Grinberg Dana et al. [43,44] consider nitrogen-based fuels in non-toxic, safe-to-handle aqueous solutions such as ammonium nitrate-based compositions including ammonium hydroxide or urea. The authors have compared seven synthetic fuels, namely methane, methanol, DME, ammonia, and such nitrogen-containing aqueous fuels in terms of a power-to-fuel-to-power assessment [43]. This methodology relates the available output power by the fuel's combustion to the energy required for its production (considering air separation, water splitting, and fuel synthesis) and distribution. While some of the proposed aqueous fuels perform quite well in this analysis [43], their combustion reactions and efficiency are not sufficiently known, with only exemplary laboratory studies of their combustion behavior [44].

Most previously mentioned conversion schemes concern rather small molecules as energy vectors that could be also used directly as combustion fuels or in fuel combinations. In view of rapidly needed alternatives, Schemme et al. [45] have focused on synthetic, liquid drop-in fuels from power-to-fuel pathways. "Renewable electrofuels" such as *n*-alkanes from power-to-fuel concepts could provide – different from CTL, GTL, or biomass-to-liquid (BTL) routes for synthetic fuels – non-fossil, non-biological alternatives that could be used widely and in the near future in existing passenger cars and trucks and could be mixed with fossil diesel in increasing proportions [45].

Liquid organic hydrogen carriers (LOHCs) present another pathway to chemically store and handle hydrogen in liquid form without the need for dedicated and complex H<sub>2</sub> storage infrastructures [46]. Such LOHC systems are pairs of hydrogen-rich and hydrogen-lean compounds that can store hydrogen by repeated catalytic hydrogenation and dehydrogenation cycles without binding or releasing other substances from or to the atmosphere [46]. Hydrogen carrier molecules are typically high-boiling, and the hydrogen-rich compounds can be stored stably for extended periods and transported, also over long distances, with existing technology [46]. Hydrogen-lean molecules can be aromatic systems, with an early LOHC pair being toluene-methylcyclohexane. Catalytic steps for LOHC systems need further attention, and while stationary use has been demonstrated already at a pilot stage, mobile applications will involve further research [46].

The substances just discussed contain preferentially the elements H, C, and N. The periodic table

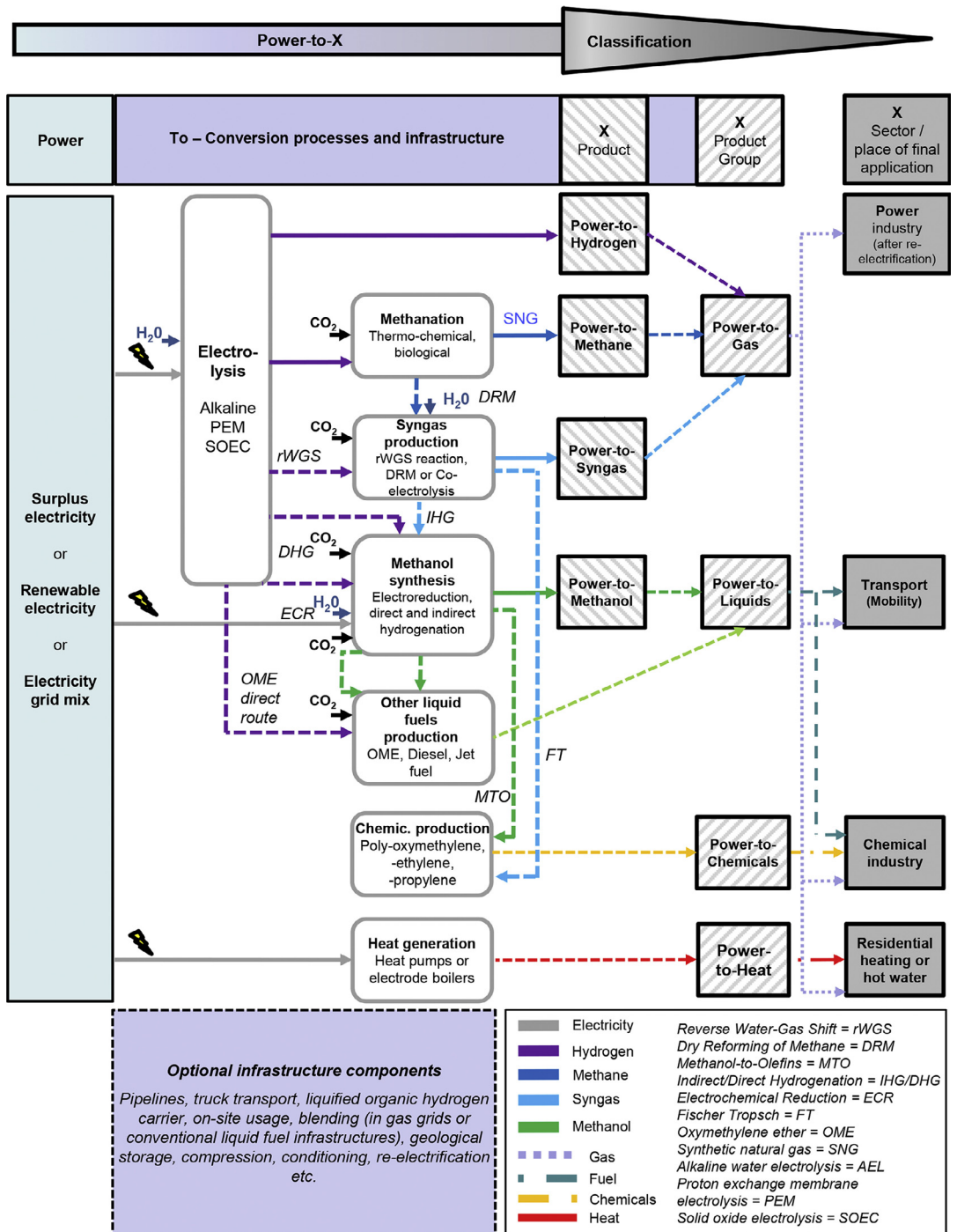


Fig. 3. Schematic illustration of main inputs, products, processes, and technologies of different Power-to-X process chains and their classification. Reprinted from [33] with permission from Elsevier.

offers more choices regarding potential combustion fuels [47,48]. Particularly high energy densities are available from metals that have been proposed as recyclable, zero-carbon energy carriers, including lithium, boron, magnesium, aluminum, silicon, iron, and zinc [48,49]. The combustion behavior of such heterogeneous systems for different applications is, however, much less understood than that of conventional liquid fuels [47].

It is beyond the scope of this article to provide a comprehensive discussion of available storage and conversion technologies. However, it should be recognized that beyond in-depth understanding of the relevant combustion systems, chemical knowledge is also required for pertinent reaction systems such as dry and steam reforming, partial oxidation, and synthesis routes. The development and optimization of technologically viable pathways can be enhanced by interaction with the combustion community. Also, the combustion community should not leave the choice of chemicals as fuels solely to others. High-efficiency, low-emission combustion techniques and integration of combustion into the changing energy landscape with the related conversion processes are areas deserving intense investigation.

#### 1.4. Combustion-generated materials

Combustion techniques provide opportunities to produce functional materials with attractive properties, including mechanical, optical, catalytic, magnetic, and electronic characteristics that makes them interesting for various applications, e.g., for coatings, ceramics, sensors, batteries, photovoltaics, and other – also energy-related – use [50–53]. Millions of tons of flame-made materials, including carbon black, fumed silica, pigment titania, and optical fibers, are reported to be produced at more than 15 billion \$/year [52,53]. As recently reviewed by Schulz et al. [50], combustion reactors can be used for gas-phase synthesis of nanoparticles, particularly oxides, complemented by plasma reactors that can be employed in similar processes to provide non-oxide materials. To tailor and control the properties of such materials including their composition, phase, morphology, size distribution, and further desirable characteristics, a necessary prerequisite is the fundamental understanding of the reaction process from the precursors to the particles. This knowledge is also vital to scale up synthesis processes from the laboratory to industrial scale. Compared with conventional combustion, the chemistry of gas-phase material synthesis includes additional elements, compounds, and

reactive species, with generally lesser knowledge about their reactions and kinetic parameters [50]. It is therefore highly useful to characterize the process under well-controlled laboratory conditions as shown in Fig. 4 [50]. Here, the authors have coupled a shock tube – a well-suited reactor to investigate the kinetics of high-temperature processes – with several *in-situ* diagnostic techniques including atomic resonance absorption spectroscopy (ARAS), emission spectroscopy, time-resolved laser-induced incandescence (TiRe-LII), extinction measurements, and high-repetition-rate time-of-flight mass spectrometry (HRR-TOF-MS) to provide insight into the species composition, its temporal development, and the particle growth.

Similarly, Kelesidis et al. [51] show that combustion synthesis can provide access to a multitude of products useful for photovoltaics, sensors, catalysis, electronics, and magnetic applications. In each case, and particularly when high purity or metastable compositions are desired, in-depth understanding of the process dynamics and tight control of the synthesis conditions are essential [51]. The authors underline how the understanding of combustion synthesis has enabled progress towards scalable production routes, including control of impurities, particle size distribution, composition, and morphology. They also highlight the importance of understanding particle dynamics and fluid mechanics for metastable product formation, and of thermophoretic sampling to understand the particle growth during the combustion process [51]. Moreover, Li et al. [52] have summarized flame aerosol synthesis routes towards supported metal nanocatalysts, including spinel and perovskite oxides and core-shell structures, of doped photocatalysts, and of carbon-metal oxide nanocomposites, using different burner configurations. To describe and scale up such flame synthesis processes, computational fluid dynamics (CFD) simulations should include information on the combustion kinetic mechanisms [54], and molecular modeling can assist in understanding their physico-chemical basis as a means to facilitate process design [55].

From the large number of systems and applications, some examples pertaining to energy- and fuel-related aspects may be interesting in the present context. Targeting the Fischer-Tropsch process as part of the GTL route towards cleaner fuels, a double flame spray pyrolysis technique was demonstrated to offer individual control over the properties of the catalyst and support materials, providing an alumina-supported cobalt catalyst that showed promising performance [56]. Gockeln et al. [57] have used a similar approach to synthesize *in-situ* carbon-coated  $\text{Li}_4\text{Ti}_5\text{O}_{12}$  (LTO) nanoparticles as electrode materials for lithium ion batteries, important in electromobility and large-scale energy storage. Again, the flexible operation of the double flame spray pyrolysis technique enabled control over the process by individually addressing the

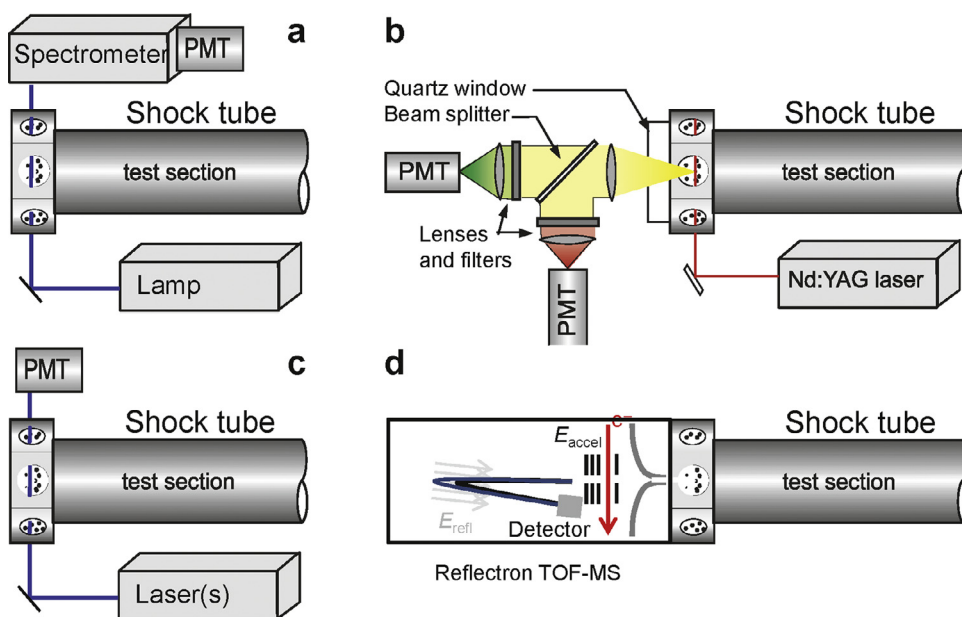


Fig. 4. Shock tube with a variety of diagnostics for particle growth processes: (a): Absorption and emission (without lamp) measurements for species concentration, and ignition delay time detection (without spectrometer), (b): time-resolved laser induced incandescence for particle size determination, (c): absorption and extinction measurements for determination of species concentration, temperature, and particle formation induction times, (d): high-repetition-rate time-of-flight mass spectrometer for multi-species measurements. Reprinted from [50] with permission from Elsevier/The Combustion Institute.

LTO nanoparticle size and their surface modification. With this technique, solvents or binders could be avoided, potentially improving the energy density, reducing the need for non-electrochemically-active materials, as well as complexity and costs, while providing opportunities for up-scaling [57]. Another example is the synthesis, again by flame spray pyrolysis using a methane/oxygen flame, of Cu/ZnO/Al<sub>2</sub>O<sub>3</sub> catalysts for direct DME production from synthesis gas [58]. Combustion processes with defined temperature, pressure, composition, and mixing properties can thus be a valuable means to provide the adjustable reaction environment for controlled synthesis of materials for multiple applications. The flexible and scalable operation of such flame reactors can offer opportunities for the energy sector, including energy storage and conversion systems. Nevertheless, the process chains must be evaluated in terms of their greenhouse gas signature, for example when using fossil-fueled, e.g., natural gas flames as the reaction environment.

Flames are especially well suited to produce carbon nanomaterials with highly attractive properties [59–66]. The double-faced nature of soot as both, an air pollutant and a high-tech product has been recognized, and Mulay et al. [59] have recently reviewed production and applications of candle soot. For example, candle soot is known to be superhydrophobic, useful in water-repellant surface

coatings, self-cleaning glasses, smart textiles, or oil-water separation [59,60]. Depending on parameters such as temperature, residence time, and wax composition, differently structured carbon materials can result, including, for example, fluorescent carbon nanoparticles and single- and multi-walled carbon nanotubes [59,61]. As discussed by the authors [59], fluorescent carbon nanoparticles derived from candle soot can be used, e.g., as hydrogen sensors, infrared (IR) sensors, ultrasound transducers, disposable immunosensors, for glucose detection in blood, in fluorescence resonance energy transfer (FRET) and similar chemiluminescence schemes; related to energy storage, conversion, and harvesting, candle-soot-derived carbon nanomaterials can find valuable applications, e.g., in supercapacitors, PEM fuel cells, lithium ion batteries, and in photo- and electrocatalytic processes. Carbon materials for supercapacitor electrodes from candle soot can offer good electrochemical performance and could thus contribute to cost-effective production pathways for building blocks of high-density energy storage devices [62]. Making different carbon nanostructures in candle flames has thus come a long way since the seminal article of Liu et al. [61]. However, understanding of the combustion parameters, in particular of the flame's reactive species composition, and of the carbon growth processes are necessary not only for using such reactive

environments stably and reproducibly, but also to bring such production options from demonstration experiments into larger-scale applications.

Flames also provide opportunities to produce different two- and three-dimensional carbon structures as e.g., carbon nanodisks of atomic thickness and tens of nanometers lateral dimension [63], three-dimensional graphene structures [64], and flame-soot nanoparticle thin films [65]. Two-dimensional materials such as graphene have received considerable attention, and well-controlled combustion conditions might permit to synthesize carbon-based 2D materials with characteristics that could be tailored for specific applications [63]. Three-dimensional structures incorporating graphene are suggested for catalysis, energy storage, and oil absorption, and flames offer appropriate reaction conditions for the fast and facile growth of such structures, as demonstrated by Qian et al. [64] in an acetylene/oxygen flame on nickel foams as substrate. From carbon nanoparticles grown in a premixed acetylene/air flame, thin films were thermophoretically deposited at low kinetic energy on stainless steel substrates with the aim to explore routes towards low-cost electronics or nanosensors [65]. Again, the facile, one-step method may show potential for tuning physico-chemical properties of the nanoparticles and thin films. As an exciting further aspect of carbon nanoparticles from flames, their quantum dot behavior has been recently investigated systematically [66], with an analysis of their optical bandgap, photoemission ionization energy, and electrochemical ionization behavior. The findings of these authors and earlier research summarized in their report [66] regarding the light absorption and emission properties of carbon nanoparticles from flames will have impact not only for applications in photovoltaic or electrochemical devices, but also for assessing the effects of radiative forcing from combustion-generated soot.

The apparent simplicity of combustion synthesis methods of carbon-based nanomaterials should, however, not lead to underrating the complexity of the chemical mechanisms that relate flame conditions and desired nanomaterial characteristics with catalytic, electrical, optical, magnetic, or other properties. Without understanding the physico-chemical basis, design, reliability, reproducibility, control, and scaling of such synthesis processes is left to phenomenological approaches.

Examples such as those given in this article underline that solving combustion problems and exploring combustion opportunities needs chemical understanding. Important knowledge is available from the classic physico-chemical domains, from surface

science, synthesis, and reaction engineering. Thermodynamics, for example, provides important criteria for the energetic feasibility of chemical conversion routes as well as for life-cycle analyses. Kinetics provides insight into the principles and pathways for the transition from the initial to the final state, e.g., to understand the formation of desirable nanomaterials as well as of undesired by-products such as harmful emissions. Spectroscopy and microscopy provide reliable and reproducible experimental evidence for the involved phenomena not only in a laboratory system, but also in a technically representative environment. In combination, fundamental knowledge and quantitative analysis methods from combustion chemistry can assist to conceive strategies to abate pollutants, to design fuels, to develop chemical conversion and storage routes, and to provide access to functional materials – important future fields of action for combustion science.

## 2. Selected combustion chemistry advances – overview and recent progress

Combustion proceeds in a wide range of pressure, temperature, and composition and in a large variety of systems. Relevant processes may include pretreatment, delivery, and mixing of fuel and oxidizer, ignition, reaction progress for safe and efficient energy conversion, and aftertreatment. Understanding such processes to the necessary level of detail is a prerequisite for performance optimization and control. Chemical knowledge is important for many combustion-related areas and includes diverse subjects from coal and biomass combustion to fire safety. In this chapter, selected advances and directions will be presented with a focus on gas-phase combustion.

Chemical knowledge on such systems is generated by the interplay of experiment, theory, and simulation of their characteristics and behavior by chemical-kinetic combustion models. Many seminal investigations combine several of these aspects. The following sections should thus not be regarded as independent. A first focus will be combustion chemistry diagnostics, highlighting experimental techniques and approaches to obtain chemical information from a combustion system. Such chemical information is important to understand the ignition and combustion behavior of conventional and alternative fuels, to understand the formation of pollutant emissions, and thus to enable design of efficient, clean combustion systems. The following two sections will then present aspects of chemically particularly complex areas, including combustion at low temperatures on the one hand and soot pre-

cursors, polycyclic aromatic hydrocarbons (PAHs), and soot on the other. The work highlighted in these two sections will also refer to the respective chemical concepts and models. Nevertheless, a final section will focus particularly on model development including selected recent work on mechanism reduction, uncertainty analysis, and data treatment. It is hoped that this overview will thus provide a flavor for the powerful methods, approaches, and developments that could also be applied in related areas beyond immediate combustion.

### 2.1. Insight into the reactive system – combustion chemistry diagnostics

Understanding combustion chemistry in relevant detail needs experimental information directly from the reactive system. Multiple parameters characterize the combustion state and its development along the reaction progress, including temperature, pressure, density, velocity, mixing status, species composition, reactivity, heat release, and others, many of which can be experimentally determined. Specifically designed laboratory experiments permit access to information such as ignition delay time, flame speed, flame structure, autoignition and extinction behavior, reactive species identification, their relative or absolute concentrations, and occurrence of specific chemical reactions as a function of boundary conditions and the fuel's molecular structure. As simplified in Fig. 5 for the reaction progress in a gas-phase combustion system, information from diagnostics and theory can support development and validation of chemical combustion models based on fundamental thermodynamics, transport, and reaction kinetics. Insight gained from such partly idealized systems can serve to develop, advance, and validate transferable combustion chemistry models that bridge between fundamental chemical knowledge and practical systems behavior.

Beyond gas-phase reactions, further characteristics of the combustion system may include the formation of droplets, sprays, and particles, phase changes, heat transfer, flame–wall interactions, heterogeneous reactions, and aftertreatment performance. Challenges to investigate chemical aspects in practical combustion systems are presented, for example, by the interaction of multiple species with a turbulent flow field [67,68] and the reactions of multi-component conventional as well as chemically diverse future transportation fuels, with different properties and reactivity, in current and advanced engines [69–73].

Laser sensors and optical imaging techniques can determine relevant parameters such as temperature, pressure, and species concentrations in practical combustion systems and reactive flows [74–76]. Such applications span an impressive range from measurements of individual reaction rate coefficients to advanced propulsion systems

[74,75], often resorting to absorption and fluorescence techniques. Diagnostic advances include highly sensitive and real-time species detection in gas-phase systems [77–79]. Also, diagnostic techniques permit to capture temporal and spatial variations of important reactive species [80], to probe flame–wall interactions [81,82], to sample correlated temperature and velocity information with high repetition rates and spatial precision [83], and to follow the formation and growth of soot and other particles [84,85].

Comprehensive reactive species information that is essential for a deeper understanding of the reaction processes as a function of temperature, pressure, fuel–oxidizer mixture, reaction time, and other system variables is often not available from laser diagnostics, but from specific methods, including mass spectrometry as a universal technique [86–89]. Advanced instrumentation includes synchrotron-based vacuum ultraviolet (VUV) photoionization (PI) molecular-beam mass spectrometry (MBMS) to determine species profiles in reactors and flames [87–91]. An example for a jet-stirred reactor (JSR) coupled with PI-MBMS is shown in Fig. 6 [92]. A sample of the reactive mixture at a pre-selected temperature and residence time is withdrawn from the heated JSR by a quartz probe. The species are then ionized with tunable single-photon VUV radiation, here generated at the Advanced Light Source (ALS) in Berkeley, and their mass is determined with a TOF-MS [92]. Combining high-mass-resolution MBMS and measurement of photoionization efficiency (PIE) curves, obtained by scanning the photon energy, typically enables detection of molecules of C/H/O(N) elemental constitution and identification of isomeric structures.

Such isomer-discriminating photoionization experiments have served to investigate the kinetics of individual combustion-relevant reactions [93,94], to determine VUV photoionization cross sections for the quantitative detection of decisive low-temperature species such as the hydroperoxyl radical ( $\text{HO}_2$ ), hydrogen peroxide ( $\text{H}_2\text{O}_2$ ), and formaldehyde ( $\text{H}_2\text{CO}$ ) [95], and to detect previously elusive molecules such as Criegee intermediates [96,97]. Moreover, photoelectron photoion coincidence (PEPICO) spectroscopy, a technique that provides species-selective information from mass-selected photoionization and the coincident photoelectron spectra (PES), has great potential to obtain in-depth species- and structure-selective information in complex reactive systems [98–101].

The detection of intermediate species profiles with species-selective techniques is important to reveal mechanistic details and evaluate the performance of kinetic models, as shown in the examples in Figs. 7 and 8. Hemken et al. [102] have studied the combustion of the high-octane biofuel candidate 2-butanone in a laminar premixed low-pressure flame combining results from two

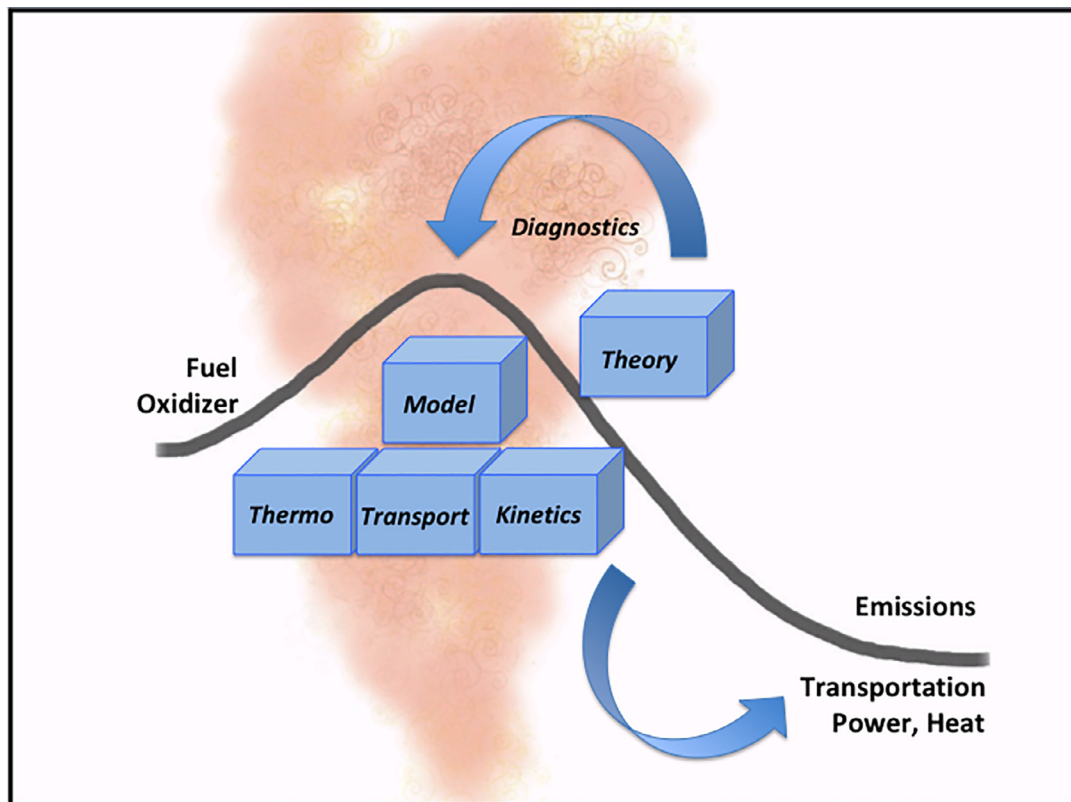


Fig. 5. Essential contributions to characterize the chemical reaction progress in gas-phase combustion systems.

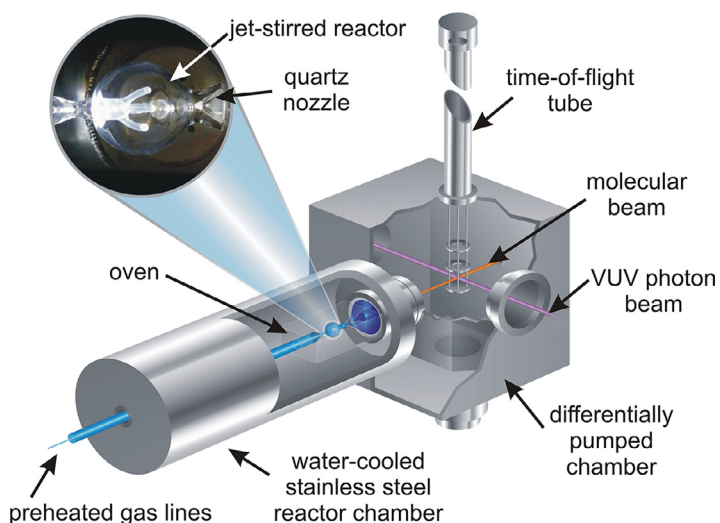


Fig. 6. Schematic representation of a jet-stirred reactor that is located within an oven, all surrounded by a water-cooled stainless-steel chamber. Molecules are sampled from the reactor through a quartz probe, ionized via single-photon ionization with vacuum-ultraviolet photons, and the respective ions are mass-selected using a reflectron time-of-flight mass spectrometer. Reprinted with permission from [92]. Copyright (2015) American Chemical Society.

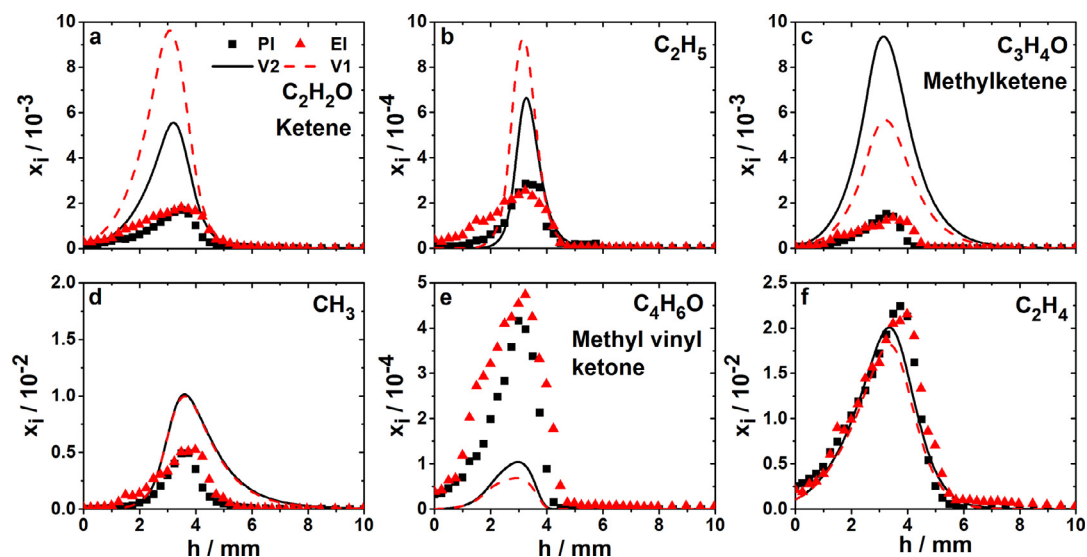


Fig. 7. Mole fraction profiles in a laminar low-pressure flame of 2-butanone (40 mbar, equivalence ratio  $\Phi = 1.6$ , fuel/O<sub>2</sub>/Ar: 0.113/0.388/0.5 mole fraction), showing first detectable intermediates after H-abstraction and  $\beta$ -scission. Symbols: PI- and EI-MBMS experiments, lines: simulation with versions V1 and V2 of a flame model (see text and original publication). Reprinted from [102] with permission from Elsevier/The Combustion Institute.

different MBMS instruments, one using VUV-PI at the ALS in Berkeley and the other electron ionization (EI) in Bielefeld. Since detailed reaction kinetic models for this fuel were still largely lacking, the combined experimental analysis was thought to provide a useful target for model inspection and development. Fig. 7 shows quantitative mole fraction profiles for six intermediates formed as products of first H-abstraction and subsequent  $\beta$ -scission reactions from the different fuel radicals. Included are (a) ketene (C<sub>2</sub>H<sub>2</sub>O) and (b) ethyl (C<sub>2</sub>H<sub>5</sub>) from H-abstraction at the primary C1-atom and subsequent  $\beta$ -scission; (c) methylketene (C<sub>3</sub>H<sub>4</sub>O) and (d) methyl (CH<sub>3</sub>) as products of 2-butanone-1-yl  $\beta$ -scission, and (e) methyl vinyl ketone (MVK, C<sub>4</sub>H<sub>6</sub>O) as well as (f) ethene (C<sub>2</sub>H<sub>4</sub>) from reactions involving the 2-butanone-3-yl and -4-yl radicals [102].

The results from the two experiments are in excellent agreement, especially considering the experimental uncertainties of both independent instruments and the different cross sections of the two ionization processes for the respective quantification. Clearly, the simulation deviates significantly from the experiment in most cases, even after introduction of some modifications regarding the initial decomposition reactions and the MVK sub-mechanism [102]. Because of the unambiguous identification and mutually supportive, quantitative experimental detection of these intermediates with two techniques, it could be concluded that further development of the model was warranted and the deviation between experiment and model

was not due to experimental errors, which is the more important since MVK is a toxic species and its correct prediction would be useful [102].

In the previous example, the fuel radicals were not identified experimentally, and information on branching between the different possible channels was only accessible indirectly from the respective first stable decomposition products. Using the PEPICO technique, Oßwald et al. [99] were the first to determine species profiles of the initially formed fuel radicals in a flame. These are particularly important since they are at the origin of further reaction pathways and thus provide information on the expected radical pool. However, they are hard to detect because of their reactivity and low concentrations. Fig. 8 shows the results for the four different butyl radicals at a mass-to-charge ratio of  $m/z=57$ , detected in the reaction zone of an isobutane flame from mass-selected threshold photoelectron spectra (TPES) in coincidence with photoionization mass spectrometry [99], using the instrument at the Swiss Light Source.

Although the PIE spectra in the top panel of Fig. 8 are of exceptional quality, given the low concentrations of these reactive intermediates, a potential assignment of the different radicals by the slight changes in slope is considerably less conclusive than the identification from the PES given in the bottom panel, especially considering that changes in geometry might occur during ionization (adiabatic versus vertical transitions, as indicated in Fig. 8). From reference spectra of all possible butyl radicals, the branched isomers were unambiguously



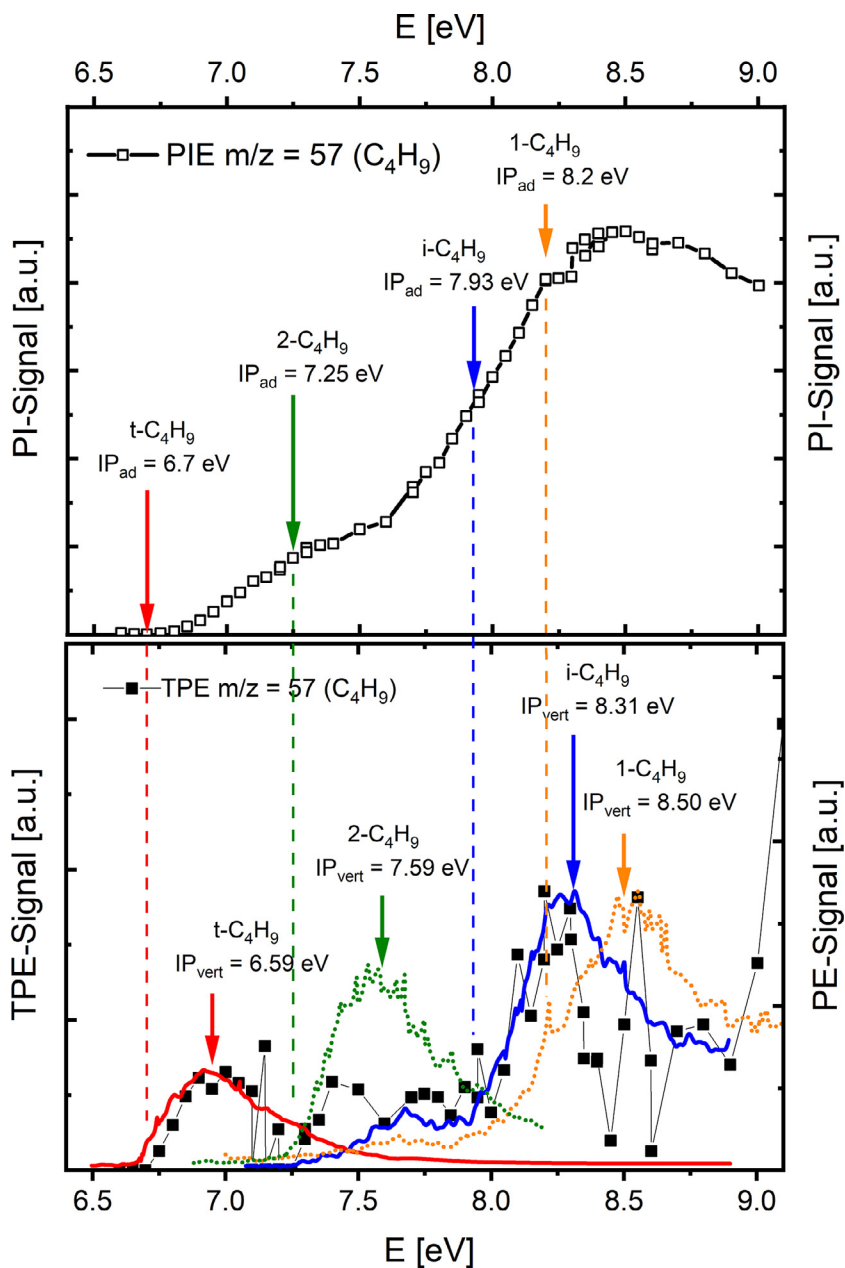


Fig. 8. PIE curve (*top*) and threshold photoelectron spectrum (TPES, *bottom*) of the  $m/z=57$  signal (butyl radicals) obtained from the reaction zone of a fuel-rich isobutane flame. Signals are compared to the adiabatic (*top panel and dashed lines*) and vertical (*bottom*) ionization thresholds ( $IP$ ) and photoelectron spectra (PES) of *tert*-butyl (*solid, red line*), *iso*-butyl (*dotted, green line*), 1-butyl (*solid, blue line*), and 2-butyl (*dotted, yellow line*). Literature for the reference PES is given in the original article. Reprinted from [99] with the permission of AIP Publishing.

identified, in good agreement with the assumed major fuel destruction routes [99]. The technique has thus demonstrated excellent sensitivity and superior isomer identification potential for highly reactive species in reacting flows of chemical complexity such as a flame.

Understanding combustion processes and concurrent development of combustion models needs information in a wide range of temperatures and pressures. It is therefore important to consider multiple reaction environments with their specific target conditions and advantages for studying

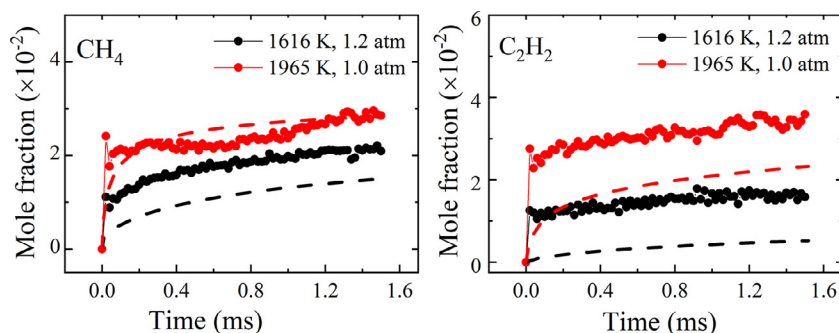


Fig. 9. Mole fractions of methane and acetylene as a function of reaction time for two reflected-shock experiments at 1616 K, 1.20 bar and 1965 K, 1.01 bar. (Dashed lines: simulations with a chemical-kinetic model; see original publication). Reprinted from [113] with permission from Elsevier/The Combustion Institute.

a given question, since they may show different sensitivity to certain species and specific reaction pathways. Also, especially in a flame environment, uncertainties in transport and heat transfer might obscure the influence of reactions of particular interest for model development. Jet-stirred and other types of reactors [103–106], shock tubes [107–115], and rapid compression machines (RCMs) [116–118] offer opportunities for mechanistic investigations for fundamental and practically relevant conditions. Different analytic methods have been used to determine important chemical information, including mass spectrometry [104,108], Fourier-transform infrared (FTIR) spectroscopy [103], gas chromatography (GC) [109], and laser absorption [107,109–114], also in the mid-infrared spectral region [112], as well as cavity-enhanced laser absorption spectroscopy (CEAS) [115,117]. Great potential for the on-line analysis of chemical composition in highly complex mixtures is also offered by advanced two-dimensional GC techniques with flame ionization or MS detection [119]. The development of laser sensors enables increasingly facile, simultaneous detection and quantification of several species in reactive mixtures, including multi-species detection approaches in shock tubes [110–113]. As a recent example, Zhang et al. [113] have used an integrated quantum cascade laser (QCL) with an extended wavelength range to provide mole fraction profiles for methane (CH<sub>4</sub>) and acetylene (C<sub>2</sub>H<sub>2</sub>) in shock tube laser experiments. Fig. 9 shows the concentration–reaction time history for two reflected-shock conditions in the pyrolysis of 2% isooctane in argon.

The production of both species increases with temperature; observed differences between experiment and simulation might be caused by imperfections in the model or potential contributions from other absorbing intermediate species in this spectral region [113]. Nevertheless, these demonstration experiments with a sensitivity at 1300 K of or below 100 ppm and an effective time resolution of 20

μs show promising potential to follow the reaction progress quantitatively in such systems.

Beyond fundamental investigations, it is important to obtain information about the combustion process – including the reaction progress – for practically relevant transportation fuels and engine conditions [118–128]. Ignition behavior, flame development, heat release, the effects of injection, mixing, exhaust gas recirculation (EGR), and other characteristics can be monitored, often using optical diagnostic methods and chemical markers for certain process aspects. For example, laser-induced grating spectroscopy (LIGS), suitable for applications in engines [121,122], has been developed to jointly measure temperature and water concentration [123]. Sampling-free in-cylinder concentration measurements have been performed with high-speed tunable diode laser absorption [124]. Tomographic imaging in the chemically sensitive near-IR has been demonstrated as a tracer-less means to monitor evaporation and mixing development; the results were cross-compared to planar laser-induced fluorescence (PLIF) measurements of naphthalene as a fuel tracer and give useful indications on combustion behavior and pollutant formation [125]. In a reactivity-controlled compression ignition (RCCI) engine, *in-situ* chemical species information from single-shot PLIF of formaldehyde was used to investigate effects of the injection procedure and the interplay of autoignition, flame propagation, and heat release [126]. Different ignition processes, early flame development, and cycle-to-cycle variations in heavy-duty natural-gas-fired engines were accessible with rapid-frame-rate borescopic IR imaging of water spectral lines in the 1–1.7 μm region [127]. Furthermore, soot formation and in-cylinder soot oxidation were analyzed in an optical engine with high-speed extinction measurements [128]. These and other examples highlight the progress in combustion diagnostics towards real-time process monitoring and control, especially for chemically sensitive advanced engine conditions.

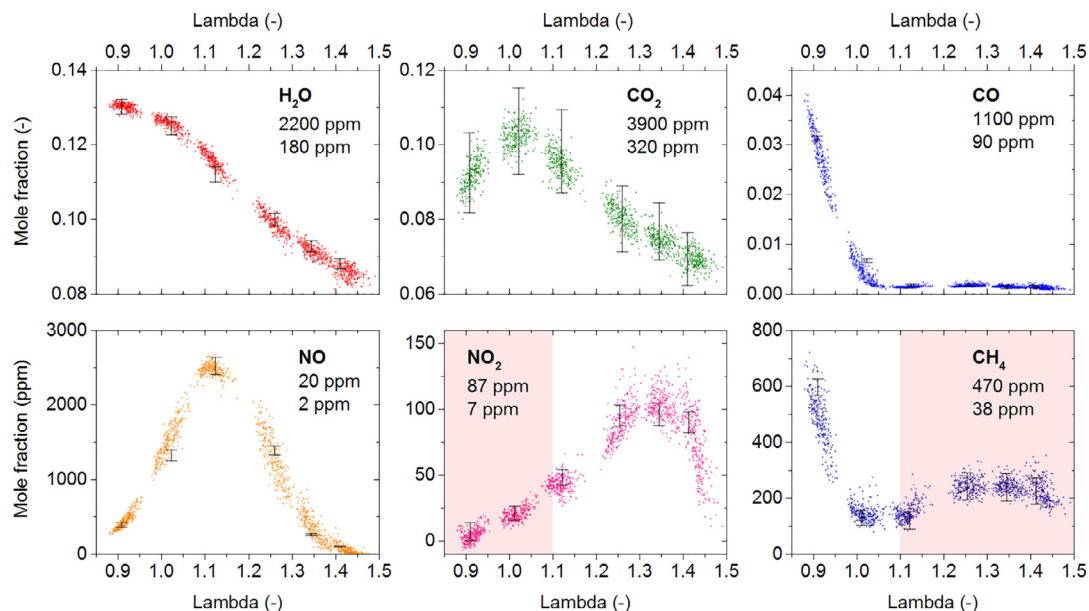


Fig. 10. Mole fractions as a function of the air–fuel equivalence ratio  $\lambda$  for all measured species. Each point corresponds to a single engine cycle. Estimated detection limits are reported for a signal-to-noise ratio (SNR) of  $\text{SNR} = 2$  at effective measurement rates of 4.8 °CA (upper value) and 720 °CA (lower value). Reprinted from [129] with permission from Elsevier/The Combustion Institute.

Chemical information is also valuable to characterize engine exhaust with appropriate sensitivity *in-situ*, in real-time, on-board, with portable devices [129–132]. Such methods are especially useful to monitor real emissions as a function of driving performance, to assure compliance with regulations, and to provide a critical assessment of associated health risks. An in-depth overview of instrumentation to determine particulate emissions is given in [130]. Diemel et al. [129] have recently demonstrated an *in-situ* sensor for the cycle-resolved measurement of six exhaust species, including H<sub>2</sub>O, CO<sub>2</sub>, CO, NO, NO<sub>2</sub>, and CH<sub>4</sub>. Results from their analysis are given in Fig. 10.

The measurements are based on tunable diode laser absorption spectroscopy (TDLAS) in the wavelength range of 1.4  $\mu\text{m}$  to 5.2  $\mu\text{m}$ , using a fiber-coupled sensor device with four optical channels and time-divided multiplexed detection and an effective measurement rate as high as 1 kHz [129]. The absorption length was up to about 1 m (test) and 2 m (engine), with miniature White cells for the detection of the nitrogen-containing species to enhance the sensitivity (for details see [129]). The data in Fig. 10 mainly show expected trends with varying air–fuel equivalence ratio  $\lambda$  for H<sub>2</sub>O, CO<sub>2</sub>, and NO. Also, CO and CH<sub>4</sub> as indicators for incomplete combustion are found in the rich regime. However, NO<sub>2</sub> has its maximum at slightly lower  $\lambda$  than expected, affecting also the maximum NO/NO<sub>2</sub> ratio, potentially due to cooling effects in the optical engine [129]. Cycle-to-cycle variations are evident but

with a different level of scatter for different species, which may be related to the different complexity of the selected spectral features. The CH<sub>4</sub> concentrations at lean conditions should be regarded with caution because of spectral overlap with NO<sub>2</sub> [129].

Further information surrounding the combustion process in the engine can be obtained, for example on preheating and evaporation of the fuel streams [133–135]. Moreover, combustion diagnostics research is also directed to gas turbine combustors and furnaces, with ambitious techniques such as femtosecond two-photon LIF imaging of CO applied to piloted liquid spray flames [136]. The analysis of different flame regimes with respect to premixed and non-premixed reaction zones in turbulent lifted flames has been demonstrated with Raman/Rayleigh line measurements [137,138] without necessitating 3D gradient information. From combined detection of several chemical species, heat release can be remarkably well predicted in turbulent jet flames [139]. As a particularly challenging example, quantitative species diagnostics has contributed to analyzing the structure of a swirl-stabilized kerosene flame with up to 180 kW thermal power using an industrial lean-premixed aero-engine injection system at near-atmospheric and elevated pressures [140,141]. Selected results of these investigations that have combined OH and kerosene PLIF for temperature and concentration measurements from two different planes are presented in Fig. 11 [141].

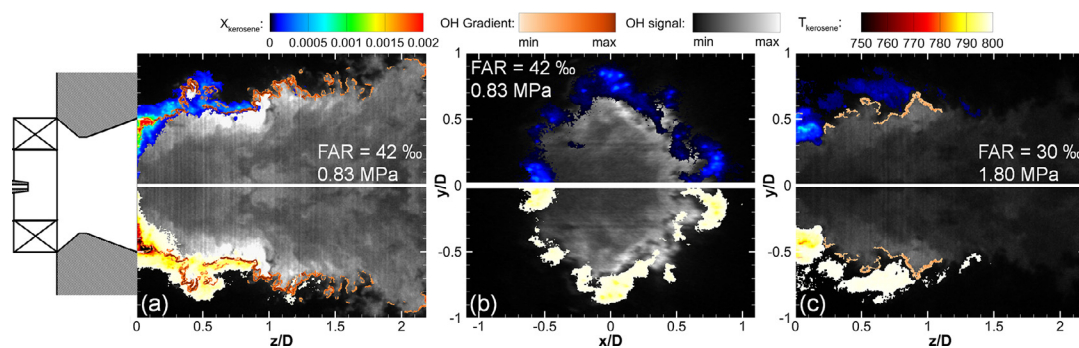


Fig. 11. Flame characterization at two different pressures combining several PLIF channels and measurement planes. Instantaneous kerosene mole fraction (*top*), OH-PLIF signals and temperature (*bottom*) at 0.83 MPa in axial configuration (a) and in radial configuration at a position  $z/D = 0.75$  (b), at 1.80 MPa in axial configuration (c) with an air inlet temperature of 670 K. Color coding: grey-to-white scale: OH signal; color scale (*top*): kerosene mole fraction; color scale (*bottom*): temperature; beige coloring (*bottom*): OH gradient. Reprinted from [141] with permission from Elsevier/The Combustion Institute.

In this series of experiments, two particle imaging velocimetry (PIV) systems were applied to characterize the flow field by 2D measurements of velocity in the axial ( $x$ - $z$ ) and radial ( $y$ - $z$ ) planes [140], using stereoscopic PIV in the radial measurements. In stream-wise direction, a high-speed PIV system with 5 kHz frame rate was used. OH PLIF at 10 Hz ensured good signal-to-noise and spatial resolution; crosstalk between the fluorescence of OH and that of the aromatics in kerosene was reduced by appropriate choice of excitation wavelength and filtering. Flame structure and dynamics were revealed with a high-speed OH-PLIF system with 10 kHz repetition rate [140]. The fluorescence spectra of commercial JET A1 fuel and the contributions of mono- and di-aromatics were analyzed in high-pressure reference measurements that were used in the calibration for both, fuel mole fraction and temperature distribution. For further geometry and characterization details for the PLIF and PIV experiments refer to [140,141].

The single-shot measurements in Fig. 11 and the averaged results in [141] obtained under these harsh conditions show impressively, how such joint information from several quantities and measurement planes in practically relevant combustion environments can be obtained based on a deep understanding of the fundamental physico-chemistry underlying the laser spectroscopic detection. The characterization of industrial-type injection systems and combustion processes at elevated pressures with realistic liquid fuels is key for the design of aero-engines and transportation fuels that can significantly reduce combustion emissions.

The development, monitoring, and control of low-emission combustion processes have be-

come feasible with diagnostics methods that can analyze the combustion process and reaction progress in chemically complex laboratory systems as well as in practical applications, using chemical markers for important properties such as evaporation, mixing, flame dynamics, heat release, and pollutant formation. Such methods, procedures, and combinations of techniques can be exploited to investigate reacting systems beyond combustion.

## 2.2. Towards efficient, clean processes – combustion at low temperatures

The need to reduce emissions drives the development of high-efficiency internal combustion (IC) engines, particularly in the low-temperature combustion (LTC) regime [142–145]. Homogeneous charge compression ignition (HCCI) concepts [144,145], low-temperature partially-premixed diesel combustion [143], and dual-fuel reactivity-controlled variants of LTC processes [142] hold high promise in both, reductions of  $\text{CO}_2$  and pollutant emissions. Fuel design provides appropriate candidates for these LT processes [146,147], including advanced fuels from biomass [17,148] or from other renewable sources, such as OMEs [23]. To predict the behavior of chemically sensitive LTC systems, in-depth knowledge on the fuel-specific reaction kinetics is needed, an issue that has motivated substantial fundamental work. Some years ago, Zádor et al. [149] and Battin-Leclerc [150] described some general features of LT reaction mechanisms; these are characterized by numerous mostly quite labile oxygenated intermediates that are hard to detect experimentally.

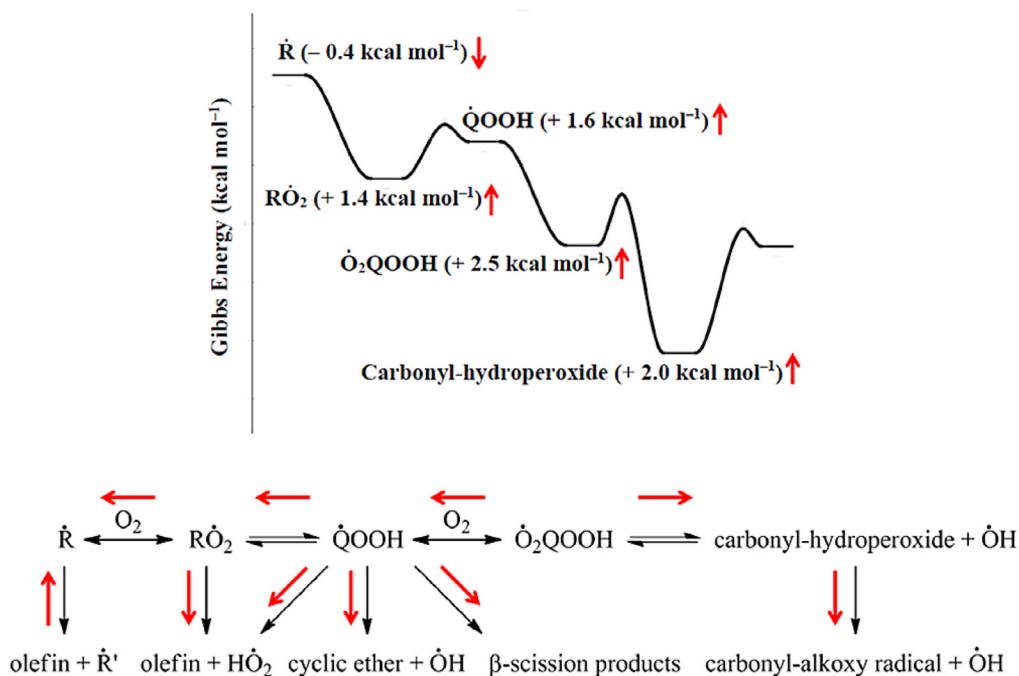


Fig. 12. Representation of average changes in Gibbs energies at 298.15 K for important classes of species as a result of updated thermochemical values for *n*-pentane and subsequent shifts in equilibria for important reaction classes. Reprinted with permission from [157]. Copyright (2015) American Chemical Society.

Experimental observations of previously elusive oxygenated species [91,151–153] led to inclusion of new reaction pathways originating from some of these compounds such as the Korcek sub-mechanism [152]. Wang et al. [154] summarize recent progress in the detection of hydroperoxides and assess their roles in combustion, atmospheric oxidation of VOCs, and SOA formation.

Knowledge on the fuel-specific autoignition chemistry in the LT regime has developed hand-in-hand from experiment and theory [155,156]. To reveal fuel-specific aspects, analysis of fuel families with different molecular structures is highly valuable, as shown by Bugler et al. [157] in their study of the three pentane isomers; a scheme for *n*-pentane is given in Fig. 12.

RCM ignition experiments over a wide range of temperatures and pressures were combined with kinetic and thermochemical evaluations to establish an LT oxidation mechanism [157]. Although close to realistic fuels, the pentane molecules are small enough to ensure a good quantum-chemical foundation for relevant thermochemical and kinetic parameters. As shown in the bottom row of Fig. 12, the low-temperature reactions proceed through fuel-specific radicals involving several oxidation and isomerization steps [157]. Specifically, fuel radicals ( $\dot{R}$ ), alkylperoxy ( $\dot{R}O_2$ ), hydroperoxyalkyl ( $\dot{Q}OOH$ ), and hydroperoxyl

alkylperoxyl radicals ( $\dot{O}_2QOOH$ ), as well as other reaction intermediates have been considered here. Quite detailed information for each fuel structure is thus needed, adding significant complexity to the overall reaction mechanism for a reliable description of fuel-specific ignition and LTC behavior. The authors [157] performed a systematic screening of the kinetic and thermochemical data for the pertinent reaction classes that led to significant changes in the Gibbs energies and subsequent shifts in the associated equilibria (see Fig. 12). The significantly updated mechanism was capable to represent the experimental data for the three fuel isomers quite accurately in the large sampled parameter space [157]. Further investigations on *n*-pentane kinetics in JSR experiments have been reported [158–160], including results on the interaction of the fuel reactions with nitrogen oxides [158,159] and on the detection of  $H_2O_2$  and hydroperoxides that act as chain branching agents in the oxidation mechanism [160]. These investigations were experimentally highly challenging and relied on combinations of EI-MBMS, PI-MBMS, micro-GC, mid-IR Faraday rotation spectrometry, and cavity ring-down spectroscopy (CRDS) [158–160].

For different fuels including linear and branched alkanes, synchrotron-based studies [92,160–164] (see also Section 2.1) have revealed

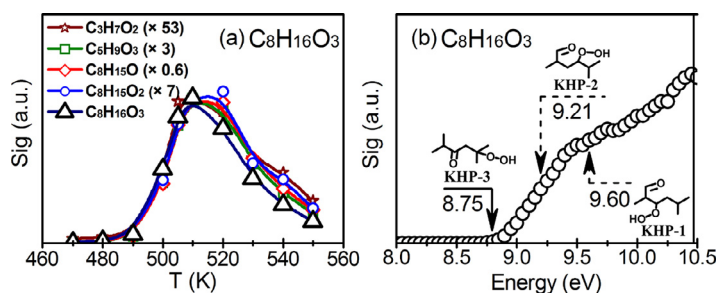


Fig. 13. (a) Temperature-dependent signal profiles of  $m/z=160.11$  ( $C_8H_{16}O_3$ ) and its potential fragments ( $C_8H_{15}O_2$ ,  $C_8H_{15}O$ ,  $C_5H_9O_3$ , and  $C_3H_7O_2$ ) from 2,5-dimethylhexane low-temperature oxidation in a JSR measured at a photon energy of 9.5 eV. The fragment signals are normalized by the  $C_8H_{16}O_3$  signal at 510 K (normalization ratios in parentheses). (b) Photoionization energy scan of  $C_8H_{16}O_3$  produced from 2,5-dimethylhexane LT oxidation at 505 K. The solid arrow indicates the calculated ionization energy threshold for KHP-3; the dashed arrows indicate the calculated IEs of the other two probable KHP isomers (see text and original publication for details). Reprinted from [162] with permission from Elsevier/The Combustion Institute.

numerous previously not detected reaction intermediates whose occurrence may shed further light on specific reaction pathways in the LT regime. Highly oxygenated intermediate species were found as a common motif in LT oxidation, presenting also a link between combustion reactions and atmospheric oxidation pathways [163]. Wang et al. [163] involved H/D exchange reactions and isotope labeling experiments using  $^{16}O_2$  and  $^{18}O_2$  as the oxidizer to assign certain intermediate structures and analyze specific reaction pathways. Fig. 13 shows signal intensity profiles from PI-MBMS experiments for  $C_8H_{16}O_3$  and some fragmentation products (a) determined in a JSR at 510 K and a photon energy of 9.5 eV in the oxidation of 2,5-dimethylhexane, and the associated PIE curve (b) [162].

The mass spectra at these conditions revealed intermediates with one to three oxygen atoms [162]. In agreement with general LT oxidation pathways, detected  $C_8$ -species were assigned to alkenes ( $C_8H_{16}$ ), cyclic ethers ( $C_8H_{16}O$ ), and ketohydroperoxides (KHPs,  $C_8H_{16}O_3$ ), respectively. The size and structure of the fuel molecule 2,5-dimethylhexane – representative of compounds in realistic fuels – leads to formation of intermediates of large structural diversity for whose detection and identification established and emerging synchrotron-based techniques may be uniquely suited. The formation of three different alkenes that have been quantitatively detected occurs *via* the primary, secondary, and tertiary fuel radicals, oxygen addition towards different ROO structures, and elimination of  $HO_2$ . Competing reactions lead to the respective QOOH intermediates, important in chain propagation and branching [162]; these can form cyclic ethers and OH radicals (compare also Fig. 12). Four of these  $C_8H_{16}O$ -species were assigned from their PIE curves and fragmentation patterns [162]. Second oxygen addition can then form OOQOOH radicals that can further isomerize

and form  $HOOQ'OOH$  structures ( $Q'=C_nH_{2n-1}$ ) that can decompose to KHPs and OH. The respective signal profile in Fig. 13(a) could correspond to three probable KHPs originating from the primary and secondary fuel radicals, whereas the tertiary-fuel-radical-derived OOQOOH has no available H-atom site for the KHP-forming reaction. The arrows in Fig. 13(b) indicate the calculated adiabatic ionization energies (IEs) for the three KHP structures; the experimentally observed onset is closest to KHP-3. Identical temperature dependences of fragment signal intensities in Fig. 13(a), consistent with KHP-3 scission *via* CO–OH (towards  $C_8H_{15}O_2$ ), C–OOH (providing  $C_8H_{15}O$ ),  $C_3H_7$ – $C_5H_9O_3$  ( $C_5H_9O_3$ ), and  $C_3H_7$ – $C_5H_9O_2$  ( $C_5H_9O_2$ ), underline the plausible assignment of KHP-3 [162].

The detection of a large number of fuel-specific highly oxygenated intermediates in the LT regime provokes discussion whether those are also significant under engine conditions. Wang et al. [164] successfully detected a large number of hydrocarbon and oxygenated intermediates in a JSR and in the exhaust of a motored HCCI-type research engine during LT oxidation of *n*-heptane. A similar composition was detected by VUV PI-MBMS in a synchrotron-based JSR and was also found by atmospheric pressure chemical ionization (APCI) Orbitrap mass spectrometry (OTMS) in another JSR and in the research engine exhaust [164]. The enormous wealth of compounds detected in the  $C_1$ – $C_7$  regime, including those resulting from up to three sequential oxygen additions, underlines the success of the discriminative MS techniques but also the enormous challenge regarding a complete assessment of the chemically reactive intermediate pool and the concurrent model development [164]. Nevertheless, qualitative species profiles and fuel-structure-dependent analogies in reaction pathways can be valuable even in the absence of in-depth information on different conformer

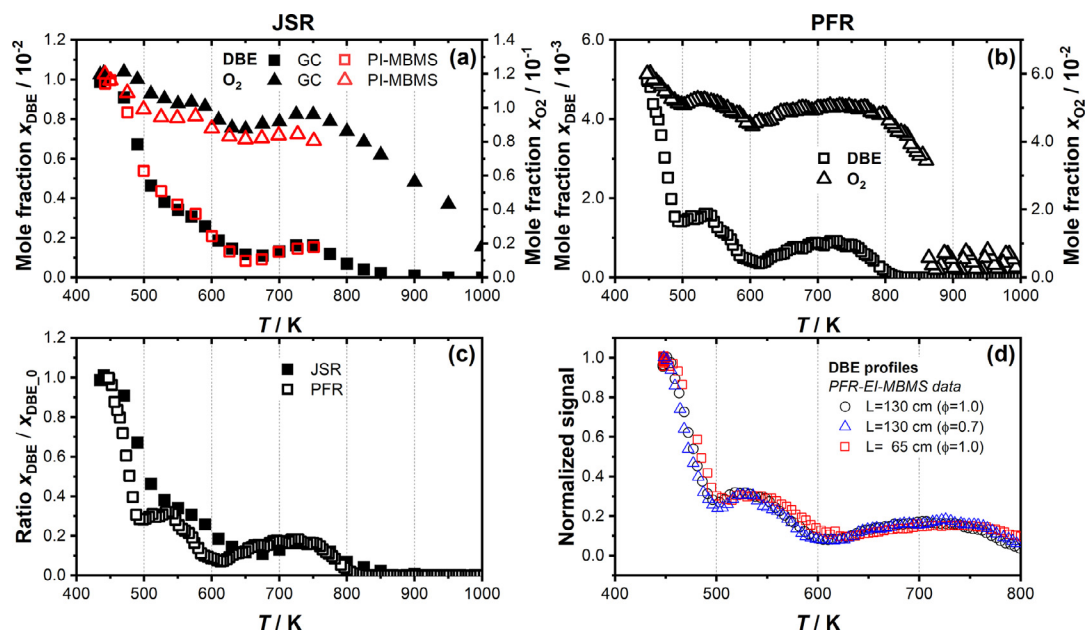


Fig. 14. Experimental mole fraction profiles of DBE and O<sub>2</sub>. (a) JSR ( $\Phi = 1.0$ , 1% DBE), (b) PFR ( $\Phi = 1.0$ , 0.5% DBE), (c) DBE profiles in JSR-GC and PFR-EI-MBMS experiments, (d) DBE profiles for different equivalence ratios  $\Phi$  and PFR lengths  $L$ . Profiles in (c) and (d) are normalized by the respective inlet DBE mole fractions. Reprinted from [171] with permission from Elsevier/The Combustion Institute.

contributions, respective IEs, and ionization cross sections.

Low-temperature oxidation has also been investigated for various oxygenated fuels [92,163,165–174]. Regarding the discussion on OMEs and their potential as clean alternative fuels, the LTC of ethers has received particular attention, including DME (as OME<sub>0</sub>) [92,166,167], diethyl ether (DEE) [168,169], and di-*n*-butyl ether (DBE) [170,171]; further studies have been devoted to e.g., dimethoxyethane [172] and aldehydes [173,174]. Recent work includes high-pressure investigations [175], *ab initio* kinetics studies [176], as well as quantitative measurements of key intermediates, in part with optical methods [160,177].

For many fuels, the LT oxidation features an NTC region that reflects the changing reactivity with temperature as a consequence of fuel-specific pathways, including oxygen addition and chain-branching reactions. Low-temperature chemistry can be even more complex with two NTC zones as recently observed for DEE and DBE [169–171]. The temperature-dependent fuel and oxygen consumption for DBE measured in two JSRs and a plug-flow reactor (PFR) is shown in Fig. 14 [171]. Good general agreement is seen between PI-MBMS-JSR, GC-JSR, and EI-MBMS-PFR results.

The double-NTC behavior was analyzed following the main reaction path starting from the

C<sub>4</sub>H<sub>9</sub>OC<sub>4</sub>H<sub>8</sub>-a radical, formed by H-abstraction from the fuel molecule at the C <sub>$\alpha$</sub> -position next to the ether function. Reactions start well below 500 K; here, C<sub>4</sub>H<sub>9</sub>OC<sub>4</sub>H<sub>8</sub>-a can react by two sequential O<sub>2</sub> additions that result through several steps in the production of *n*-C<sub>3</sub>H<sub>7</sub> and two OH radicals, thus enhancing the reactivity [171]. Both NTC zones are characterized by decreasing reactivity with temperature, and the overall behavior reflects delicate competitions between decomposition reactions of the formed intermediates to produce mainly stable products (as e.g., cyclic ethers) *versus* those reactions that can form chain carriers (as e.g., OH radicals) [171]. Similar analyses have been performed for the two NTC zones observed in LT DEE oxidation [169]. Beyond analyzing the reactivity, the combination of several diagnostic techniques and reactors has also permitted detection of a number of previously unobserved LT intermediates [171].

Many details of LT oxidation have been investigated in reactors under conditions with imposed temperature. A special flow reactor design has permitted to study periodic ignition phenomena and flame propagation, thus addressing the transition from "cool" to "hot" reaction regimes [178]. For practical systems, the question arises how LT chemistry influences the combustion behavior of realistic fuels [179] under conditions where coupling between chemical reactions, transport,

and heat release must be considered [180,181]. Ju et al. [181] have recently reviewed the importance of cool flame phenomena for ignition, flame extinction, and knock, and the possibility to study LT chemistry under flame conditions. Ozone addition has been demonstrated as being valuable [182–189], albeit not necessary [190], to enhance or control the reactivity in cool flames. Recent work includes premixed [191] and non-premixed [183,184,186,189,190], laminar and turbulent regimes [192] as well as engine combustion systems [185].

Numerous investigations have shown the LT oxidation chemistry of realistic fuels to be highly complex, with continuing detection of additional species and reaction pathways, but also with challenges regarding the unambiguous identification of such intermediates. Not only kinetics matters in this regime, but also flame dynamics, concerning ignition, potential oscillations, and extinction, necessitating measures to ensure stabilization and control. The interplay of fuel composition and molecular structures of its components, temperature, pressure, mixture conditions, flow field, and potentially, EGR rates will influence the balance between timescales of chemistry and turbulent mixing under engine conditions, with consequences for stable operation, efficiency, and emissions. Regarding the large chemical diversity of present and alternative fuels and the need for reliable prediction of their ignition and combustion behavior, it is unfeasible to perform similarly detailed experiments as exemplarily selected here for every newly discussed alternative fuel. Rather, the present knowledge about the reaction classes involved is being incorporated in systematically established models, using extensive chemical-kinetic mechanisms that can be applied beyond a single fuel and suitably reduced for practical applications. As will be discussed further in Section 2.4, such models, validated by well-selected examples, are expected to predict essential combustion characteristics under pertinent conditions.

### 2.3. From fuels to particles – soot precursor and soot formation

Because of the importance of soot particle formation for climate, environment, and health, the complex reaction chemistry from the fuel molecule to particle formation has motivated intense research over decades. Challenges are manifold in connecting (i) the decomposition reactions of fuel molecules with different structures towards differ-

ent intermediate species, (ii) the multitude of postulated routes contributing to PAH and carbon cluster formation, (iii) the process of particle inception based on this variety of precursor species and reactions, (iv) the influence of the particular combustion system conditions on particle nucleation and growth, (v) the oxidation and aging processes of the formed particles, and (vi) the effects of real emissions on radiative forcing, cloud formation, reactive processes in the environment, and health-related conditions. A comprehensive mechanism that would provide physico-chemically founded predictions of fuel–combustion-system–particle-property relationships could serve as a basis for realistic estimates of such environmental, climate- and health-related effects. A significant *desideratum* is the experimental confirmation of each part of such mechanisms, which is particularly difficult in the transition range from higher-molecular-weight precursors and PAH structures to the first particles.

Recent reviews summarize important aspects of the particle-forming reaction sequences as well as methods to analyze the soot formation process [51,84,85,193–195]. Further work has described the physico-chemical characterization of particle emissions from engines [130,196,197] and of flame-sampled, aircraft-type soot with potential impact on cloud formation [198]. The importance of processes leading to carbon nanostructures in other domains, especially in material science and astrochemistry, contributes to the interest in the overall carbon growth chemistry. Johansson et al. [199] have recently highlighted the importance of resonance-stabilized radical chain reactions in the formation of carbonaceous particles in combustion and interstellar dust, and Zhao et al. [200] have provided indications for a gas-phase synthesis pathway to large PAH structures, for the example of [4]-helicene, that could be active in combustion and interstellar media.

Chemical-kinetic models, often based on systematic analyses of earlier work, have profited from the interplay of experiment and theory. For selected  $C_1$  and  $C_2$  fuels, specific aspects of the growth process were inspected concerning, e.g., the formation of benzene and PAHs in laminar flames of methane (as the main component of natural gas) [201], ethane [202], and ethene [202,203]. Model results were examined against available experimental data for these fuels, and decisive influences on the formation of small PAHs were noted regarding  $C_2$ – $C_4$  species, resonantly stabilized radicals such as propargyl ( $C_3H_3$ ), benzyl ( $C_7H_7$ ), and indenyl ( $C_9H_7$ ), and further aromatic radicals such as phenyl ( $C_6H_5$ ) and naphthyl ( $C_{10}H_7$ ) [201]. PAH-forming pathways for  $C_2$  fuels include the well-established hydrogen abstraction acetylene addition (HACA) mechanism [204], hydrogen atom migration, radical addition, and methyl substitution/acetylene addition reactions as well as those of



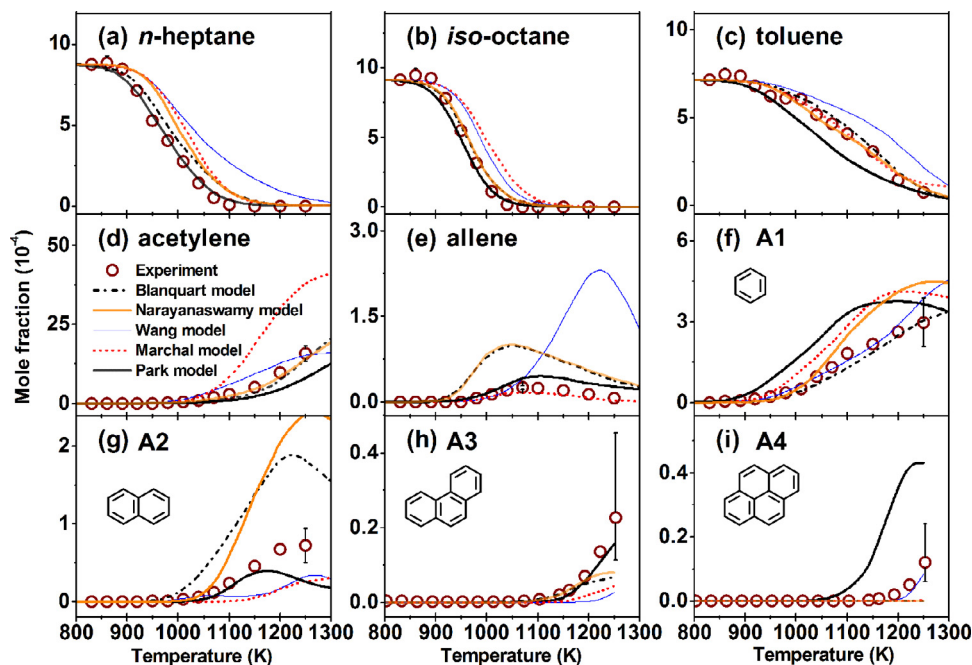


Fig. 15. Comparison between experimental and simulated mole fractions of toluene primary reference fuel (TPRF) components, acetylene, allene, and one to four ring aromatics in TPRF 70 pyrolysis. The experimental data for A3 and A4 were taken from flow reactor pyrolysis while the rest were from JSR pyrolysis. Reprinted from [215] with permission of Elsevier/The Combustion Institute.

the cyclopentadienyl ( $C_5H_5$ ) radical [202]. Small intermediates such as methyl have been considered as further growth species [205–208]. For larger PAHs, theoretical work has provided insight into the role of curvature and surface growth processes involving, e.g., HACA reactions and additions to specific sites such as graphene edges [209–212]. Gas-phase and soot-forming reactions have been linked to predict the particle distribution in ethene flames [213]. Also, soot oxidation has been considered, using a reduced model formalism because of the associated complexity [214].

While numerous previous investigations have concerned  $C_2$  fuels, Shao et al. [215] have recently provided an experimental and modeling study of the PAH formation in the pyrolysis of toluene primary reference fuels (TPRFs), composed of toluene, *n*-heptane, and iso-octane, to approach the properties of real gasoline fuels. Experiments with two different TPRF mixtures were performed in a JSR using GC analysis and a flow reactor coupled to synchrotron-based PI-MBMS, and several chemical-kinetic models were compared with the data. Mole fractions of the reactants, important stable  $C_1$ – $C_3$  intermediates, and small aromatics including benzene (A1) and naphthalene (A2) were determined by GC, whereas larger PAHs including phenanthrene (A3) and pyrene (A4) were determined by PI-MBMS. Illustrative results in Fig. 15

for the pyrolysis of a low-octane TPRF 70 mixture, *i.e.* with a research octane number (RON) of 70, show profiles of the three fuel components, of acetylene and allene as  $C_2$  and  $C_3$  species, and of A1–A4 as PAH structures with up to four aromatic rings [215].

The TPRF 70 fuel features similar amounts of the three constituents, providing a good test case for the simulations. The chosen mechanisms should represent the behavior of the mixture, but none can predict the decomposition of each of the three fuel components equally well. Differences are seen in the formation of acetylene, allene, benzene, and of the larger PAHs [215] where none of the models consistently predicts all species profiles. Model improvements were achieved by updating selected reactions and rate expressions in the PAH-forming sub-mechanisms concerning, e.g., reactions of toluene ( $C_6H_5CH_3$ ), indenyl ( $C_9H_7$ ), and methylindene ( $C_9H_7CH_3$ ), and important influence on benzene and PAH formation was seen for propargyl ( $C_3H_3$ ) and benzyl ( $C_7H_7$ ) radicals [215].

Results from this recent study suggest that further mechanistic information would be useful. The fuel combination, *i.e.* three  $C_7$ – $C_8$  components with linear, branched alkane, and aromatic structure, although of practical relevance, may be too challenging to inspect kinetic details regarding

reaction pathways, rate coefficients, and their dependence on temperature and pressure. Recent contributions have concentrated on specific mechanistic avenues such as the HACA route [216–219], on individual reactions, both from experiment [220–223] and theory [224,225], shedding further light on the formation of the first and second aromatic ring and beyond [217–219,226,227], and on competing oxidation reactions [224,228].

Renewed effort based on numerous studies for an extensive range of fuels has been devoted to establishing a hierarchically constructed model for the sequence from molecular precursors to particles, starting from a  $C_0$ – $C_3$  core mechanism [229]. The sectional soot mechanism, coupled to the PAH-formation sub-mechanism, considers 25 classes of lumped pseudo-species to describe the process from 20 to about  $10^8$  carbon atoms [230]. Experimental corroboration remains difficult, however. Regarding model simplifications and experimental uncertainties, e.g., in temperature and PAH concentrations, the authors plead for comprehensive mechanism validation using different flames, fuels, conditions, and data from different facilities [229].

In a different systematic approach, Das et al. [231] have analyzed the sooting tendencies for more than 400 straight-chain, ring, aliphatic, aromatic, and oxygenate fuels. From pyrometry experiments for key components of fuel structure families under well-defined non-premixed flame conditions, they provided a unified yield sooting index (YSI), integrating values from two previous, incompatible YSI scales. To identify fuel-structure–sooting-tendency relations, they constructed a model in which single-carbon parts ("fragments") of fuel molecules were assigned a linearly additive sooting tendency contribution. When necessary, the analysis was supported by quantum calculations. Contributions of these fragments were determined through a multivariate linear regression against the newly established unified YSI values for different compounds [231]. Rigorous inspection of test cases with different molecular functions was performed, even referring to organic chemistry databases with millions of compounds to screen for potentially missing types of carbon chemistry, and the authors [231] report their model to be applicable to predicting the sooting tendency of most hydrocarbons contained in practical fuels, without the inclusion of chemical-kinetic mechanism details. As one of the chemical functionalities not well covered by the present approach, oxygen heterocycles were identified [231]. Influences on PAH and soot formation of such heterocyclic compounds have been analyzed, e.g., for furanic fuels [232–234].

Such approaches as briefly addressed above are pursued in parallel and concern detailed kinetic mechanisms for the molecular precursor range towards small PAHs, strategies using kinetic infor-

mation and lumped species for PAH and particle growth, and systematic analyses of experimental observations to classify the contributions of certain molecular groups to soot formation. Recent progress is illustrated below from selected examples with a mainly experimental focus.

The fuel-specific pathways of  $C_5$  fuels leading to compounds with 3–4 aromatic rings were recently investigated with a combination of PI- and EI-MBMS, motivated by the role of  $C_5$  species in aromatics formation and by the apparent lack of detailed knowledge on the fuel-structure-dependent  $C_5$  chemistry [235–238]. Quantitative mole fraction profiles of  $C_5H_6$  for non-premixed flames of *n*-pentane, 1-pentene, and 2-methyl-2-butene (2M2B) are presented in Fig. 16 [236], together with PIE curves for the two latter fuels that show the highest  $C_5H_6$  concentrations. The PI- and EI-MBMS results from independent instruments are in excellent quantitative agreement. The isomer composition for both fuels analyzed under the same conditions is evident from the PIE curves in Fig. 16 and reveal  $C_5H_6$  to be mostly 1,3-cyclopentadiene in the 1-pentene flame whereas substantial contributions are also seen for 2-methyl-1-buten-3-yne in the 2M2B flame; 1-penten-3-yne and 3-penten-1-yne are of lesser importance in both cases [236].

Among others, the  $C_5$  species play a role in the formation of indene and naphthalene that were also seen to be more abundant in the 2M2B flames than in those of 1-pentene and *n*-pentane [236]. A closer analysis of the pathways leading to the dominant  $C_5H_6$  isomers reveals fuel structure dependences, including cyclization reactions from  $C_5H_7$  radicals and 1,3-pentadiene ( $C_5H_8$ ) in the 1-pentene case. In the 2M2B flame where 1,3-pentadiene was not detected, 1,3-cyclopentadiene can be formed from the reaction of acetylene with propene [236]. Detailed analyses of the intermediate species composition for the three fuels point towards considerable influence of the nature and concentration of early fuel-specific decomposition products on the PAH formation pathways [236]. Experimental results from premixed flames of these  $C_5$  fuels have contributed to further model development [235,238], with substantial improvements, e.g., for the prediction of several small PAHs [235]. As one aspect of these comparative, systematic studies, it should be kept in mind that fuel-specific, small hydrocarbon decomposition products can influence the amount and nature of PAH precursors and their contributions to PAH-forming reactions. The capability of  $C_0$ – $C_8$  models to represent the fuel decomposition reactions in relevant detail can thus be considered of importance, if not a prerequisite, for the accurate description of PAH formation.

Beyond the formation of small PAHs, recent work has been devoted to systematically analyze the prevalence of higher-mass compounds and soot in flames of different structure by combining *ex-*

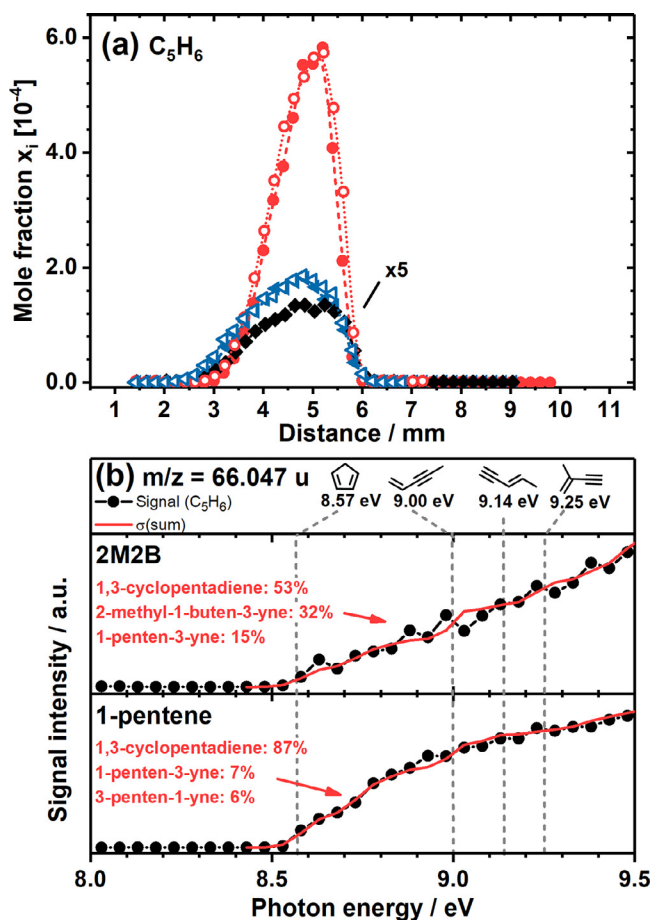


Fig. 16. (a) Experimental mole fraction profiles of C<sub>5</sub>H<sub>6</sub> in laminar non-premixed flames of 2-methyl-2-butene (circles), 1-pentene (triangles), and *n*-pentane (diamonds). Open symbols: PI-MBMS, closed symbols: EI-MBMS. The experimental data are fitted by dotted lines (B-spline) for better visualization. (b) Flame-sampled PIE curve of  $m/z=66.047$  u (C<sub>5</sub>H<sub>8</sub>). Closed symbols (connected to guide the eyes) represent the measured signal, and the obtained sum signal is shown as solid line. Reproduced from [236] with permission from the PCCP Owner Societies.

*situ* secondary ion mass spectrometry (SIMS) and LII, using data mining and multivariate analyses to classify the observations and extract characteristic features from numerous samples such as e.g., the existence of species of certain mass ranges and/or particles in different flame regions [239]. Experimental techniques to analyze PAHs of different structures and sizes include detection of high-molecular-weight soot precursors by means of an aerosol mass spectrometer and photoionization with synchrotron-generated VUV radiation [240], laser desorption/laser ionization/TOF-MS to detect PAHs adsorbed on soot particles [241], jet-cooled LIF with the capacity of isomer discrimination [242], and the detection of aromatic excimers by visible broadband LIF [243]. These and other studies have, piece-by-piece, provided informative contributions towards assem-

bling a more consistent picture of the formation of condensed-phase particles from gas-phase building blocks.

The particular reaction conditions in terms of molecular fuel structure, temperature, pressure, and other variables affect the internal nanostructure, chemical composition, mobility, and reactivity of soot particles [244–249], which may be different in technical devices from laboratory reactors and flames. Attempts to link between PAHs, high-molecular-weight carbon structures, and initial particles has motivated theoretical work [199,250] as well as experimental approaches including *in-situ* LII [251–253], probe-sampling tandem mass spectrometry (MS-MS) [254], and *ex-situ* microscopy [207,252,255–258] to image carbon structures and particles while considering also probe sampling effects [259].

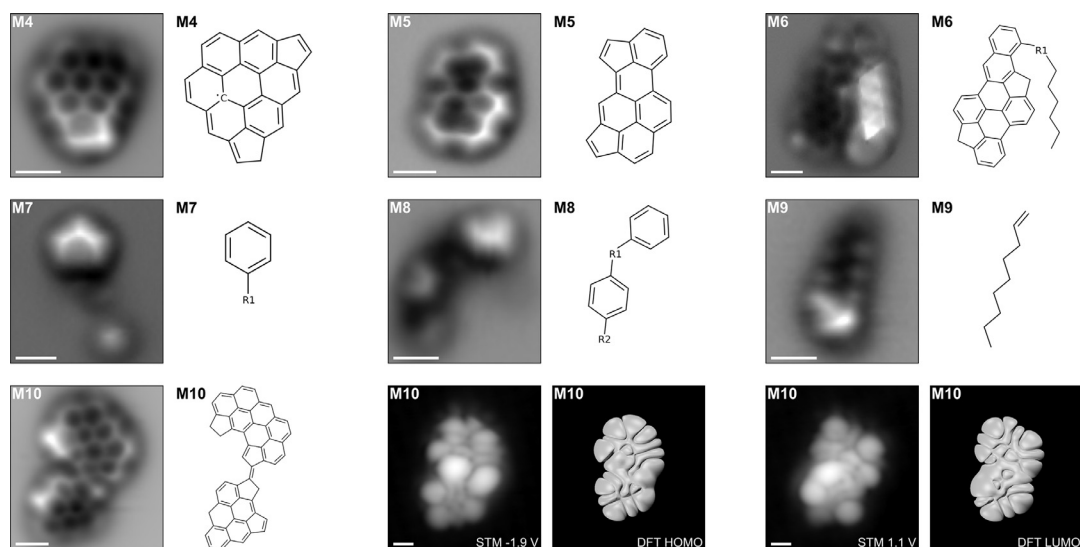


Fig. 17. AFM images and chemical structure of some representative molecules, as well as molecular orbital densities measured by scanning tunneling microscopy (STM) for **M10** and corresponding density functional theory (DFT) simulations. "R" labels denote unidentified parts of the molecules. Scale bars are 0.5 nm. Reprinted from [256] with permission from Elsevier/The Combustion Institute.

Particularly exciting results revealing aspects of the PAH-to-soot growth process are provided in Fig. 17 that shows images from high-resolution atomic force microscopy (AFM) of carbon structures found in soot sampled near the nucleation zone of a slightly sooting premixed ethene/air flame [256]. The sampling process was conducted at low temperature and high dilution to prevent PAH condensation from the gas phase.

The depicted molecules, imaged at 5 K and  $10^{-10}$  mbar with a CO-functionalized tip after a rapid sublimation procedure from the collected soot samples, are considered as building blocks in the nucleation process. They feature 6- and 5-membered rings, aliphatic side chains, and cross-linked aromatic structures, underlining the diversity of building blocks that may contribute to particle nucleation [256].

Soot sampled in a premixed ethene/air flame served to follow the aromatic growth process by means of a fringe analysis using high-resolution transmission electron microscopy (HRTEM) as shown in Fig. 18 [258]. The size distribution of aromatic structures in terms of carbon density *versus* number of aromatic rings was determined with a mathematical morphological analysis to extract the fringe length (with fringes assumed as parallelogram shapes) and further geometrical parameters of soot nanostructures. The soot samples were collected at different heights above the burner (HAB) reflecting the growth status. Similar data for comparison is also available from benzene flames [258].

With increasing height, the distribution is shifted towards larger aromatic structures, evident in the cumulative analysis in the insert in Fig. 18. The growth process was found to be particularly sensitive to specific structural changes, including an observed decrease of the percentage of nearly straight fragments *versus* an increase of that of fringes with high tortuosity, suggesting that structural order is established in more mature soot from longer, more planar layers [258]. This evaluation can contribute valuable hints on the growth process. Unlike the AFM results [256,257], however, it does not provide structural information. Also, it should not be assumed that growth favors only condensed aromatics, as evident from the aliphatically linked structures detected in recent MS-MS experiments [254]. The combination of many such details from complementary techniques with their specific advantages and disadvantages contributes to a more detailed, yet still incomplete picture of the complex molecules-to-particles growth process.

Remaining aspects under debate concern particularly the nucleation phase. Recent experiments target this phase from both directions: advances in diagnostics provide intriguing evidence for pathways from molecules to large carbon structures while they also shift the limits to detection of ever-smaller-size

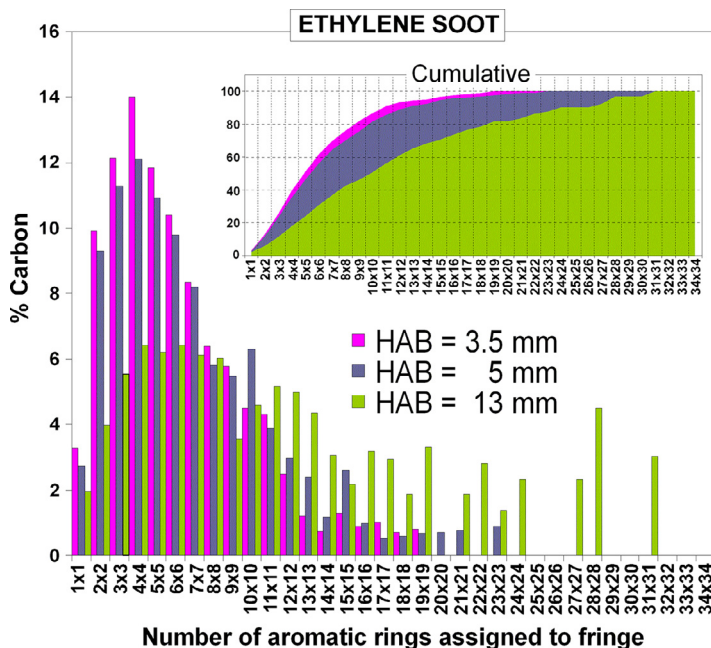


Fig. 18. Carbon number density vs. number of aromatic rings assigned to each fringe assuming a parallelogram catenation for the ethylene soot at various heights above the burner (HAB). Reprinted from [258] with permission from Elsevier/The Combustion Institute.

particles. From the lower-molecular precursor end, it has been noted how sensitively the formed large variety of aromatic compounds depends on the chosen fuel and reaction conditions. Fundamental studies, often for  $C_2$  fuels, have analyzed the respective precursor species pool and their reactions. At the particle end, dependences of the chemical functionalities, internal structure, as well as the physical and chemical properties of the formed particles on the inception process are being investigated. Much of the experimental results have been gained with sampling and *ex-situ* processes, which remains a certain impediment in chemically reactive atmospheres. Theoretical work in combination with such recent experimental results has supported the conception of systematic models that target the entire growth chain. Reliable modeling for practical situations such as predicting aero-engine emissions, with realistic multi-component fuels and complex boundary conditions including high pressure and turbulent flow fields, however, will not feasibly include all elementary steps from the fuel molecule *via* all conceivable carbon structures to soot. Influences of aromatic components in such fuels may also need further attention [260]. Properties of combustion-formed

particles are important in many different contexts and impact, e.g., heat transfer in combustors, albedo and optical properties in relation to climate development, formation of aerosols and particulate matter including UFPs and their reactivity in the environment and the human body, design of carbon-based materials, and understanding of astrochemical phenomena. Prediction of such properties is at the same time a valuable target and an utmost challenge. It may be an option to include phenomenological approaches and to look at a fuller picture along the buildup chain by extracting useful correlations, potentially using data mining procedures, from the multitude of individual investigations devoted to limited aspects of the process.

#### 2.4. Towards reliable prediction – combustion chemistry models

Combustion models should provide a realistic representation of a given system, including all relevant processes. With a valid combustion model, a simulation of a given operating condition should be possible. Moreover, it is desirable to predict the combustion behavior, including required resources,

efficiency, emissions, safety hazards, and other important parameters for conditions beyond those that have been explored in detail experimentally (see also Section 2.1). Combustion chemistry models comprise particularly thermodynamic, kinetic, and molecular transport properties and aim to describe fuel ignition and decomposition, the actual combustion reactions, heat release, and product as well as pollutant formation under relevant conditions. Such chemical-kinetic models must then be integrated in a feasible way into more complete combustion models that describe the characteristic aspects of the process; these may include fuel preparation and delivery, associated phase changes, particle, spray, or droplet formation, mixture preparation, fluid dynamics and its interaction with the chemical processes, heat and exhaust management, and other parameters of interest. Regarding the complexity of the associated systems and processes, reductions are often necessary. It is therefore useful to first examine chemical models critically under somewhat idealized conditions that are sensitive to the chemical changes in question but decoupled from other complex influences of the respective technical combustion system, before they are reduced and incorporated into global process models for system design and optimization.

Detailed combustion chemistry models have been developed concurrently with experiments in dedicated laboratory reactors and flames (see also examples in previous sections). Although a plethora of chemical models have been published and subsequently modified by stepwise inclusion of some additional reactions or changes in specific reaction coefficients, it should be recognized that systematic combustion chemistry modeling requires specific expertise. The critical comparison of model predictions to experiments under different relevant conditions is crucial for model validation and development. Validation, however, does not mean that a single experimental study can approve or verify a model. Such a study merely tests the feasibility of the model and its underlying assumptions under the particular conditions. Also, it is unfeasible to expect an experimental study to be valuable only if just any available model accompanies it. Significant effort has been devoted to systematic combustion chemistry model development, and only selected aspects can be highlighted here.

Several seminal reviews provide an excellent summary of recent combustion chemistry modeling efforts [261–268]. They discuss kinetic mechanism development from fundamental physico-chemical principles [261,262,268] and the contributions of theoretical chemistry for this purpose [263,268]. Targets range from hydrogen [264] over realistic transportation fuels [265] to pollutant formation from combustion systems [267–269]. Some overview articles that report model development aspects have been already briefly mentioned

in the context of low-temperature chemistry [149,150,154] and soot formation [193,214]. The basis for many mechanisms for larger hydrocarbons are extensively validated C<sub>0</sub>–C<sub>4</sub> core models, for which thermochemical and kinetic data are mostly well established or estimated [261]. Unified or comprehensive, detailed kinetic models have been developed for different fuel families [270–276], including, e.g., normal and branched alkanes [270,272,273] and esters in biodiesel [274–276]. Systematic approaches have also recently been reported for multi-component fuels [277–279].

Reliable experimental data from a wide range of well-defined conditions must be available for model validation, and this is indeed one of the major concerns for model development [261]. Section 2.1 has presented experimental methods to obtain chemical information from combustion processes, although not with an immediate focus on their reliability for model validation. Excellent data quality with good uncertainty quantification is desirable for this purpose. Some systematic influences on data quality should thus not be overlooked. Although they are invasive, in contrast to laser techniques, probe-sampling methods, especially synchrotron-based mass spectrometry, have become indispensable for measuring extensive sets of chemical species profiles of particular value for model development [86–89]; such methods have been coupled with flames, JSRs, and other reactors including miniaturized shock tubes [88,89,92,99–101,154,163,164,280].

Because of their widespread use for (full) speciation measurements, it is necessary to keep in mind that probe perturbations can significantly affect temperature and species profiles [281–287]. Sampling techniques may influence the detection of important combustion intermediates such as the OH radical [286], and they might contribute to the formation of low-temperature intermediates *via* cooling effects [287]. As clearly demonstrated by Hansen et al. [281,282], probe perturbations in flat laminar premixed flames are typically not one-dimensional. However, such deviations from one-dimensionality are typically not considered in modeling approaches for validation, and perfect agreement of experiment and model can thus not be expected [282]. As a superior strategy, the specific probe-sampling conditions could be included in two-dimensional model predictions. Furthermore, experimental data for the same conditions from different techniques and/or instruments can provide a more realistic assessment of the uncertainty for interpreting model–experiment comparisons [101,102,236,283,288]. Examples have been given in Fig. 7 [102] and Fig. 16 [236] showing PI-MBMS and EI-MBMS measurements from two independent set-ups. Struckmeier et al. [283] have discussed typical uncertainties of MBMS *versus* CRDS experiments and the consequences for model vali-

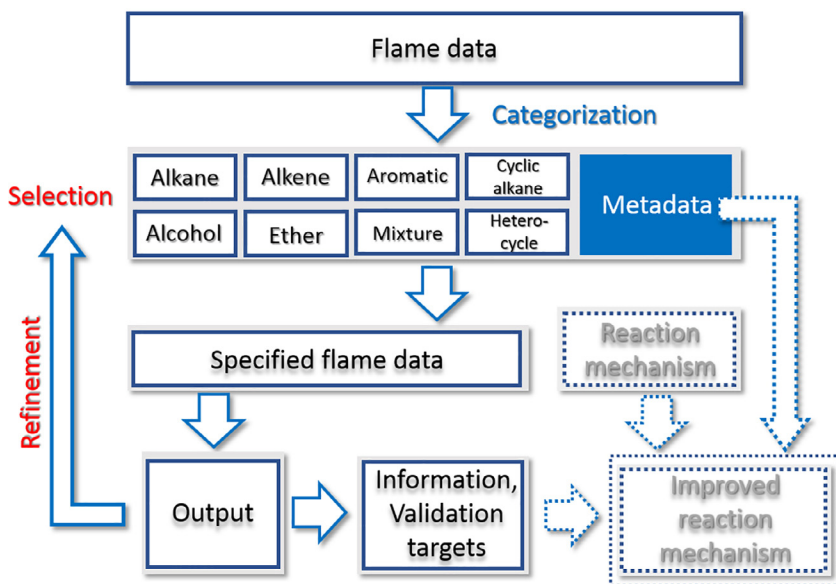


Fig. 19. Conceptual hierarchical data structure and work flow (see text for details). Dotted lines symbolize conceivable expansion of the concept. Reprinted from [294] with permission from Elsevier/The Combustion Institute.

dition for the example of  $\text{CH}_3$  and  $\text{CH}_2\text{O}$  profiles. Hansen et al. [288] have compared  $\text{CH}_2\text{O}$  and  $\text{CH}_3\text{CHO}$  profiles using EI-MBMS and Fourier transform microwave spectroscopy in DME and ethene flames. A round-robin comparison of  $\text{C}_2\text{H}_2$  profiles involving several synchrotron-based instruments [101] has demonstrated the range of uncertainty in the quantitative interpretation of probe-sampling MBMS measurements caused by different cross section values in the literature, again underlining the value of cross-comparison between different techniques. High-level theoretical calculations to provide ionization energies and cross sections may favorably support speciation measurements [289,290]. Complementary experimental techniques are highly valuable for quantitative species analysis and validation purposes, and combinations of sampling with non-invasive laser techniques may be particularly useful [177,291,292].

Although perturbations seem to place probe-sampling experiments at a certain disadvantage, they can provide excellent chemical insight and guidance for model validation by species identification [153,163,164], by comparisons of trends between fuels of different structures under identical conditions [161,236,293], by considering signal-intensity or mole-fraction ratios [208,236], and by the analysis of correlations in combustion experiments [294]. The approach presented by Hansen et al. [294] makes use of a large number of combustion experiments for model validation rather than of individual "one-by-one" experiment-model comparisons, with the general procedure explained

in Fig. 19 [294]. The authors aim to interpret apparently correlated information on peak mole fractions of certain intermediate species across an ensemble of 55 flames of different fuels and stoichiometries ("Flame data") as indications for specific reaction pathways. The categorization of flame data according to chemical details of the fuel enters the "Metadata", and a subset ("Specified flame data") can be analyzed regarding correlation plots ("Output") for two selected species, possibly using several iterations ("Refinement") [294]. Their paper gives examples for such (linear) correlations observed across different flames, e.g. for toluene/benzene, benzene/fulvene, allene/propyne, or diacetylene/vinylacetylene. Such correlations can be used as additional model validation targets and to identify potential inconsistencies or chemically interesting cases. Broader databases and automated analysis are suggested as further perspectives [294].

Beyond the base chemistry in core models, a wide range of validation experiments and a focus on determination and analysis of respective kinetic details have greatly supported the development of systematically constructed comprehensive reaction mechanisms for individual, technically relevant fuels and fuel components, including isooctane [295,296], *n*-heptane [297,298], further normal alkanes [299], aromatic compounds [300,301], and primary reference fuels (PRFs) or surrogate mixtures [118,302]. While core mechanisms for  $\text{C}_1$ – $\text{C}_2$  hydrocarbon and oxygenated fuels are systematically updated [303], comprehensive mechanisms

for certain oxygenates are increasingly becoming available including alcohols in general [16] and specifically, butanols [304], pentanols [305,306], and *n*-octanol [307], the latter as one of the linear C<sub>8</sub> compounds that are discussed favorably as sustainable, low-emission diesel-type fuel from biomass [308–310]. As targets for modeling efforts, further oxygenated fuels receive attention, including, e.g., C<sub>4</sub>–C<sub>8</sub> ethers [168–171,311], ketones [312], furanics [313,314], small esters [315,316], and other compounds such as dimethyl carbonate [317]. Regarding the practical relevance of fuel blends including hydrocarbon and oxygenated compounds, interactive effects in the reaction chemistry of such mixtures are being studied [318–321]. Also, nitrogen-containing fuel molecules have been targeted for kinetic investigations [322–324], because of potential pathways to make such fuels from biomass and the renewed interest in hydrogen-rich fuel molecules such as ammonia for energy conversion and storage (see also Section 1.3). Similar concerns as above regarding data quality should apply to such detailed investigations of particular fuels.

With the extension of the fuel spectrum, additional functional groups and a large variety of molecular fuel structures require systematic approaches to develop chemical mechanisms that can embrace combinations of petroleum-derived and non-fossil alternative fuels [325]. Consolidated, detailed mechanisms tend to encompass thousands of reactions and are typically too large to be embedded into CFD calculations for given applications. Reliable reduction of systematically constructed, detailed, well-validated mechanisms is possible by lumping of chemical isomers and elimination of unimportant species and reactions [325–328]. Indeed, sensitivity analyses in large mechanisms often show that only few reaction types dominate the overall conversion of reactants to products [329]. Introducing concepts of reaction classes and rate rules has thus supported the development of chemically consistent mechanisms for large and complex reaction networks [329,330]. For example, such reaction classes include, among others, H-abstraction and  $\beta$ -scission reactions as well as radical addition, recombination, and isomerization reactions. Given the availability of computational resources, theoretical calculations become increasingly feasible as a means by which rate coefficients for smaller members of a given reaction class can be assigned, enabling also reasonable approximations for larger representatives [329]. Such methods complement earlier approaches, e.g., using statistical methods to identify contributions to the reaction behavior by the presence of particular structural groups [331]. Also, systematic merging of a parent mechanism and problem-specific, modular sub-mechanisms in terms of a fuel component library framework can approximate the reaction behavior of multi-component real fuels [332].

Systematically identified reaction classes and rate rules may form the basis for automatic mechanism generation [333–335] with the advantage of internal consistency in rate constant assignment [329]. Several prerequisites must be considered in automated mechanism construction, *i.e.*, species must be unambiguously represented, reactions between species described, kinetic and thermodynamic parameters determined, and boundaries set for in- or exclusion of species and reactions [334–336]. The functional-group-based reaction mechanism generator (RMG) approach [333,334] defines reaction families by templates and uses chemical graph theory to represent molecules and substructures. A recipe for a reaction class is depicted in Fig. 20 [334], here for the case of the H-abstraction family.

A reaction template with the reactive sites represents the respective reaction family, and the corresponding reaction recipe shows how bonds are broken and formed during the reaction. To each reaction family, a hierarchical set of estimation rules is provided, acknowledging that reactions between similar sites will have similar rates [334]. In the example of Fig. 20, a radical species Y abstracts an H-atom from a molecule XH. Representatives for XH could be, e.g., saturated or unsaturated, branched or non-branched hydrocarbons of different chain length, and Y could be various kinds of small radicals [334]. Thermodynamic and kinetic parameters are then determined for such families using appropriate rules. From this information, the RMG software can generate a core mechanism for the specified reactants and reaction conditions that is then expanded iteratively by sequentially including further species that can be involved in reactions with those in the core mechanism [334]. Rather than taking the necessary parameter values from libraries, thermochemical values for each species can be calculated with high quality from theory, starting with reference geometries and stepwise improvements by geometry optimization [337]. This predictive automated computational thermochemistry (PACT) approach was applied for *n*-butane as a reasonably sized fuel molecule using approximately 10<sup>5</sup> CPU hours, and it might be expanded towards mechanisms for larger alkanes with 2–3 orders of magnitude larger computational time [337]. Similarly, thermochemical data for combustion species are made available in the Active Thermochemical Tables (ATcT) project [338].

With larger target fuel molecules, the consumption of memory space associated with growing numbers of species may become a challenge, because the automatic mechanism generation sequence considers numerous potentially unimportant species; a problem that can be counteracted by dynamic pruning algorithms [339]. Accurate rate expressions that are essential for a reliable performance of chemical-kinetic mechanisms are often scarce, and targeted experiments are highly



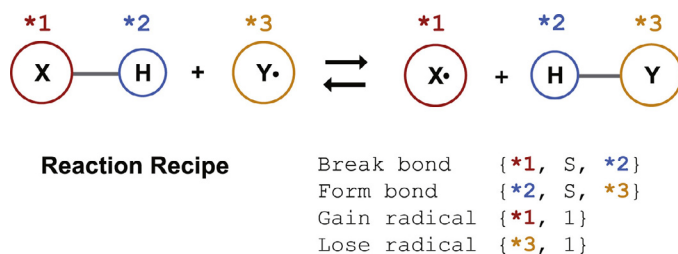


Fig. 20. Reaction template and recipe for the H-abstraction family. Reprinted from [334] available under Creative Commons Attribution License (CC BY).

valuable. Furthermore, efficient on-the-fly *ab initio* calculations are becoming available for automatic mechanism generation [340]. Powerful automatic methods must thus balance consistency of mechanisms, effectiveness of calculation, and incorporation of fundamental kinetic advances, e.g., regarding prediction of pressure-dependent reaction kinetics [341,342].

Mechanism development can also become difficult regarding abundant structural diversity, as, e.g., in low-temperature oxidation of larger alkanes [343]. On the one hand, lumping all structurally similar isomers can lead to oversimplification while on the other, including all isomers generates very large mechanisms that may become impractical regarding computational and memory resources [343]. For example, internal H-atom abstraction produces 18 QOOH isomers (see also Section 2.2) for *n*-heptane, and 60 QOOH isomers for *n*-hexadecane [343]. To reduce the number of species for subsequent reactions, structural isomers were assigned to different lumped groups, e.g., by similar geometrical features or functional groups at primary or secondary sites [343]. From consistent, detailed mechanisms, using predictive chemical kinetics approaches [344] and systematic reduction and optimization procedures [345–348], kinetic schemes may be derived for fuel design and engine applications [349–352], considering also uncertainties of the involved kinetics expressions [348,353–355].

Especially for larger fuels, experimental data remain scarce, making validation and further model development difficult. In such cases, automated optimization procedures [330], using rate rules for shorter fuels of similar chemical structure, may be used for calibration and assist model development for larger ones [348]. A result from a mechanism optimization procedure for *n*-alkanes is shown in Fig. 21 [348]. First, a training of the rate rules was performed using extensive experimental data for  $C_7$ – $C_{11}$  *n*-alkanes, and the optimized rate rules were used to derive a mechanism for *n*-dodecane that could be examined against previous experimental and modeling results [348]. Using a Bayesian approach, existing information on model param-

eters was represented in terms of probability density functions (PDFs) of random variables [348]. Fig. 21 depicts 2D joint prior PDFs (in logarithmic form) for the non-optimized model for ignition delay times  $\tau_{ig}$  in several *n*-heptane ("Hep") and *n*-decane ("Dec") calibration cases; the plots show correlations in terms of kernel density estimation (KDE) plots.

Since significant deviations were found between the non-optimized mechanism and the experimental data, specifically regarding an under-prediction of the first-stage ignition, these plots served to analyze the underlying kinetic behavior in more detail [348]. In each panel in Fig. 21, the width of the area indicates to which extent a change in one rate parameter will influence other parameters. While a wide distribution, corresponding to a weak correlation, is seen in Fig. 21a between *n*-heptane first-stage and total ignition delay times,  $\tau_{ig}(Hep_{F,LP})$  and  $\tau_{ig}(Hep_{LT,HP})$ , respectively, much stronger correlations are seen for the other three cases. The weak correlation in Fig. 21a might suggest that the first-stage ignition delay time could potentially be increased within its uncertainty levels without changing  $\tau_{ig}(Hep_{LT,HP})$ ; this is not observed after optimization, however, because of the strong interdependences at intermediate temperatures and changing pressures with a significant influence of LT oxidation chemistry (Fig. 21b,c). Correlations between *n*-heptane and *n*-decane cases reflect the use of common rate rules (Fig. 21d) [348].

Although such procedures may seem somewhat involved, systematic analyses using mathematical routines appear highly preferable over manual case-by-case tuning, especially in chemically complex systems. Much recent work has been devoted to systematic uncertainty assessment in combustion kinetics [353–362] with the aim to improve confidence in chemical models with thousands of reactions and associated rate parameters [353,354]. In such conditions, especially when using rate rules for reaction classes, the uncertainty of a given rate coefficient could be a factor of ten or more [353]. Since individual assessment of the uncertainty of each rate parameter becomes unfeasible in such multi-parameter systems, a useful consideration is to con-

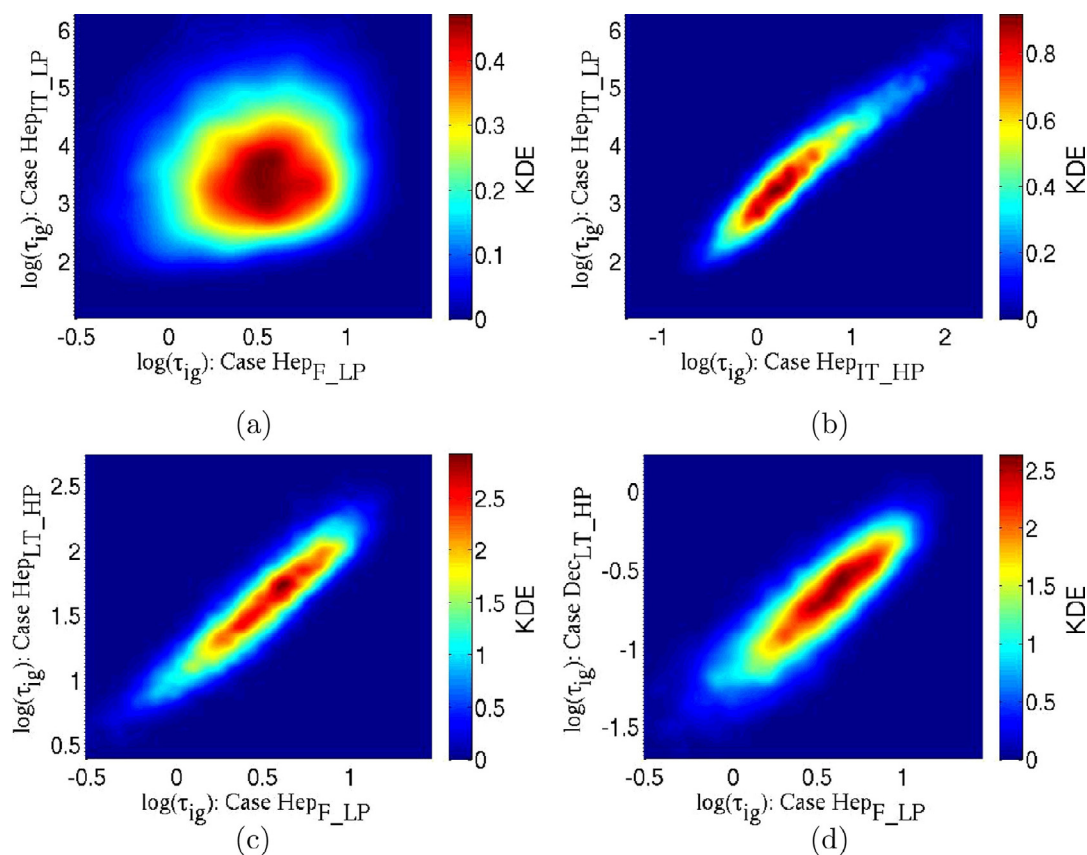


Fig. 21. 2D prior joint PDFs of prediction targets. The log values of these prediction targets are presented. For details, see the original paper. Reprinted from [348] with permission from Elsevier/The Combustion Institute.

strain the parameter set to available results from measurements or theory [353–355]. Experimental data may thus not only be useful *per se*, or serve for a model–data comparison, but are also, in an inverse problem approach, constraining values for a model, thus reducing the uncertainty distribution that reflects the joint uncertainties of individual parameters propagated through the model. Recent reviews of uncertainty quantification and minimization strategies [353–355], as well as dedicated articles on specific aspects [356–359] are available for further information. Such procedures have been applied to a number of examples, including hydrogen [360],  $\text{H}_2/\text{CO}$  [361], methane [361], formaldehyde [361,362], methanol [361,362], DME [363], ethene [361], and ketene [364] mechanisms.

An optimization example for methanol/air flames is given in Fig. 22 [362]. Experimental data for laminar burning velocities from several configurations are shown together with modeling results of an initial mechanism, further kinetic models available in the literature, and an optimized mechanism resulting from optimization of numerous rate parameters of important elementary

reactions identified by a local sensitivity analysis [362]. In total 24,900 data points for a wide range of operating conditions were considered, narrowing the posterior uncertainty limits considerably *versus* the prior ones [362]. As one target, the temperature-dependent branching ratio of the  $\text{CH}_3\text{OH}+\text{OH}$  reaction towards either  $\text{CH}_2\text{OH}$  or  $\text{CH}_3\text{O}$  was analyzed because of reported discrepancies. At each temperature, the grey shading in Fig. 22 represents the PDF of the branching ratios that were calculated from the posterior covariance matrix as a measure for the joint uncertainty of the optimized rate parameters [362]. The optimized mechanism provides a good compromise between the experimental results, with a simulation uncertainty on the order of the experimental scatter, based on optimized, consistent rate parameters for the most sensitive reactions [362].

Further recent work concerns, e.g., increasing computational speed for global sensitivity and uncertainty analyses by using artificial neural networks [365,366] or other schemes that may accelerate computation [367]. Also, uncertainty minimization strategies can be employed to guide ex-

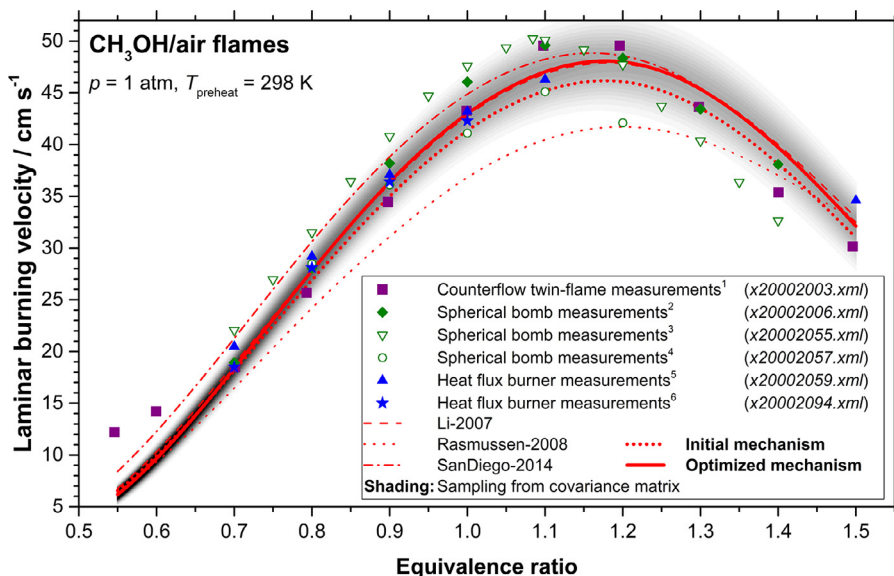


Fig. 22. Simulation results vs. experimental data for methanol/air flames at  $T=298 \text{ K}$  and  $p=1 \text{ atm}$ ; comparison of the optimized and initial mechanisms against several published mechanisms and experimental data. At each temperature, the gray shading represents the PDF of the branching ratios calculated from the posterior covariance matrix. Experimental uncertainties and further details are given in the original paper. Reprinted from [362] with permission from Elsevier/The Combustion Institute.

periment design [368]. When large training sets are used for model optimization, a consistency analysis may be useful to detect outliers [353]. The agreement between various experiments and models can be tested using a curve matching procedure [369] that identifies differences in values, in curve shapes, and shifts between curves. The example in Fig. 23 shows a comparison of experiments that have determined laminar flame speeds in *n*-heptane/air mixtures [369]. Four dissimilarity measures are calculated in the procedure for a group of  $N$  datasets of similar nature (approximated by continuous functions) represented by  $M$  models. All dissimilarity measures have zero as their minimal value; the quantity  $d_{L2}^0(\text{orig})$  in Fig. 23 is the original (before alignment) L2 norm of the difference between the functions, and the boxplot describes the position and dispersion of a dataset [369].

From the representation of  $N=20$  experiments simulated by  $M=8$  models in Fig. 23, significantly different performance is evident, with the experimental datasets 23 and 29 not as well described by the models, because either all models are not well suited for the particular experimental conditions, or the experimental data are systematically in error [369]. As a consequence, these data can be further inspected critically and potentially excluded from further analysis, or the critical conditions of such experiments can guide further model development. The combined analysis from different kinds of validation experiments including shock tubes, reactors, RCMs, and flames against different mechanisms

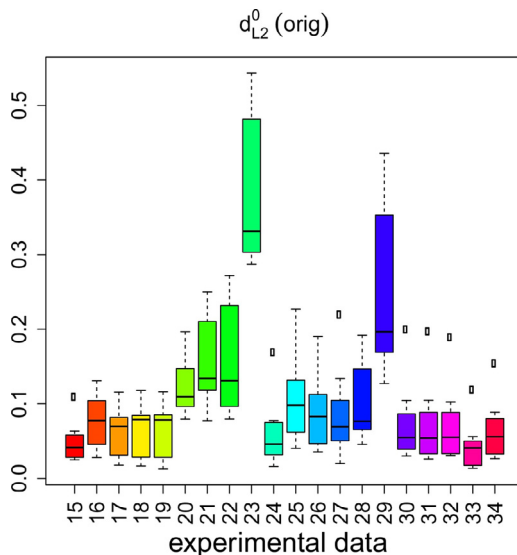


Fig. 23. Boxplot for  $d_{L2}^0(\text{orig})$  for a group of experiments “Laminar Flame Speed” for *n*-heptane/air mixtures. Reprinted from [369] with permission from Elsevier/The Combustion Institute.

can thus assist to constrain the useful database for further comparison and identify conditions which need further inspection in both experiment and model.

Chemical combustion models have experienced huge developments, targeting more advanced problems, practical fuels, and extreme conditions. They serve a dual purpose of providing fundamental understanding of a reacting system and of designing and optimizing processes and devices for practical applications. For the former, reactions should be represented in appropriate detail on the molecular level, and for the latter, desired qualities include ease of implementation, computational speed, robustness, and reliability. Physically-based, automatically-generated mechanisms show a way to couple these requirements, providing detailed, systematically-constructed models that can then be reduced, again following systematic procedures, for the purpose in question. Nevertheless, they need a solid foundation in experiment and theory against which the results can be tested. Initiatives to collaboratively evaluate pertinent kinetic data can prove helpful in this respect [370,371]. In complex reaction systems, direct, reliable measurements for multiple parameters may be scarce, however. While assessing experimental uncertainties and causes for systematic errors – as was pointed out earlier in this section – is common practice, such uncertainty considerations have only recently become more widespread for combustion modeling. To reduce the uncertainties, ensembles of experimental data are useful to constrain models, and with mathematical procedures to minimize uncertainties, to optimize, and to reduce mechanisms to meet specific requirements and conditions in a wide range of potential applications, earlier practices such as tuning and adapting rate parameters for certain individual questions have become obsolete. As a result, models are becoming more comprehensive, inclusive, and of broader relevance, without losing their physical foundation. Knowledge remains incomplete in many cases, for example in the case of unknown or missing pathways and lacking experimental guidance. Machine learning approaches for complex chemical systems [372] might also offer perspectives to contribute to model development in the future.

### 3. Combustion, chemistry, and beyond – a few examples

The previous chapter has highlighted selected areas of active combustion research with an emphasis on gas-phase reactive systems. With sophisticated experimental and theoretical methods and systematically constructed combustion chemistry models, recent work has advanced the understanding of the reaction behavior in increasingly complex conditions and furthered the application of such knowledge to practical combustion systems. As a major step to enhance the confidence in com-

bus-tion chemistry results, critical assessment of uncertainties of both experiments and models, and increasing use of larger datasets instead of individual experiments for model validation, permits identifying useful – or lacking – information for these purposes. With these tools sharpened, they can find application to investigate chemical aspects in combustion-related systems and beyond (see also Chapter 1). Some exemplary recent work on reactive processes under complex conditions will be highlighted in the following, emphasizing different aspects in often interlinked areas.

In his seminal review, Haynes [373] has addressed chemical production processes with relation to combustion, including among others flame synthesis, partial oxidation, and chemical looping. It has become apparent how much information can be provided by advanced chemical diagnostics (see Section 2.1), also beyond direct combustion. Measurements of chemical species and process parameters that have proven useful in combustion can be adapted to investigate complex reactive environments in more general terms [374–379]. They include application of synchrotron PI-MBMS to detect species of atmospheric relevance [374], of mobile MS combining different ionization techniques to analyze complex gas mixtures [375], and of various laser methods to provide *in-situ* information on the respective reaction chemistry: offering high sensitivity over a broad spectral range [376], detecting labile LTC species in engines [377], characterizing gasification reactor performance [378], or distinguishing particle phases in nanoparticle production under reaction conditions [379].

The following sections will highlight selected primarily fundamental studies from plasma-assisted processes (Section 3.1), coal- and biomass-related conversion processes (Section 3.2), and catalytic conversion processes (Section 3.3). Section 3.4 will focus on some specific aspects of reforming processes, and Section 3.5 will give several examples devoted to the coupling of combustion, chemistry, and energy conversion. The structure into these sections is somewhat arbitrary, since a given example could be highlighted under different topics. As a unifying motif, these chemistry and reaction engineering examples could both, profit from and further amplify combustion expertise.

#### 3.1. Unraveling plasma-assisted processes

Diagnostics and mechanistic analysis common to combustion studies (as discussed in Sections 2.1 and 2.4, respectively) have been increasingly used to investigate chemically complex plasma-assisted processes. As one example, Fig. 24 [378] shows the adaptation of a Raman instrument to a plasma-assisted biomass gasification reactor.

The reactor could perform flexibly in a chemical storage system utilizing renewably produced

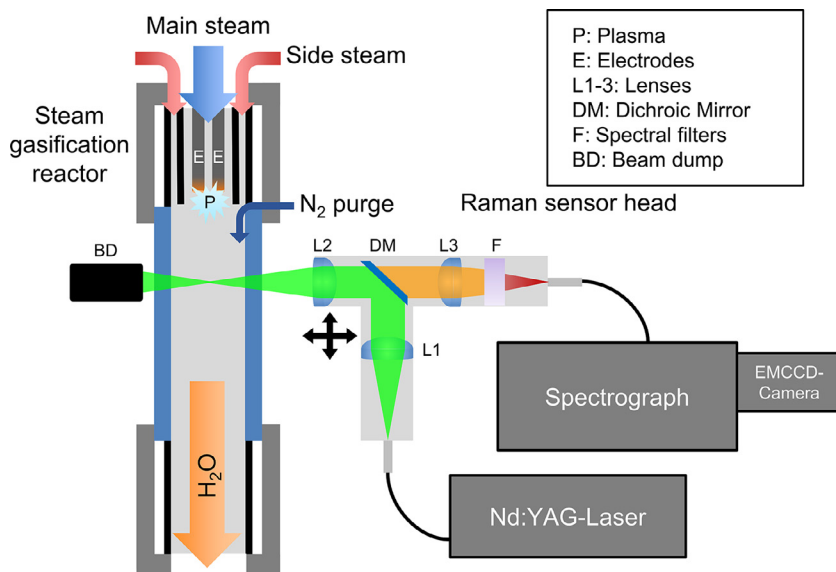


Fig. 24. Optical Raman measurement set-up at steam gasifier reactor. Reprinted with permission from [378] © The Optical Society.

surplus electricity to produce base chemicals or fuels from hydrogen-rich synthesis gas derived from carbon-rich materials such as municipal waste and biomass. Depending on operating conditions, methane and  $C_2$  hydrocarbons could be generated. A plasma-assisted, entrained-flow gasification process with preheated water steam as the gasification agent and plasma medium was established that can be dynamically operated with available electrical energy; it can attain high temperatures and consequentially, enhance reaction rates [378]. Temperature plays an important role in both thermal and plasma-assisted gasification processes, e.g., to control and optimize biomass conversion into chemicals. Using the temperature sensitivity of the rotational-vibrational water  $\nu_1$  stretching vibration, Raman spectroscopy permitted to establish a non-invasive temperature measurement technique that can operate effectively also under the challenging conditions near the plasma and in the presence of intense radiation from the hot walls [378]. The Raman sensor is based on a frequency-doubled high-power continuous-wave Nd:YAG laser (see Fig. 24) and is fiber-coupled to the steam gasifier reactor. The signal is filtered against thermal radiation and directed through an optical fiber to a high-resolution spectrograph and an appropriate camera. The sensor is movable to acquire position-dependent temperature information [378].

Detailed analyses of reactive media were also performed in further combustion-related systems that involve plasma-assisted processes and enhancement by electric and magnetic fields [380–392]. Nonthermal plasma-assisted processes

offer means for reduction of pollutant emissions and extension of the combustion-operating regime [383,384], including ultra-lean [384] and low-temperature combustion [384–386] (see also Section 2.2). The presence of charged and excited species in plasma-assisted combustion adds significantly to their chemical complexity, especially regarding the larger molecules in liquid fuels, contributing further to diagnostic and mechanistic challenges [385,387]. Nevertheless, well-established diagnostics techniques such as MBMS and TD-LAS have shown potential in characterizing the reactive environment under such conditions, including relevant neutral, charged, and excited species [387,388]. Rapid diagnostics can enable the measurement of multiple quantities and follow dynamic interactions in such processes, relying, e.g., on picosecond degenerate four-wave mixing (DFWM) [380], spectrally filtered Rayleigh scattering, femtosecond laser electronic excitation tagging, and radar resonance-enhanced multi-photon ionization (REMPI) [389]. Kinetics investigations and mechanism development [385,387,390] in such systems are highly desirable, with the eventual aim to reach an advanced modeling status as described in Section 2.4.

The effects of a nanosecond repetitively pulsed plasma on *n*-pentane pyrolysis and oxidation were investigated by Rouso et al. [387] in a flow reactor with an in-built Herriott cell (24 passes) from mid-IR TDLAS measurements using different quantum cascade lasers; Fig. 25 shows some of their species-reaction-time profiles together with model simulations.

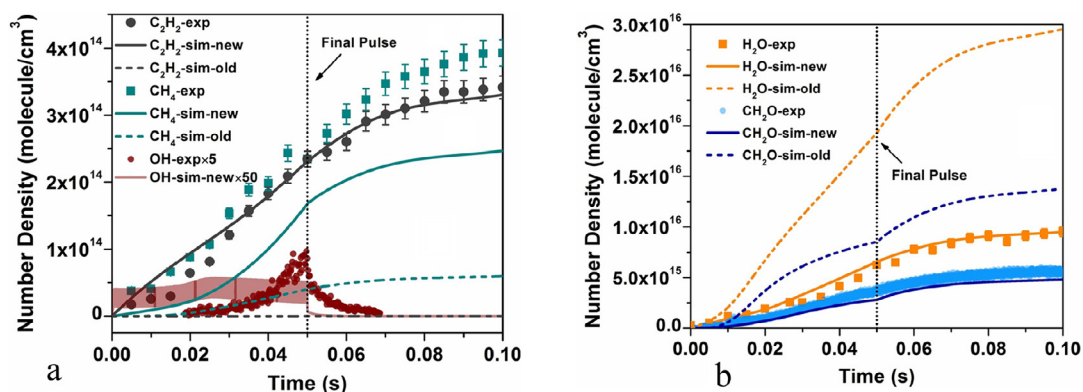


Fig. 25. Time evolution measured by tunable diode laser absorption spectroscopy of (a) C<sub>2</sub>H<sub>2</sub>, CH<sub>4</sub> and OH, and (b) H<sub>2</sub>O and CH<sub>2</sub>O together with model predictions. Reprinted from [387] with permission from Elsevier/The Combustion Institute.

While *n*-pentane combustion has been addressed in this article before, especially regarding the LTC regime [157–160] (see also Fig. 12 in Section 2.2) and PAH formation [236] (see also Fig. 16 in Section 2.3), modeling the plasma-assisted combustion of *n*-pentane demands inclusion of additional reaction pathways. Predictions of selected species with the "new" model in Fig. 25 show significant improvement over the previous "old" model, attained by inclusion of numerous electron-impact dissociation reactions and respective cross sections [387]. The detailed analysis shows that direct electron-impact dissociation of *n*-pentane is almost entirely responsible for the formation of C<sub>2</sub>H<sub>2</sub> whose profile is now well captured, and that plasma-generated radicals and excited species enhance the low-temperature fuel oxidation [387]. However, the remaining discrepancy between experiment and model for OH points towards necessary further model development.

Plasma-assisted processes show attractive potential for reactive systems involving gas-phase reactions in and beyond combustion, such as in the production of nanoparticles from gas-phase precursors [391] and in the conversion of CO<sub>2</sub> and gaseous hydrocarbons, e.g., from flares, in an efficient single-step GTL process towards methanol [392]. A common aim for the understanding and optimization of such chemical processes is to establish fundamental knowledge of the reaction behavior, including that of charged particles, obtained from direct measurement of the relevant process parameters, and to use this information to develop appropriate, transferable models, needed for safety, efficiency, selectivity, and scaling purposes.

### 3.2. Analyzing multi-phase processes involving solid fuels

As for gas-phase systems, fundamental chemical kinetics knowledge and *in-situ* process information from the reacting system is highly valuable to understand and optimize heterogeneous processes and to predict their behavior under relevant conditions with regard to material resources, energy demands, potential pollutant formation, and generation of waste. Similar diagnostics and kinetics approaches as described before can be valuably applied in coal and biomass utilization [393–410].

In this context, oxy-fuel combustion is one of the promising technologies that can capture CO<sub>2</sub> from power plants [393], which is the more important in an era of increasing energy and electricity demand and an only gradual increase of the global share of renewables (see also Chapter 1). Carbon capture and storage schemes have the potential to use fossil fuels in power plants while abating associated CO<sub>2</sub> emissions. Carbon dioxide harvested from large point sources such as power plants can also be viewed as a valuable commodity for fuel and base chemical production. Implementing oxy-fuel combustion necessitates changes in plant and process configuration; especially the need for pure O<sub>2</sub> from separation processes imposes energy penalties [393]. Molecular nitrogen is absent from the combustion system, with flue gas composed mainly of carbon dioxide and water. To control the flame temperature, flue gas is typically recirculated to the burners, and the combustion chemistry is altered by the replacement of N<sub>2</sub> with CO<sub>2</sub>- and H<sub>2</sub>O-containing flue gas. The associated effects on ignition, reactivity, heat release, burnout, radiative and convective heat transfer, pollutant emissions, flue gas processing, and on residual products such as fly ash remain incompletely understood; oxy-fuel combustion processes thus require further comprehensive fundamental research [393]. To develop ap-

appropriate chemical models, the secondary pyrolysis and oxidation reactions of gas-phase products of coal devolatilization under oxy-fuel conditions have been investigated using counterflow flames probed with molecular-beam mass spectrometry for speciation measurements [394,395]. Specifically, Baroncelli et al. [394] have studied the combustion behavior of  $C_2H_2$  and a  $C_2H_2/CH_4$  mixture with addition of  $CO_2$  as representative of light coal volatiles. Felsmann et al. [395] introduced a coal-plate burner to explore gas-phase kinetics of volatiles above the coal surface under oxy-fuel conditions, again using MBMS to determine multiple species concentrations for two different coal types.

The characterization of multi-phase flows poses significant challenges regarding insight into relevant properties of all phases and the nature and dynamics of their interactions, but a detailed understanding of the relevant physico-chemical processes is a prerequisite for the further development of promising combustion technologies. Köser et al. [396] have reported non-invasive multi-parameter diagnostics to investigate the volatile combustion duration for single coal particles in a premixed laminar flow reactor into which coal particles were injected. The system can operate with both, oxy-fuel and air combustion conditions. The flame was visualized by its luminosity and by high-speed OH-PLIF, and a stereoscopic backlight-illumination approach was used to determine particle geometries. Simultaneously, ignition, volatile combustion, and particle size, shape, and velocity were captured for individual particles. While OH-PLIF was found to be superior to determine ignition because it is not very sensitive to the composition of volatiles, flame luminescence was the better choice to mark the end of volatile combustion [396].

Tufano et al. [397] present a chemical model for the heating, ignition, combustion of volatiles, and char conversion of single coal particles that incorporates heterogeneous kinetics and information on the inner particle structure such as porosity. The model considers the elemental analysis of the coal and its properties assigned from reference samples [397]. An experimental configuration is modeled, with enhanced  $O_2$  levels and in the presence of  $CO_2$ , where 0.1 mm diameter coal particles are injected into the hot combustion gases of a Hencken burner [397]. In the computation, the boundary layer around the particle is fully resolved with 20 cells in the radial and more than 70 cells in the circumferential direction to access both, the external gas phase and the particle interior, and the enveloping flame is also resolved with at least 20 cells [397]. Results from this study are shown in Fig. 26.

In this configuration, hot combustion products are introduced from the left side. The particle, indicated by a circle in the left panels, is captured at selected times [397]. After heating up, volatile matter is released, and homogeneous gas-phase ignition occurs at 29.5 ms, accompanied by OH forma-

tion and a temperature increase first observed in the wake; at 29.6 ms, the particle is surrounded by a region of elevated OH and temperature [397]. The flame then consumes the available volatile gases completely so that at 35 ms, OH and temperature are decreased. Additional time is needed to decompose the heavy tars, and until about 50 ms, heterogeneous char reactions at the particle surface again cause OH formation and heat release, forming a circular chemical conversion region around the particle [397].

The right side of Fig. 26 shows the associated  $O_2$  mass fraction, temperature, and velocity vectors in the particle interior for the same temporal sequence; note that different sets of equations were solved for the exterior (standard gas-phase conservation equations) and the interior (two-phase intra-particle model) [397]. Ignition occurs when both gas phase and particle reach about the same temperature and is associated with high mass release with a peak velocity of about 2.4 m/s. Subsequent cooling and lower mass release are observed until about 35 ms. Then surface ignition occurs from heterogeneous reactions, and the conversion process results in higher particle temperature and increased mass release at 50 ms [397]. Regarding oxy-fuel combustion, boundary conditions with  $CO_2$ -containing atmospheres can affect the described combustion behavior [397].

Further detailed diagnostics studies have been devoted, e.g., to lignin and lignite co-pyrolysis investigated by PI-MS [398] and laser sensors to determine chemical species in a high-pressure coal gasifier [399]. Similarly, kinetics investigations have addressed fundamentals of pollutant formation in solid fuel combustion [400] and mechanisms of biomass pyrolysis [401–403], while progress in biomass gasification [404,405] and its conversion to chemicals and liquid fuels [406,407] has been reported. The complex chemistry of lignocellulosic biomass pyrolysis has recently been addressed using molecular modeling to describe cellulose, hemicellulose, and lignin pyrolysis, respectively [403], profiting of the advances of quantum chemistry towards treatment of large molecular structures. Thermochemistry and reaction pathways have been provided with particular success for cellulose pyrolysis, whereas it remains difficult to understand hemicellulose conversion and the effects of ions [403]. Process engineering and optimization can benefit from the quantitative understanding of reaction rates, temperature effects, and of factors controlling selectivity towards desired chemical products [403]. Chemical diagnostics in such complex environments is being reported, e.g., with real-time monitoring of biomass pyrolysis by on-line ultra-high-resolution photoionization mass spectrometry [408]. This technique, using a micro-fixed-bed reactor coupled to a VUV-lamp photoionization Orbitrap mass spectrometer combination, has successfully provided the chemical composition

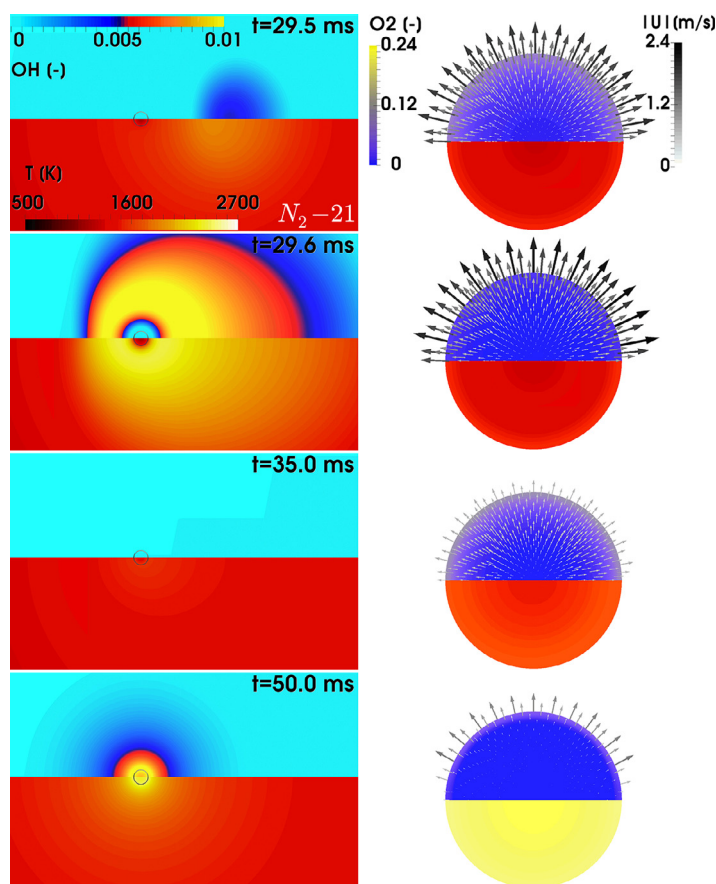


Fig. 26. Selected time instants during ignition and combustion of a coal particle in a specific gas mixture termed  $N_2-21$ . A circle marks the particle surface. *Left:* Mass fraction  $Y_{OH}$  (top frames) and temperature (bottom frames) contours in the vicinity of the particle. *Right:* Velocity vectors colored by magnitude, mass fraction  $Y_{O_2}$  (top frames) and temperature (bottom frames) contours for the particle interior. Reprinted from [397] with permission from Elsevier.

upon pyrolysis of dehydrated, pulverized camphor wood [408]; selected results are shown in Fig. 27.

The diagram relates O/C and H/C ratios and categorizes the types of compounds found in the complex pyrolysis mixture; the relative abundance of the compounds assigned from their molecular formulae is color-coded [408]. The approximate range of O/C of 0.2–0.7 and H/C of 0.7–1.3 corresponds to phenolic compounds derived from lignin, while species with a higher H/C ratio of about 1.4–2.0 are assumed to represent lipids. Fig. 27 also shows the time evolution of compounds during the pyrolysis process. Initially, hydrocarbons are produced whose early appearance suggests their formation from devolatilization rather than from bond cleavage; later stages indicate H/C ratios consistent with aromatics formation [408]. Further analysis included examination for double-bond equivalents to assess chemical structures, MS-MS to investigate fragmentation patterns, off-line GC-MS in the pyrolysis gases, and on-line single-photon

ionization MS [408]. The ultra-high-resolution MS revealed a much more complex pyrolysis gas composition than that detected with conventional methods, with more than 90% of the detected signals corresponding to oxygenated compounds with 1 to 5 oxygen atoms and double bond equivalents of 2 to 7. Although the assignment of structures remains a challenge, the on-line diagnostics could be used for process monitoring in biomass pyrolysis and might find application also in catalytic conversion systems for biomass valorization [408–410].

Diagnostics developments and real-time monitoring techniques, combined with theoretical insight and numerical modeling, can assist in understanding fundamental aspects of practically relevant processes involving



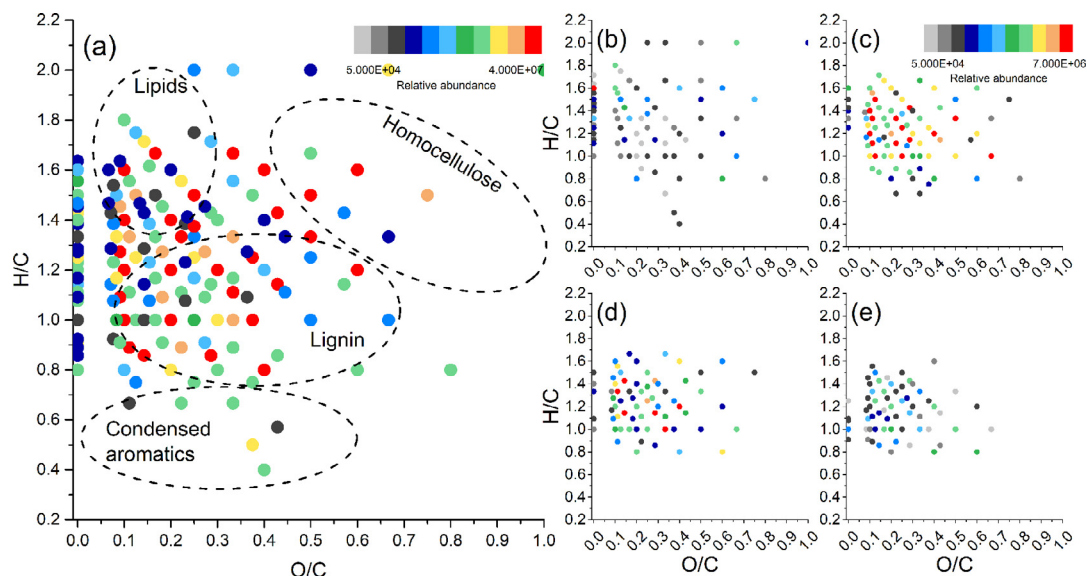


Fig. 27. (a) Van Krevelen diagram derived from the accumulative mass spectra in biomass pyrolysis. Pyrolysis products with similar characteristics fall within specific regions, and their origins are shown in the circles. (b–e) van Krevelen diagrams derived from mass spectra recorded at 0.31, 0.64, 0.91 and 2.01 min, respectively. Reprinted from [408] with permission from Elsevier.

solid fuels such as coal or biomass pyrolysis, gasification, and combustion under conventional as well as oxy-fuel operating conditions. Attention should be paid to designing appropriate partly idealized systems that can be subjected to extensive diagnostics and mechanistic inspection while still representing essential aspects of the technical process. Considering the large variability of solid fuel characteristics, comparing and integrating fundamental results across laboratories might be valuable, potentially supported by data science procedures and uncertainty assessment as in approaches discussed in Section 2.4.

### 3.3. Characterizing catalytic combustion and conversion processes

Mantzaras [411] has recently documented progress in using laser-based diagnostics near catalytic surfaces to understand the homogeneous and heterogeneous reactive processes of relevance for diverse chemical and energy conversion systems, including power generation from the microscale to full-size power plants, fuel reforming, and exhaust aftertreatment for automotive engines and fuel cells. Hybrid hetero-/homogeneous processes can be useful, for example, in new combustion concepts using pre- and post-combustion CO<sub>2</sub> capture; here the presence of catalytic devices and heteroge-

neous reactions can help to avoid flashback and blowout due to significantly different reactivity of hydrogen-enriched mixtures in pre-combustion technologies, or flue-gas-enriched mixtures in post-combustion capture strategies [411]. Requirements for combustion-related systems include catalysts with high activity and thermal stability. To understand the interaction and dynamic progress of gas-phase and surface reactions, spatially and temporally resolved diagnostics must be able to access the boundary layer close to the catalytic surface, desirably under practically relevant conditions (see also Section 2.1). Challenges include probing reactive species near hot walls, in turbulent media, and in confined channels, in the presence of intense thermal radiation or combustion instabilities, at elevated pressures or low densities, and for a wide range of reactant compositions and catalytic surface characteristics. Advances in theory and measurement techniques, including PLIF and Raman spectroscopy to detect reactive intermediates and stable species, provide data that can support model development and simulation of such systems [411]. Further research is needed, for example, regarding the coupling of chemistry and turbulence in catalytic systems. Diagnostics developments should include detection and quantification of reactive species in chemically complex mixtures at suitable pressures and temperatures and under confined conditions, e.g., in channels or near surfaces. While non-invasive laser-based experiments can determine the local catalytic reactivity as a crucial system parameter, combinations with *in-situ* surface science techniques

as, e.g., X-ray absorption spectroscopy (XAS) or diffuse reflectance infrared Fourier transform spectroscopy (DRIFTS), are needed to monitor also the surface properties under operation [411].

Laser-based and other gas-phase diagnostics, *ex-situ* microscopic characterization, kinetic model development, and numerical simulations in catalytic systems have been applied to investigate combustion-related emission reduction and control regarding, e.g.,  $\text{NO}_x$  [412,413],  $\text{CH}_2\text{O}$  [414], and soot [415,416]. Furthermore, catalytic and homogeneous (partial) oxidation of methane [417–420], methane/*n*-heptane mixtures [421], ethene [422], jet fuel surrogates [423], and other volatile organic compounds [424,425] has been the subject of detailed chemical analyses. Understanding the reaction processes in such hydrocarbon (partial) oxidation systems is important for methane leakage abatement from natural gas usage [417], VOCs abatement from industrial processes [424], and other emission reduction purposes [425], for (on-board) reforming for fuel cells, to generate syngas as feedstock for Fischer-Tropsch fuel production or chemical synthesis [418–421,423], for energy conversion from renewable power to chemicals [421], and for improving ignition in hypersonic engine combustion [422].

Natural-gas-fired engines, while potentially reducing PM emissions, may contribute to GHG emissions from methane leakage (compare Section 1.2). Methane oxidation in exhaust gas aftertreatment systems relies on palladium catalysts whose operation must be understood in more detail, however, to improve technical applications [417]. Aspects such as the dependence of catalyst aging on the gas mixture composition, influences of the catalyst support material, effects of the Pd particle size on the turnover frequency, and the origin of oscillations in reactivity observed as a function of feed rate, have motivated Stotz et al. [417] to develop a microkinetic model for the surface reactions in this system based on DFT calculations and *in-situ* DRIFTS studies. Similarly, PLIF and Raman experiments in an optically accessible reactor and two-dimensional numerical simulations of the homogeneous and heterogeneous kinetics led to an improved understanding of syngas formation from fuel-rich  $\text{CH}_4/\text{O}_2/\text{N}_2/\text{CO}_2$  mixtures over rhodium or platinum catalysts [418]. An example for the interplay of homogeneous and heterogeneous kinetics is given in Fig. 28 from an investigation of the catalytic partial oxidation of methane in rhodium-coated channels [419]. Numerical simulations were performed with detailed catalytic and gas-phase chemistries, heat transfer, and transport for pressures of 1–25 bar, inlet temperatures of 300–900 K, different stoichiometries, and various channel diameters [419]. Operation conditions were investigated with respect to factors such as the importance of gas-phase chemistry,

thermal stability of the catalyst, and thermal management of the system [419].

Profiles of wall temperature, radially-averaged species mole fractions, and conversion rates are given in Fig. 28 for Case B ( $\Phi = 4.0$ , 600 K, 15 bar, 1.2 mm channel diameter) [419]. Adiabatic equilibrium values are indicated on the right ordinates in Fig. 28 (top panels). Volume changes due to chemical reactions have been considered in the calculations [419]. The left panels show results with only catalytic chemistry (conversion rates denoted with C, solid lines), while gas-phase conversion (indicated with G, dashed lines) is included in the right panels; negative rates denote species production and positive rates indicate species destruction. Considering both, catalytic and gas-phase reactions, the end of the oxidation zone (at 1%  $\text{O}_2$ ) is found at 14 mm (Fig. 28, b1), and 82% of  $\text{CH}_4$  was converted in this zone. The oxidation zone extended further to 36 mm with only catalytic reactions (Fig. 28, a1). In both cases, CO,  $\text{H}_2$ , and  $\text{H}_2\text{O}$  increased significantly, and smaller amounts of  $\text{CO}_2$  were formed, dominantly from catalytic reactions [419]. From their parameter variation, the authors attempted to answer the technically relevant question under which conditions gas-phase reactions might be safely neglected in predicting the system's operation; they concluded that wider channels and lower equivalence ratios supported gas-phase reactions, whereas lower inlet temperatures and pressures suppressed them [419].

Experimental, theoretical, and modeling investigations combining treatment of surface and gas-phase chemistry will – best jointly – advance the knowledge to optimize hetero-/homogeneous systems. Catalytic processes studied with MS include co-pyrolysis of cellulose and polyethylene [426] as well as selective conversion of syngas to light olefins [427]. PEPICO as a highly discriminative and sensitive synchrotron-based technique (see also Section 2.1) has provided isomer-specific analyses of intermediates in the catalytic fast pyrolysis of guaiacol as a lignin model compound with the aim to develop more detailed understanding of such processes; from the species desorbed from the catalytic surface, the role of various reaction pathways was analyzed and fulvenone was identified as a key intermediate [428]. PEPICO has also been successfully combined with other techniques in *operando* mode and DFT calculations to catalytic oxychlorination, a selective process for light alkane functionalization to olefins, to determine gas-phase reaction intermediates and investigate their involvement in alkane activation [429].

Further catalytic systems of interest include the conversion of methanol to hydrocarbons [430,431], for example in the methanol-to-olefin (MTO) system [432–434] as one of the important  $\text{C}_1$  chemical processes that can contribute to alternative pathways to base chemicals and fuels from non-petroleum feedstock [432,434]. Methanol can be

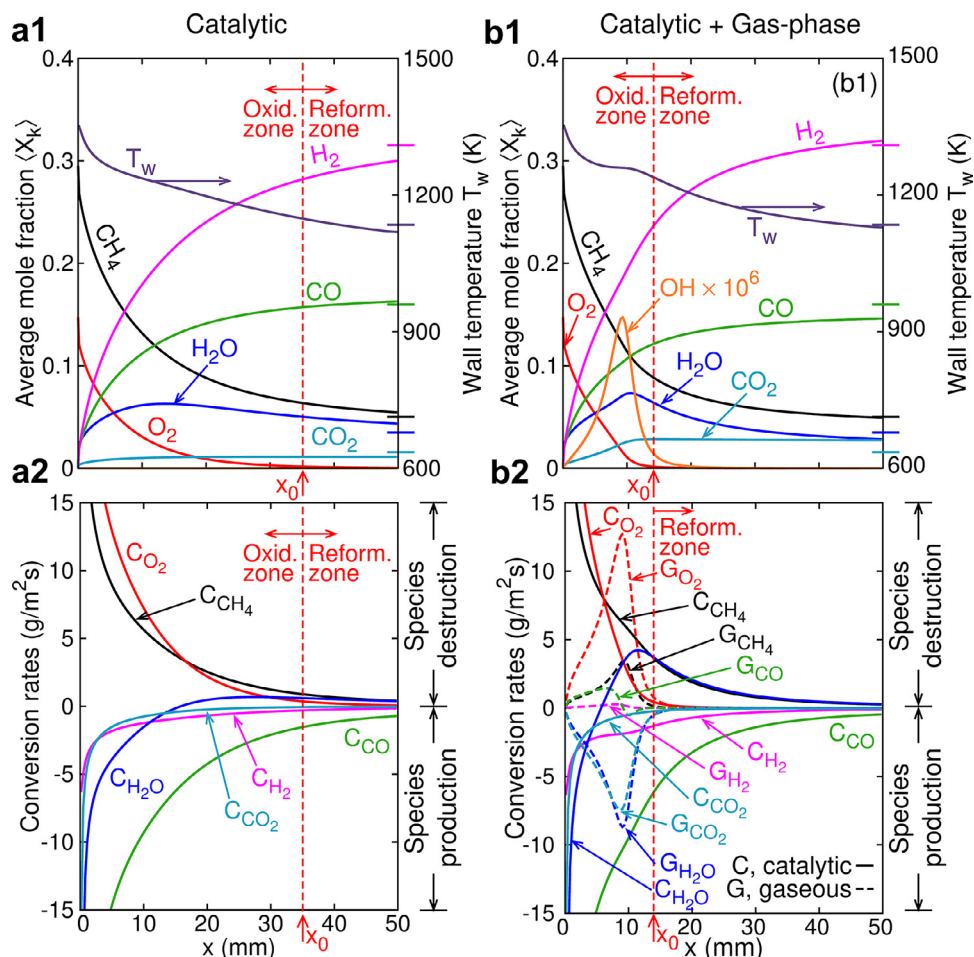


Fig. 28. (a1, b1) Streamwise profiles of wall temperature and radially-averaged species mole fractions and (a2, b2) species conversion rates for Case B: (a1, a2) with only catalytic chemistry and (b1, b2) with catalytic and gas-phase chemistry. *C* and *G* refer to catalytic and gaseous conversion rates, respectively. Horizontal ticks on the right ordinates of (a1, b1) provide the adiabatic equilibrium compositions and temperature. The axial locations marked  $x_0$  and the vertical dashed lines delineate the end of the oxidation zone. Reprinted from [419] with permission from Elsevier/The Combustion Institute.

obtained from natural gas or by gasification of coal or biomass, and it could serve as a potential energy storage compound [432] (see also Section 1.3). In spite of long-term research, important questions remain regarding the reaction mechanism because it involves gas-phase and surface reactions occurring in the pores of the molecular-sieve- or zeolite-based catalysts [431–434]. Insight into mechanistic details has been provided from *in-situ* spectroscopy and computational chemistry [431,433]. Although methanol is a small molecule and the chemistry seems simple on first glance, the formation of the initial C–C bond and the identification of potential intermediates has remained a controversial issue [433,434]. Solid-state NMR spectroscopy, *operando* diffuse reflectance spectroscopy in the ultraviolet and visible spectral regions, and on-line mass spectrometry have been successfully combined to iden-

tify gas-phase species and surface acetate, methyl acetate, and dimethoxymethane during the early stages of the MTO reaction and led to a suggestion of a surface-species-assisted direct mechanism [433].

Challenges in catalytic systems include control of selectivity and product distribution as well as catalyst deactivation, e.g., by carbon deposition, as a function of catalyst properties and reaction conditions [431,432] – questions that might be resolved with the aid of *in-situ* diagnostics (see also Section 2.1). Models based on fundamental insight to predict the performance of such heterogeneous, dynamic

reaction processes of technical relevance are often not yet sufficiently advanced; such processes may thus offer as valuable targets for mechanistic inspection and model validation as genuine combustion systems. Catalytic processes of technological impact for future energy conversion and chemical production environments that can involve also gas-phase reactions are often investigated in communities outside of combustion, a situation that suggests bringing in existing combustion expertise.

### 3.4. Investigating reforming processes

Hydrogen, now produced in large quantities from fossil fuels, will be in increasing demand for hydrogenation and hydrodeoxygenation processes, e.g. for the production of methanol as a key building block as discussed above, for the synthesis of ammonia that is also being discussed as an energy vector (see also Section 1.3), as a feedstock for fuel cells, and in the production of biofuels and synthetic fuels (see also Section 1.2). The current industrial processes use reforming of natural gas or oil and coal gasification; biomass gasification could contribute hydrogen from renewable sources [373]. Steam reforming from methane over nickel catalysts at high pressure and temperatures of about 980–1200 K generated from combustion heat is the dominant large-scale process, while partial oxidation of methane offers control to produce specific molar  $H_2/CO$  required, e.g., in methanol or FT synthesis [373]. (Catalytic) partial oxidation routes are also interesting in the context of green chemistry to provide oxygen-functionalized compounds, and as stated recently by Haynes [373], many of the involved reactions are closely related to combustion.

Unraveling kinetic and mechanistic aspects of reforming processes is a key element of recent research [435–440]. For example, Liu et al. [435] have analyzed thermal *versus* plasma-assisted steam reforming of methane to assess effects of electron-induced chemistry on product distribution and selectivity. Schulz et al. [436] have investigated coke formation mechanisms in the dry reforming of methane to synthesis gas over Ni- and Pt-based catalysts from a multi-technique experimental approach. In-cylinder reforming processes in IC engines could change the fuel–air mixture reactivity on board [437], and fuel-specific reforming products and respective mechanisms were recently studied in detailed speciation experiments performed with synchrotron-based mass spectrometry in a single-cylinder research engine [437]. Such in-cylinder reforming strategies could reduce emissions and enhance the engine efficiency and performance range with liquid fuels through gaseous

hydrogen-rich reformates produced on board (e.g., *via* waste heat recovery), in this regard superseding the need for a hydrogen fueling and storage infrastructure [438].

Considerations and challenges towards optimization and control of such processes concern the selection of appropriate combinations of reforming technology (steam, autothermal, exhaust gas reforming) and fuel (methane, small alcohols, conventional engine fuels), effects of pressure and mixture conditions, mixing properties upon direct injection of multi-component reformates, influences on burning velocity, and prevention of coking [438], suggesting dedicated more detailed investigations. The interaction of hetero-/homogeneous reactions and heat transfer in reforming processes for on-board auxiliary devices, e.g., for reforming diesel and gasoline during short contact times or operating solid-oxide fuel cells (SOFCs) with non-pure hydrogen, is not understood in appropriate depth [439]. Importantly, SOFCs are considered as highly valuable reactors for electricity generation by methane conversion from natural gas because they could potentially double the efficiency (to above 60%) and thus decrease the  $CO_2$  emissions significantly in natural gas power plants *versus* existing combustion technology [440], again demanding detailed characterization and mechanistic understanding of the process. For the oxidation of biogas as a non-fossil feedstock to generate electricity in an SOFC, Kirtley et al. [441] have employed *in-situ* optical techniques such as near-IR thermal imaging, FTIR emission spectroscopy, and vibrational Raman spectroscopy in combination with electrochemical measurements to provide spatially, temporally, and thermally resolved gas-phase and surface-specific information that can be used for mechanism development and detailed performance characterization.

Reversibly operating solid oxide cells are promising elements for the storage and conversion of fluctuating and distributed renewable energy, considering also that a significant storage capacity will be needed in the future [442,443]. Inversely to SOFC mode, operation as a solid oxide electrolysis cell (SOEC) can utilize electricity to convert  $H_2O$  and/or  $CO_2$  into  $H_2$  and/or  $CO$ . Menon et al. [443] have investigated the  $H_2O/CO_2$  co-electrolysis in an SOEC to develop a model for the processes at the three-phase boundary, considering electrochemical performance, transport in the channels and the porous electrode media, and heterogeneous reactions. Results of model simulations compared with experiments performed at the European Institute for Energy Research described in [443] are provided in Fig. 29.

The electrolysis was performed with different  $H_2O-CO_2-H_2$  mixtures and air, respectively, supplied to the cell at two different temperatures, and the detailed model is capable to reproduce the experimentally determined cell performance quite ac-

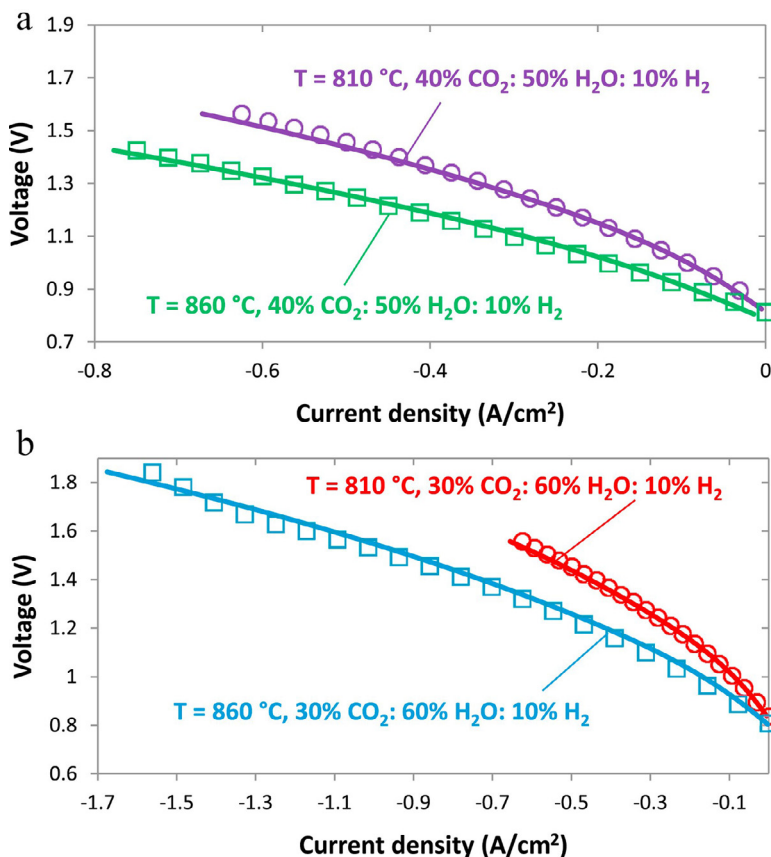


Fig. 29. Comparison between numerical simulations (*lines*) and experiments (*symbols*) for inlet gas compositions of (a) 40% CO<sub>2</sub>, 50% H<sub>2</sub>O, 10% H<sub>2</sub> and (b) 30% CO<sub>2</sub>, 60% H<sub>2</sub>O, 10% H<sub>2</sub>. Reprinted from [443] with permission from Elsevier.

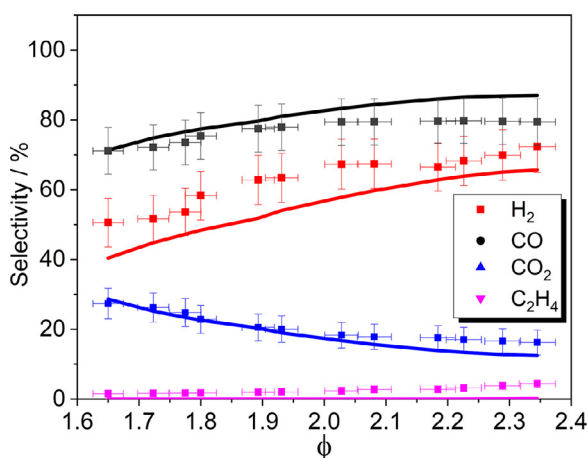


Fig. 30. Selectivities of product-gas species. *Symbols*: experiment, *lines*: simulation. Reprinted from [444], available under Creative Commons CC-BY-NC-ND license.

curately [443]. While Fig. 29 shows electrical characteristics, it should be pointed out that the model includes numerous heterogeneous elementary reactions, involving  $O_2$ ,  $CH_4$ ,  $CO$ ,  $CO_2$ , and  $H_2O$  in the gas phase and on the nickel-based catalyst surface and their interaction with surface species such as  $H$ ,  $OH$ ,  $CH$ ,  $CH_2$ ,  $CH_3$ ,  $HCO$ , and other intermediates known from heterogeneous combustion processes.

While the analysis of multi-phase systems involving gas-phase chemistry can profit of the developments made in combustion diagnostics and kinetics, progress in their detailed understanding and optimization must involve combinations with methods from surface science and, potentially, electrochemistry, especially to assess the complex dynamic behavior of such systems. Knowledge acquired in a combustion context could valuably improve the investigation, understanding, and optimization of systems of different scales as building blocks in energy and chemical conversion.

### 3.5. Coupling combustion, chemical, and energy conversion processes

Polygeneration processes that couple between heat and/or power generation and the production of synthesis gas, fuels, and/or chemical compounds offer efficient and flexible conversion opportunities [373,444–449]. HCCI engines have been described as particularly useful and versatile elements for such chemical and energy conversion processes [444–447], because it is possible with a single engine combustion process to obtain variable ratios of mechanical work, process heat, and chemicals [444]. Specifically, Banke et al. [444] have used the HCCI engine as a reactor for partial oxidation for fuel-rich methane/DME mixtures. DME increases the reactivity of methane in the low-temperature regime (see also Section 2.2), and operation with the two-component mixture in HCCI mode also enables using fuel-rich conditions that are not prone to soot formation [444]. DME was also chosen as an additive because it can be derived from biomass. The experimental and modeling investigation explored the selectivity towards potentially valuable products ( $CO$ ,  $H_2$ ,  $C_2H_4$ ) and the conversion efficiency of the process as a function of operating conditions; Fig. 30 shows selected results [444].

Methane conversion decreases with equivalence ratio  $\Phi$  as a result of decreasing temperature and lower  $O_2$  content, while the sensitivity towards  $H_2$ ,  $CO$ , and  $C_2H_4$  increases to about 72%, 79%, and 4%, respectively, at  $\Phi = 2.34$  [444]. These

tendencies are in line with the lower oxygen content at higher  $\Phi$  that precludes full conversion to  $H_2O$  and  $CO_2$ . The simulations agree reasonably well with the experimental results within the measurement uncertainties; deviations, especially for  $C_2H_4$ , might result from using a single-zone engine model that cannot resolve regions of different temperatures [444]. Work and heat outputs were seen to decrease with  $\Phi$  and the according lower temperature. It is interesting to consider the overall exergetic efficiency of the polygeneration process that takes work, heat, and energy content of the chemical products into account: it is as high as 82% at  $\Phi = 2.34$  and exceeds that of synthesis gas production by methane steam reforming of typically 63% as well as those of some other polygeneration processes [444]. Flexible operation between work and chemical output is possible by adjusting the equivalence ratio.

Saylam et al. [446] have also, by numerical simulation, explored the potential for chemical production in an HCCI engine under fuel-lean conditions; they considered the conversion of methane as a rather inert major component of natural gas or biogas, and of ethane and propane (further components of natural gas) to oxygenated compounds such as formaldehyde, methanol, and hydrogen peroxide as well as to ethene. On the one hand, the process could form reactive intermediates on board that might serve to stabilize low-temperature engine operation (see also Section 2.2), and on the other, it could serve to produce base chemicals in a flexible polygeneration reactor [446].

Polygeneration processes are of interest in a variety of contexts, and only two further examples, namely the production of biogas, bio-oil, and bio-char in biomass pyrolysis [448] and of liquid fuels and electricity in coal gasification [449] are mentioned here. The former [448] shows potential for efficient, low-emission conversion processes of huge amounts of seasonally available agricultural waste in China towards several valuable and transportable products, rather than to burn the biomass locally in the field or use it directly in combustion for power generation. The latter study [449] utilizes an interesting hybrid coal gasification strategy with solarthermal energy input. To reduce GHG emissions of the CTL process (see also Section 1.2), concentrated solar power can be employed to support the high-temperature coal gasification process, with a hybrid approach incorporating pressurized storage of syngas and oxygen to allow for transient response to the varying solar irradiation [449].

Solarthermal energy can be coupled in different ways with combustion as recently reviewed by Nathan et al. [450]. Such hybridization strategies that combine both sources in a single plant have several advantages including GHG reductions, continuous stable operation, and efficiency gains and cost reductions by shared infrastructure [450]. Solarthermal-combustion hybrids can

also be used with oxy-fuel and chemical looping combustion, and they could operate with fossil or biomass resources. Different thermodynamic cycles and operating conditions can be considered, and understanding the physical and chemical processes and limitations will assist in optimizing and scaling as well as controlling the operation [450]. Concentrated solarthermal power offers also pathways towards fuel synthesis [451]. It should not be overlooked that direct photocatalytic conversion of biomass to fuels is an active research area [452], with production efficiencies and scales, however, that are not yet competitive against those of thermochemical processes.

Design, coupling, and critical assessment of technical-scale conversion processes between heat, power, and chemicals is a complex task, especially when different feedstocks are used, different process components and conditions are applied, and different criteria are suggested to consider technical, economic, or environmental constraints. Systematic approaches may be beneficial with respect to process integration and plant design [453], considering especially GHG emissions associated with combustion-related and chemical production technologies for the industrial sector [454–457] and potential resulting environmental issues, e.g., for CO<sub>2</sub> capture, transport, and storage [458]. Similarly important issues concern the projected developments of emissions in the transportation sector [459–462]. Systematic lifecycle analyses considering energy and material streams along entire process chains may provide guidance, but they are not commonly adopted within the combustion community.

Environmental risks and health impacts of combustion-associated processes raise increasing public concern. It is not easy, even for those working in the field, to form a sound and balanced view of the interdependent aspects in chemical and/or energy conversion and storage. Moreover, reception of scientific arguments can depend on many factors, as recently inspected for climate science [463]. It may thus be a useful endeavor for the combustion community to contribute to a more efficient communication and better public understanding of the role of combustion in a future energy, transportation, and industrial production scenario.

#### 4. Final thoughts

Combustion must be regarded in context. The present article has mainly considered its connec-

tions with chemistry, attempting a larger background in the first chapter, and providing examples in active combustion areas in the second. Encouragement to explore connections of combustion and chemistry in some exciting and important fields was intended in the third. Examples have been selected from a personal view with a first goal to highlight especially the potential of *in-situ* chemical diagnostics and of kinetics and dynamics to unravel fundamental physico-chemical aspects and thus to contribute to a mechanistic understanding and potentially, model development enabling numerical simulation and prediction even in highly complex and challenging reactive environments. Secondly, I wished to point out selected recent developments, and thirdly to be reasonably inclusive regarding the contributions of many researchers and groups worldwide. There could have been so much more material!

Due to multiple connections between the addressed topics, examples could have been sorted differently. However, it is suggested to take a birds-eye view rather than a columnar perspective to appreciate a more complete picture. Connections have been pointed out to other areas including, e.g., atmospheric chemistry, astrochemistry, surface science, material synthesis, nanochemistry, catalysis, reaction engineering, and chemical production. Also, coupling combustion-related processes with renewable feedstocks and renewable energy, and integrating production of fuels and chemicals with that of heat and power have been briefly addressed. While many genuine combustion problems need attention, as has been pointed out throughout this article, the future role for combustion will be different from that today, regarding, for example, decreased production of combustion cars and investment in renewable energy and green processes.

Which perspectives would this offer for the combustion community? An attempted answer can only be personal and speculative, the more so since the COVID-19 outbreak has introduced additional uncertainties regarding global developments. I have already given some observations and partial answers in the summaries at the end of each section that can be viewed together as an unfinished list of suggestions for further research directions. Moreover, I wish to briefly highlight three aspects that – in my view – will gain importance: The use of digital tools, a focus on small molecules with their double role as fuels and energy vectors, and the potential to adapt to an increased importance of hydrogen.

Since Frenklach has highlighted the value of process informatics for combustion [464], exciting digital tools have become available. Automated mechanism development, optimization, and analysis routines have already been highlighted in Section 2.4. Further opportunities arise regarding databases, frameworks, methodologies, and platforms for chemistry and reaction engineering

[465–470]. Systematic and consistent approaches to numerical simulation of reacting systems [465], preserving fundamental model details while saving computational time [466,467], facile intercomparison of mechanisms and kinetic information [468,469], recommendation of reaction routes to optimize synthesis strategies [470], environmental information considering real-time combustion emissions and their local dispersion [469,472] are only a few examples that may spark off further ideas and applications for chemical processes and energy conversion systems [470–473]. The need for high-quality experimental data should, however, be stressed again in this context to ensure that simulations and models remain physically trustworthy.

Experimental and modeling effort has evolved in the direction of larger, chemically more complex, "realistic" fuels and fuel mixtures (see Section 2.4). For applications in the future, smaller molecules such as methane, methanol, methyl formate, DME, ammonia, as well as blends such as syngas and hydrogen-enriched methane or ammonia deserve renewed attention. It is widely believed that mechanisms, including validation experiments, for such "simple" molecules are in good shape. Nevertheless, it may be wise to verify this impression in detail, considering new theoretical and experimental results, and potential gaps and needs for the conditions of interest in future applications and conversion routes. Furthermore, gas-phase mechanisms for such molecules tend also to be relied upon for modeling heterogeneous systems, e.g., for process routes as mentioned in Sections 3.3 and 3.4, for which ascertained gas-phase mechanism quality would be a prerequisite.

Hydrogen may be expected to play a more important role as an energy vector; its global demand is expected to increase by 4–5% per year [474]. This article has briefly mentioned hydrogen particularly in the context of fuels and energy conversion (Sections 1.2 and 1.3). Applications have been considered briefly in (catalytic) combustion systems [475,476] (see also Section 3.3), in fuel cells (Section 3.4), and for processes such as hydrogenation and deoxygenation for biomass conversion to fuels and chemicals. However, questions arise regarding its most efficient, sustainable production in appropriate quantities [477–482]. Electrolysis using renewable power is discussed as a likely option [479,480], but only 4% of global hydrogen is currently produced by water electrolysis; 96% is gained through conventional routes from fossil feedstock based on coal gasification, hydrocarbon pyrolysis, and steam reforming of natural gas [474]. Further approaches may also include biomass conversion, biological hydrogen production, photo- or photo-electrochemical water splitting, and solarthermal generation [474,482]. Coupling of efficient production with an appropriate infrastructure is another aspect [474]. It should be pointed out that chemical engineering processes like those mentioned in

Sections 3.3 and 3.4, including catalytic dry reforming of methane [478], are potential targets for the tools of the combustion community for process development and optimization, using fundamental knowledge and diagnostic techniques gained in decades of research.

In view of these and other important developments and expected transformations, chances and opportunities are offered for contributions. Combustion researchers can make a difference and take an active role in clean energy conversion with their expertise in advanced diagnostics, detailed kinetics and dynamics, mechanism development, and modeling of multi-phase, multi-scale reactive processes. Reductions of emissions, especially of carbon dioxide, are needed, and the combustion community is well positioned to contribute to efficient strategies to attain such goals. Such transformations must happen in a timely manner. Already Arrhenius has pointed out in 1896 [483] connections of industrial activity, CO<sub>2</sub> in the atmosphere, and its effects on temperature, however with anthropogenic contributions at his time of much lesser importance than today.

I would like to finish by quoting a statement, published 1955 but seemingly not outdated, of John von Neumann [484]: "In all its stages the industrial revolution consisted of making available more and cheaper energy, more and easier controls of human actions and reactions, and more and faster communications. Each development increased the effectiveness of the other two. All three factors increased the speed of performing large-scale operations – industrial, mercantile, political, and migratory. But throughout the development, increased speed did not so much shorten time requirements of processes as extend the areas of the earth affected by them. The reason is clear. Since most *time* scales are fixed by human reaction times, habits, and other physiological and psychological factors, the effect of the increased speed of technological processes was to enlarge the *size* of units – political, organizational, economic, and cultural – affected by technological operations. That is, instead of performing the same operations as before in less time, now larger-scale operations were performed in the same time. This important evolution has a natural limit, that of the earth's actual size. The limit is now being reached, or at least closely approached."

#### Declaration of Competing Interest

None.

#### Acknowledgments

I am grateful to numerous individuals for their support, collaboration, and discussions that fu-



eled the ideas in this article. My student and post-doctoral collaborators have inspired me with their questions regarding future energy and transportation strategies. Colleagues in different disciplines, in various institutions, academies, work groups, and boards have challenged my views and motivated a closer study of recent progress in combustion and chemistry with regard to detail and to a larger energy and climate perspective. My selection of recent examples and results cannot do justice to all the substantial contributions that have been made in the area, and I am grateful to all who pointed seminal work out to me – any major omissions are entirely my fault. I am indebted to Tiziano Faravelli, Politecnico di Milano, Nils Hansen, Sandia National Laboratories, Brian Haynes, University of Sydney, Heinz Pitsch, RWTH Aachen University, Christof Schulz, University of Duisburg-Essen, Jürgen Troe, Göttingen University, and Hai Wang, Stanford University, for a critical reading of the manuscript and helpful comments. Contributions of Regine Schröder to part of the redaction are gratefully acknowledged. Last but not least, I wish to thank my late parents for supporting my education and fostering my scientific curiosity.

## References

- [1] C.J. Smith, P.M. Forster, M. Allen, et al., *Nat. Commun.* (2019) 1–10 (2019)10:101, doi:10.1038/s41467-018-07999-w.
- [2] D.P. van Vuuren, E. Stehfest, D.E.H.J. Gernaat, et al., *Nat. Clim. Change* 8 (2018) 391–397.
- [3] J. Lelieveld, K. Klingmüller, A. Pozzer, R.T. Burnett, A. Haines, V. Ramanathan, *Proc. Natl. Acad. Sci. U.S.A.* 116 (2019) 7192–7197.
- [4] S. Fuzzi, U. Baltensperger, K. Carslaw, et al., *Atmos. Chem. Phys.* 15 (2015) 8217–8299.
- [5] N.L. Ng, S.S. Brown, A.T. Archibald, et al., *Atmos. Chem. Phys.* 17 (2017) 2103–2162.
- [6] T.D. Gordon, A.A. Presto, N.T. Nguyen, et al., *Atmos. Chem. Phys.* 14 (2014) 4643–4659.
- [7] R.-J. Huang, Y. Zhang, C. Bozzetti, et al., *Nature* 514 (2014) 218–222.
- [8] R. Burnett, H. Chen, M. Szyszkowicz, et al., *Proc. Natl. Acad. Sci. U.S.A.* 115 (2018) 9592–9597.
- [9] R. Beelen, O. Raaschou-Nielsen, M. Stafoggia, et al., *Lancet* 383 (2014) 785–795.
- [10] J.G. Anderson, C.E. Clapp, *Phys. Chem. Chem. Phys.* 20 (2018) 10569–10587.
- [11] IPCC, *Climate Change 2013: The Physical Science Basis. Contribution of Working Group I to the Fifth Assessment Report of the Intergovernmental Panel on Climate Change*, in: T.F. Stocker, D. Qin, G.-K. Plattner, M. Tignor, S.K. Allen, J. Boschung, et al. (Eds.), Cambridge University Press, Cambridge, UK, New York, USA, 2013.
- [12] G. Kalghatgi, *Appl. Energy* 225 (2018) 965–974.
- [13] K. Kohse-Höinghaus, *Prog. Energy Combust. Sci.* 65 (2018) 1–5.
- [14] F.L. Dryer, *Proc. Combust. Inst.* 35 (2015) 117–144.
- [15] L.S. Tran, B. Sirjean, P.-A. Glaude, R. Fournet, F. Battin-Leclerc, *Energy* 43 (2012) 4–18.
- [16] S.M. Sarathy, P. Obwald, N. Hansen, K. Kohse-Höinghaus, *Prog. Energy Combust. Sci.* 44 (2014) 40–102.
- [17] W. Leitner, J. Klankermayer, S. Pischinger, H. Pitsch, K. Kohse-Höinghaus, *Angew. Chem. Int. Ed.* 56 (2017) 5412–5452.
- [18] M.A. Eldeeb, B. Akih-Kumgeh, *Energies* 11 (2018) 512, doi:10.3390/en11030512.
- [19] A.K. Agarwal, *Prog. Energy Combust. Sci.* 33 (2007) 233–271.
- [20] K. Kohse-Höinghaus, P. Obwald, T.A. Cool, et al., *Angew. Chem. Int. Ed.* 49 (2010) 3572–3597.
- [21] A. Omari, B. Heuser, S. Pischinger, C. Rüdinger, *Appl. Energy* 239 (2019) 1242–1249.
- [22] C. Barro, M. Parravicini, K. Boulouchos, A. Liati, *Fuel* 234 (2018) 1414–1421.
- [23] S. Deutz, D. Bongartz, B. Heuser, et al., *Energy Environ. Sci.* 11 (2018) 331–343.
- [24] H. Thomson, J.J. Corbett, J.J. Winebrake, *Energy Policy* 87 (2015) 153–167.
- [25] P. Gilbert, C. Walsh, M. Traut, U. Kesime, K. Pazouki, A. Murphy, *J. Clean. Prod.* 172 (2018) 855–866.
- [26] Z.-M. Yao, Z.-Q. Qian, R. Li, E. Hu, *Energy* 176 (2019) 991–1006.
- [27] J. Ling-Chin, A.P. Roskilly, *Appl. Energy* 181 (2016) 416–434.
- [28] C. Zhang, X. Hui, Y. Lin, C.-J. Sung, *Renew. Sustain. Energy Rev.* 54 (2016) 120–138.
- [29] R.L. Speth, C. Rojo, R. Malina, S.R.H. Barrett, *Atmos. Environ.* 105 (2015) 37–42.
- [30] S. de Jong, K. Antonissen, R. Hoefnagels, et al., *Biotechnol. Biofuels* 10:64 (2017), doi:10.1186/s13068-017-0739-7.
- [31] S.H. Won, P.S. Veloo, S. Dooley, et al., *Fuel* 168 (2016) 34–46.
- [32] A.F. Ghoniem, *Prog. Energy Combust. Sci.* 37 (2011) 15–51.
- [33] J.C. Koj, C. Wulf, P. Zapp, *Renew. Sustain. Energy Rev.* 112 (2019) 865–879.
- [34] J.A. Martens, A. Bogaerts, N. De Kimpe, et al., *ChemSusChem* 10 (2017) 1039–1055.
- [35] M. Härtl, A. Stadler, F. Backes, G. Wachtmeister, E. Jacob, *MTZ Worldwide* 07–08 (2017) 76–83.
- [36] T. Sinigaglia, F. Lewiski, M.E. Santos Martins, J.C. Mairesse Siluk, *Int. J. Hydrogen Energy* 42 (2017) 24597–24611.
- [37] P. Dimitriou, T. Tsujimura, *Int. J. Hydrogen Energy* 42 (2017) 24470–24486.
- [38] M. Ball, M. Weeda, *Int. J. Hydrogen Energy* 40 (2015) 7903–7919.
- [39] H. Kobayashi, A. Hayakawa, K.D. Kunkuma, A. Somarathne, E.C. Okafor, *Proc. Combust. Inst.* 37 (2019) 109–133.
- [40] A. Valera-Medina, H. Xiao, M. Owen-Jones, W.I.F. David, P.J. Bowen, *Prog. Energy Combust. Sci.* 69 (2018) 63–102.
- [41] A. Yapicioglu, I. Dincer, *Renew. Sustain. Energy Rev.* 103 (2019) 96–108.
- [42] A. Valera-Medina, M. Gutesa, H. Xiao, et al., *Int. J. Hydrogen Energy* 44 (2019) 8615–8626.
- [43] A. Grinberg Dana, O. Elishav, A. Bardow, G.E. Shter, G.S. Grader, *Angew. Chem. Int. Ed.* 55 (2016) 8798–8805.
- [44] A. Grinberg Dana, B. Mosevitzky, G. Tvil, M. Epstein, G.E. Shter, G.S. Grader, *Energy Fuels* 30 (2016) 2474–2477.

- [45] S. Schemme, R.C. Samsun, R. Peters, D. Stolten, *Fuel* 205 (2017) 198–221.
- [46] P. Preuster, C. Papp, P. Wasserscheid, *Acc. Chem. Res.* 50 (2017) 74–85.
- [47] T.J. Wallington, J.E. Anderson, D.J. Siegel, et al., *J. Chem. Educ.* 90 (2013) 440–445.
- [48] J.M. Bergthorson, *Prog. Energy Combust. Sci.* 68 (2018) 169–196.
- [49] M. Schiemann, J. Bergthorson, P. Fischer, V. Scherer, D. Taroata, G. Schmid, *Appl. Energy* 162 (2016) 948–965.
- [50] C. Schulz, T. Dreier, M. Fikri, H. Wiggers, *Proc. Combust. Inst.* 37 (2019) 83–108.
- [51] G.A. Kelesidis, E. Goudeli, S.E. Pratsinis, *Proc. Combust. Inst.* 36 (2017) 29–50.
- [52] S. Li, Y. Ren, P. Biswas, S.D. Tse, *Prog. Energy Combust. Sci.* 55 (2016) 1–59.
- [53] W.Y. Teoh, R. Amal, L. Mädler, *Nanoscale* 2 (2010) 1324–1347.
- [54] P.B. Neto, L. Buss, F. Meierhofer, H.F. Meier, U. Fritsching, D. Norler, *Chem. Eng. Process.* 129 (2018) 17–27.
- [55] V.G. Mavrantzas, S.E. Pratsinis, *Curr. Opin. Chem. Eng.* 23 (2019) 174–183.
- [56] M. Minnermann, H.K. Grossmann, S. Pokhrel, et al., *Catal. Today* 214 (2013) 90–99.
- [57] M. Gockeln, S. Pokhrel, F. Meierhofer, et al., *J. Power Sources* 374 (2018) 97–106.
- [58] S. Lee, K. Schneider, J. Schumann, A.K. Mogalicherla, P. Pfeifer, R. Dittmeyer, *Chem. Eng. Sci.* 138 (2015) 194–202.
- [59] M.R. Mulay, A. Chauhan, S. Patel, V. Balakrishnan, A. Halder, R. Vaish, *Carbon* 144 (2019) 684–712.
- [60] K.D. Esmeryan, C.E. Castano, A.H. Bressler, M. Abolghasemibizaki, R. Mohammadi, *Appl. Surf. Sci.* 369 (2016) 341–347.
- [61] H. Liu, T. Ye, C. Mao, *Angew. Chem. Int. Ed.* 46 (2007) 6473–6475.
- [62] B. Zhang, D. Wang, B. Yu, F. Zhou, W. Liu, *RSC Adv.* 4 (2014) 2586–2589.
- [63] P. Minutolo, M. Commodo, A. Santamaria, G. De Falco, A. D’Anna, *Carbon* 68 (2014) 138–148.
- [64] M. Qian, C. Xu, Y. Gao, *Mater. Sci. Eng. B* 238–239 (2018) 149–154.
- [65] G. De Falco, M. Commodo, M. Barra, et al., *Synth. Met.* 229 (2017) 89–99.
- [66] C. Liu, A.V. Singh, C. Saggese, et al., *Proc. Natl. Acad. Sci. U.S.A.* 116 (2019) 12692–12697.
- [67] S.B. Pope, *Proc. Combust. Inst.* 34 (2013) 1–31.
- [68] S. Hochgreb, *Proc. Combust. Inst.* 37 (2019) 2091–2107.
- [69] J.M. Bergthorson, M.J. Thomson, *Renew. Sustain. Energy Rev.* 42 (2015) 1393–1417.
- [70] F. Hoppe, B. Heuser, M. Thewes, et al., *Int. J. Engine Res.* 17 (2016) 16–27.
- [71] G.T. Kalghatgi, *Int. J. Engine Res.* 15 (2014) 383–398.
- [72] D.A. Splitter, R.D. Reitz, *Fuel* 118 (2014) 163–175.
- [73] D. Gschwend, P. Soltic, A. Wokaun, F. Vogel, *Energy Fuels* 33 (2019) 2186–2196.
- [74] R.K. Hanson, *Proc. Combust. Inst.* 33 (2011) 1–40.
- [75] C.S. Goldenstein, R.M. Sparrin, J.B. Jeffries, R.K. Hanson, *Prog. Energy Combust. Sci.* 60 (2016) 132–176.
- [76] W. Cai, C.F. Kaminski, *Prog. Energy Combust. Sci.* 59 (2016) 1–31.
- [77] J.P. Waclawek, C. Kristament, H. Moser, B. Lendl, *Opt. Express* 27 (2019) 12183.
- [78] A.C. Johansson, J. Westberg, G. Wysocki, A. Foltynowicz, *Appl. Phys. B* 124 (2018) 79.
- [79] M. Lamperti, B. AlSaif, D. Gatti, et al., *Sci. Rep.* (2018) 1–7 (2018) 8:1292, doi:10.1038/s41598-018-19188-2.
- [80] V. Sick, *Proc. Combust. Inst.* 34 (2013) 3509–3530.
- [81] A. Dreizler, B. Böhm, *Proc. Combust. Inst.* 35 (2015) 37–64.
- [82] A. Bohlin, M. Mann, B.D. Patterson, A. Dreizler, C.J. Kiewer, *Proc. Combust. Inst.* 35 (2015) 3723–3730.
- [83] C. Abram, B. Fond, F. Beyrau, *Prog. Energy Combust. Sci.* 64 (2018) 93–156.
- [84] H.A. Michelsen, *Proc. Combust. Inst.* 36 (2017) 717–735.
- [85] H.A. Michelsen, C. Schulz, G.J. Smallwood, S. Will, *Prog. Energy Combust. Sci.* 51 (2015) 2–48.
- [86] F.N. Egolopoulos, N. Hansen, Y. Ju, K. Kohse-Höinghaus, C.K. Law, F. Qi, *Prog. Energy Combust. Sci.* 43 (2014) 36–67.
- [87] Y. Li, F. Qi, *Acc. Chem. Res.* 43 (2010) 68–78.
- [88] F. Qi, *Proc. Combust. Inst.* 34 (2013) 33–63.
- [89] N. Hansen, T.A. Cool, P.R. Westmoreland, K. Kohse-Höinghaus, *Prog. Energy Combust. Sci.* 35 (2009) 168–191.
- [90] S.R. Leone, M. Ahmed, K.R. Wilson, *Phys. Chem. Chem. Phys.* 12 (2010) 6564–6578.
- [91] F. Battin-Leclerc, O. Herbinet, P.-A. Glaude, et al., *Angew. Chem. Int. Ed.* 49 (2010) 3169–3172.
- [92] K. Moshhammer, A.W. Jasper, D.M. Popolan-Vaida, et al., *J. Phys. Chem. A* 119 (2015) 7361–7374.
- [93] J.D. Savee, T.M. Selby, O. Welz, C.A. Taatjes, D.L. Osborn, *J. Phys. Chem. Lett.* 6 (2015) 4153–4158.
- [94] J.D. Savee, S. Borkar, O. Welz, B. Sztáray, C.A. Taatjes, D.L. Osborn, *J. Phys. Chem. A* 119 (2015) 7388–7403.
- [95] L.G. Dodson, L. Shen, J.D. Savee, et al., *J. Phys. Chem. A* 119 (2015) 1279–1291.
- [96] G. Marston, *Science* 335 (2012) 178–179.
- [97] O. Welz, J.D. Savee, D.L. Osborn, et al., *Science* 335 (2012) 204–207.
- [98] D. Schleier, P. Constantinidis, N. Faßheber, et al., *Phys. Chem. Chem. Phys.* 20 (2018) 10721–10731.
- [99] P. Obwald, P. Hemberger, T. Bierkandt, et al., *Rev. Sci. Instrum.* 85 (2014) 025101.
- [100] J. Krüger, G.A. Garcia, D. Felsmann, et al., *Phys. Chem. Chem. Phys.* 16 (2014) 22791–22804.
- [101] D. Felsmann, K. Moshhammer, J. Krüger, et al., *Proc. Combust. Inst.* 35 (2015) 779–786.
- [102] C. Hemken, U. Burke, I. Graf, et al., *Proc. Combust. Inst.* 36 (2017) 1175–1183.
- [103] P. Dagaut, S.M. Sarathy, M.J. Thomson, *Proc. Combust. Inst.* 32 (2009) 229–237.
- [104] N. Leplat, P. Dagaut, C. Togbé, J. Vandooren, *Combust. Flame* 158 (2011) 705–725.
- [105] Q. Guan, K.N. Urness, T.K. Ormond, D.E. David, G.B. Ellison, J.W. Daily, *Int. Rev. Phys. Chem.* 33 (2014) 447–487.
- [106] D.W. Kohn, H. Clauberg, P. Chen, *Rev. Sci. Instrum.* 63 (1992) 4003.
- [107] R.K. Hanson, D.F. Davidson, *Prog. Energy Combust. Sci.* 44 (2014) 103–114.

- [108] S.H. Dürrstein, M. Aghsaee, L. Jerig, M. Fikri, C. Schulz, *Rev. Sci. Instrum.* 82 (2011) 084103.
- [109] A.M. Ferris, D.F. Davidson, R.K. Hanson, *Combust. Flame* 195 (2018) 40–49.
- [110] S.E. Johnson, D.F. Davidson, R.K. Hanson, *Combust. Flame* 216 (2020) 161–173.
- [111] N.H. Pinkowski, S.J. Cassidy, D.F. Davidson, R.K. Hanson, *Fuel* 269 (2020) 117420.
- [112] Z.E. Loparo, E. Ninnemann, Q. Ru, K.L. Vodopyanov, S.S. Vasu, *Opt. Lett.* 45 (2020) 491–494.
- [113] G. Zhang, K. Khabibullin, A. Farooq, *Proc. Combust. Inst.* 37 (2019) 1445–1452.
- [114] M.B. Sajid, Et. Es-Sebbar, T. Javed, C. Fittschen, A. Farooq, *Int. J. Chem. Kinet.* 46 (2014) 275–284.
- [115] X. Chao, G. Shen, K. Sun, et al., *Proc. Combust. Inst.* 37 (2019) 1345–1353.
- [116] C.-J. Sung, H.J. Curran, *Prog. Energy Combust. Sci.* 44 (2014) 1–18.
- [117] E.F. Nasir, A. Farooq, *Proc. Combust. Inst.* 37 (2019) 1297–1304.
- [118] L. Cai, A. Ramalingam, H. Minwegen, K.A. Heufer, H. Pitsch, *Proc. Combust. Inst.* 37 (2019) 639–647.
- [119] K.M. Van Geem, S.P. Pyl, M.-F. Reyniers, J. Vermammen, J. Beens, G.B. Marin, *J. Chromatogr. A* 1217 (2010) 6623–6633.
- [120] C. Gessenhardt, C. Schulz, S.A. Kaiser, *Proc. Combust. Inst.* 35 (2015) 3697–3705.
- [121] B. Williams, M. Edwards, R. Stone, J. Williams, P. Ewart, *Combust. Flame* 161 (2014) 270–279.
- [122] F. Förster, C. Crua, M. Davy, P. Ewart, *Combust. Flame* 199 (2019) 249–257.
- [123] F. De Domenico, T.F. Guiberti, S. Hochgreb, W.L. Roberts, G. Magnotti, *Combust. Flame* 205 (2019) 336–344.
- [124] O. Witzel, A. Klein, S. Wagner, C. Meffert, C. Schulz, V. Ebert, *Appl. Phys. B* 109 (2012) 521–532.
- [125] S.-A. Tsekenis, K.G. Ramaswamy, N. Tait, Y. Hardalupas, A. Taylor, H. McCann, *Int. J. Engine Res.* 19 (2018) 718–731.
- [126] H. Liu, Q. Tang, X. Ran, X. Fang, M. Yao, *Proc. Combust. Inst.* 37 (2019) 4767–4775.
- [127] A. Mazacioglu, M.C. Gross, J. Kern, V. Sick, *Proc. Combust. Inst.* 37 (2019) 4993–5001.
- [128] M. Koegl, B. Hofbeck, S. Will, L. Zigan, *Proc. Combust. Inst.* 37 (2019) 4965–4972.
- [129] O. Diemel, R. Honza, C.-P. Ding, B. Böhm, S. Wagner, *Proc. Combust. Inst.* 37 (2019) 1453–1460.
- [130] B. Giechaskiel, M. Maricq, L. Ntziachristos, et al., *J. Aerosol Sci.* 67 (2014) 48–86.
- [131] R. O'Driscoll, H.M. ApSimon, T. Oxley, N. Molden, M.E.J. Stettler, A. Thiyagarajah, *Atmos. Environ.* 145 (2016) 81–91.
- [132] J.D.K. Bishop, N. Molden, A.M. Boies, *Appl. Energy* 242 (2019) 942–973.
- [133] M. Piszko, W. Wu, S. Will, M.H. Rausch, C. Giraudet, A.P. Fröba, *Fuel* 242 (2019) 562–572.
- [134] M. Bardi, A. Di Lella, G. Bruneaux, *Fuel* 239 (2019) 521–533.
- [135] W. Zhang, X. Li, L. Huang, M. Feng, *Fuel* 246 (2019) 454–465.
- [136] Y. Wang, A. Jain, W. Kulatilaka, *Proc. Combust. Inst.* 37 (2019) 1305–1312.
- [137] S. Hartl, R. Van Winkle, D. Geyer, et al., *Proc. Combust. Inst.* 37 (2019) 2297–2305.
- [138] S. Hartl, D. Geyer, A. Dreizler, G. Magnotti, R.S. Barlow, C. Hasse, *Combust. Flame* 189 (2018) 126–141.
- [139] A. Bhagatwala, Z. Luo, H. Shen, J.A. Sutton, T. Lu, J.H. Chen, *Proc. Combust. Inst.* 35 (2015) 1157–1166.
- [140] P. Malbois, E. Salaün, A. Vandel, et al., *Combust. Flame* 205 (2019) 109–122.
- [141] P. Malbois, E. Salaün, B. Rossow, et al., *Proc. Combust. Inst.* 37 (2019) 5215–5222.
- [142] R.D. Reitz, G. Duraisamy, *Prog. Energy Combust. Sci.* 46 (2015) 12–71.
- [143] M.P.B. Musculus, P.C. Miles, L.M. Pickett, *Prog. Energy Combust. Sci.* 39 (2013) 246–283.
- [144] S. Saxena, I.D. Bedoya, *Prog. Energy Combust. Sci.* 39 (2013) 457–488.
- [145] M. Yao, Z. Zheng, H. Liu, *Prog. Energy Combust. Sci.* 35 (2009) 398–437.
- [146] X. Han, M. Zheng, J. Wang, *Fuel* 109 (2013) 336–349.
- [147] X. Lu, D. Han, Z. Huang, *Prog. Energy Combust. Sci.* 37 (2011) 741–783.
- [148] Z. Zheng, C. Li, H. Liu, Y. Zhang, X. Zhong, M. Yao, *Fuel* 141 (2015) 109–119.
- [149] J. Zádor, C.A. Taatjes, R.X. Fernandes, *Prog. Energy Combust. Sci.* 37 (2011) 371–421.
- [150] F. Battin-Leclerc, *Prog. Energy Combust. Sci.* 34 (2008) 440–498.
- [151] J.D. Savee, E. Papajak, B. Rotavera, et al., *Science* 347 (2015) 643–646.
- [152] A. Jalan, I.M. Alecu, R. Meana-Pañeda, et al., *J. Am. Chem. Soc.* 135 (2013) 11100–11114.
- [153] F. Battin-Leclerc, O. Herbinet, P.-A. Glaude, et al., *Proc. Combust. Inst.* 33 (2011) 325–331.
- [154] Z. Wang, O. Herbinet, N. Hansen, F. Battin-Leclerc, *Prog. Energy Combust. Sci.* 73 (2019) 132–181.
- [155] A.J. Eskola, O. Welz, J. Zádor, et al., *Proc. Combust. Inst.* 35 (2015) 291–298.
- [156] A.J. Eskola, T.T. Pekkanen, S.P. Joshi, R.S. Timonen, S.J. Klippenstein, *Proc. Combust. Inst.* 37 (2019) 291–298.
- [157] J. Bugler, K.P. Somers, E.J. Silke, H.J. Curran, *J. Phys. Chem. A* 119 (2015) 7510–7527.
- [158] H. Zhao, A.G. Dana, Z. Zhang, W.H. Green, Y. Ju, *Energy* 165 (2018) 727–738.
- [159] H. Zhao, L. Wu, C. Patrick, et al., *Combust. Flame* 197 (2018) 78–87.
- [160] A. Rodriguez, O. Herbinet, Z. Wang, et al., *Proc. Combust. Inst.* 36 (2017) 333–342.
- [161] Z. Wang, O. Herbinet, Z. Cheng, et al., *J. Phys. Chem. A* 118 (2014) 5573–5594.
- [162] Z. Wang, L. Zhang, K. Moshhammer, et al., *Combust. Flame* 164 (2016) 386–396.
- [163] Z. Wang, D.M. Popolan-Vaida, B. Chen, et al., *Proc. Natl. Acad. Sci. U.S.A.* 114 (2017) 13102–13107.
- [164] Z. Wang, B. Chen, K. Moshhammer, et al., *Combust. Flame* 187 (2018) 199–216.
- [165] O. Welz, J. Zádor, J.D. Savee, et al., *Phys. Chem. Chem. Phys.* 14 (2012) 3112–3127.
- [166] A. Rodriguez, O. Frottier, O. Herbinet, et al., *J. Phys. Chem. A* 119 (2015) 7905–7923.
- [167] H. Guo, W. Sun, F.M. Haas, T. Farouk, F.L. Dryer, Y. Ju, *Proc. Combust. Inst.* 34 (2013) 573–581.
- [168] J. Eble, J. Kiecherer, M. Olzmann, *Z. Phys. Chem.* 231 (2017) 1603–1623.

- [169] L.-S. Tran, O. Herbinet, Y. Li, et al., *Proc. Combust. Inst.* 37 (2019) 511–519.
- [170] S. Thion, C. Togbé, Z. Serinyel, G. Dayma, *Combust. Flame* 185 (2017) 4–15.
- [171] L.-S. Tran, J. Wullenkord, Y. Li, et al., *Combust. Flame* 210 (2019) 9–24.
- [172] W. Sun, M. Lailliau, Z. Serinyel, et al., *Proc. Combust. Inst.* 37 (2019) 555–564.
- [173] M. Pelucchi, E. Ranzi, A. Frassoldati, T. Faravelli, *Proc. Combust. Inst.* 36 (2017) 393–401.
- [174] T. Tao, W. Sun, N. Hansen, et al., *Combust. Flame* 192 (2018) 120–129.
- [175] H. Hashemi, J.M. Christensen, L.B. Harding, S.J. Klippenstein, P. Glarborg, *Proc. Combust. Inst.* 37 (2019) 461–468.
- [176] L. Ye, L. Zhang, F. Qi, *Combust. Flame* 190 (2018) 119–132.
- [177] M. Djehiche, N.L. Le Tan, C.D. Jain, et al., *J. Am. Chem. Soc.* 136 (2014) 16689–16694.
- [178] J. Gao, Y. Nakamura, *Combust. Flame* 165 (2016) 68–82.
- [179] A. Stagni, D. Brignoli, M. Cinquanta, et al., *Combust. Flame* 188 (2018) 440–452.
- [180] W. Liang, C.K. Law, *Combust. Flame* 185 (2017) 75–81.
- [181] Y. Ju, C.B. Reuter, O.R. Yehia, T.I. Farouk, S.H. Won, *Prog. Energy Combust. Sci.* 75 (2019) 100787.
- [182] W. Sun, X. Gao, B. Wu, T. Ombrello, *Prog. Energy Combust. Sci.* 73 (2019) 1–25.
- [183] C.B. Reuter, M. Lee, S.H. Won, J. Yu, *Combust. Flame* 179 (2017) 23–32.
- [184] C.B. Reuter, S.H. Won, Y. Ju, *Proc. Combust. Inst.* 36 (2017) 1513–1522.
- [185] J.-B. Masurier, F. Foucher, G. Dayma, P. Dagaut, *Appl. Energy* 160 (2015) 566–580.
- [186] A. Alfazazi, A. Al-Omier, A. Secco, H. Selim, Y. Ju, S.M. Sarathy, *Combust. Flame* 191 (2018) 175–186.
- [187] M. Hajilou, E. Belmont, *Combust. Flame* 196 (2018) 416–423.
- [188] F.E. Alam, S.H. Won, F.L. Dryer, T.I. Farouk, *Combust. Flame* 195 (2018) 220–231.
- [189] O.R. Yehia, C.B. Reuter, Y. Ju, *Proc. Combust. Inst.* 37 (2019) 1717–1724.
- [190] V.R. Katta, W.M. Roquemore, *Proc. Combust. Inst.* 36 (2017) 1369–1376.
- [191] M. Lee, Y. Fan, C.B. Reuter, Y. Ju, Y. Suzuki, *Proc. Combust. Inst.* 37 (2019) 1749–1756.
- [192] A.G. Novoselov, C.K. Law, M.E. Mueller, *Proc. Combust. Inst.* 37 (2019) 2143–2150.
- [193] H. Wang, *Proc. Combust. Inst.* 33 (2011) 41–67.
- [194] P. Desgroux, X. Mercier, K.A. Thomson, *Proc. Combust. Inst.* 34 (2013) 1713–1738.
- [195] Y. Wang, S.H. Chung, *Prog. Energy Combust. Sci.* 74 (2019) 152–238.
- [196] S.J. Harris, M.M. Maricq, *J. Aerosol Sci.* 32 (2001) 749–764.
- [197] C.K. Gaddam, R.L. Vander Wal, *Combust. Flame* 160 (2013) 2517–2528.
- [198] S. Grimonprez, A. Faccinetto, S. Batut, J. Wu, P. Desgroux, D. Petitprez, *Aerosol Sci. Tech.* 52 (2018) 814–827.
- [199] K.O. Johansson, M.P. Head-Gordon, P.E. Schrader, K.R. Wilson, H.A. Michelsen, *Science* 361 (2018) 997–1000.
- [200] L. Zhao, R.I. Kaiser, B. Xu, et al., *Nat. Commun.* (2019) 1–8 (2019)10:1510, doi:10.1038/s41467-019-09224-8.
- [201] H. Jin, A. Frassoldati, Y. Wang, et al., *Combust. Flame* 162 (2015) 1692–1711.
- [202] N.A. Slavinskaya, U. Riedel, S.B. Dworkin, M.J. Thomson, *Combust. Flame* 159 (2012) 979–995.
- [203] S.B. Dworkin, Q. Zhang, M.J. Thomson, N.A. Slavinskaya, U. Riedel, *Combust. Flame* 158 (2011) 1682–1695.
- [204] H. Wang, M. Frenklach, *Combust. Flame* 110 (1997) 173–221.
- [205] B. Shukla, A. Miyoshi, M. Koshi, *J. Am. Soc. Mass Spectrom.* 21 (2010) 534–544.
- [206] B. Shukla, M. Koshi, *Combust. Flame* 159 (2012) 3589–3596.
- [207] M. Schenk, N. Hansen, H. Vieker, A. Beyer, A. Götzhäuser, K. Kohse-Höinghaus, *Proc. Combust. Inst.* 35 (2015) 1761–1769.
- [208] N. Hansen, M. Schenk, K. Moshhammer, K. Kohse-Höinghaus, *Combust. Flame* 180 (2017) 250–261.
- [209] A. Raj, *Combust. Flame* 204 (2019) 331–340.
- [210] A. Raj, P.L.W. Man, T.S. Totton, M. Sander, R.A. Shirley, M. Kraft, *Carbon* 48 (2010) 319–332.
- [211] X. You, R. Whitesides, D. Zubarev, W.A. Lester Jr., M. Frenklach, *Proc. Combust. Inst.* 33 (2011) 685–692.
- [212] Z.-B. Ding, E. Di Marco, M. Pelucchi, T. Faravelli, M. Maestri, *Chem. Eng. J.* 377 (2019) 119691.
- [213] C. Saggese, S. Ferrario, J. Camacho, et al., *Combust. Flame* 162 (2015) 3356–3369.
- [214] M. Frenklach, *Combust. Flame* 201 (2019) 148–159.
- [215] C. Shao, H. Wang, N. Atef, et al., *Proc. Combust. Inst.* 37 (2019) 993–1001.
- [216] M. Frenklach, R.I. Singh, A.M. Mebel, *Proc. Combust. Inst.* 37 (2019) 969–976.
- [217] A.M. Mebel, Y. Georgievskii, A.W. Jasper, S.J. Klippenstein, *Proc. Combust. Inst.* 36 (2017) 919–926.
- [218] T. Yang, T.P. Troy, B. Xu, et al., *Angew. Chem. Int. Ed.* 55 (2016) 14983–14987.
- [219] T. Yang, R.I. Kaiser, T.P. Troy, et al., *Angew. Chem. Int. Ed.* 56 (2017) 4515–4519.
- [220] P. Constantinidis, F. Hirsch, I. Fischer, A. Dey, A.M. Rijs, *J. Phys. Chem. A* 121 (2017) 181–191.
- [221] F. Hirsch, P. Constantinidis, I. Fischer, S. Bakels, A.M. Rijs, *Chem. Eur. J.* 24 (2018) 7647–7652.
- [222] F. Hirsch, E. Reusch, P. Constantinidis, et al., *J. Phys. Chem. A* 122 (2018) 9563–9571.
- [223] A. Golan, M. Ahmed, A.M. Mebel, R.I. Kaiser, *Phys. Chem. Chem. Phys.* 15 (2013) 341–347.
- [224] A.D. Oleinikov, V.N. Azyazov, A.M. Mebel, *Combust. Flame* 191 (2018) 309–319.
- [225] A.N. Morozov, A.M. Mebel, *J. Phys. Chem. A* 123 (2019) 1720–1729.
- [226] V.V. Kislov, A.I. Sadovnikov, A.M. Mebel, *J. Phys. Chem. A* 117 (2013) 4794–4816.
- [227] V.V. Kislov, A.M. Mebel, *J. Phys. Chem. A* 111 (2007) 9532–9543.
- [228] V.V. Kislov, R.I. Singh, D.E. Edwards, A.M. Mebel, M. Frenklach, *Proc. Combust. Inst.* 35 (2015) 1861–1869.

- [229] W. Pejpichestakul, E. Ranzi, M. Pelucchi, et al., *Proc. Combust. Inst.* 37 (2019) 1013–1021.
- [230] W. Pejpichestakul, A. Frassoldati, A. Parente, T. Faravelli, *Fuel* 234 (2018) 199–206.
- [231] D.D. Das, P.C. St. John, C.S. McEnally, S. Kim, L.D. Pfefferle, *Combust. Flame* 190 (2018) 349–364.
- [232] M. Conturso, M. Sirignano, A. D’Anna, *Fuel* 175 (2016) 137–145.
- [233] L.-S. Tran, B. Sirjean, P.-A. Glaude, K. Kohse-Höinghaus, F. Battin-Leclerc, *Proc. Combust. Inst.* 35 (2015) 1735–1743.
- [234] H. Liu, P. Zhang, X. Liu, et al., *Combust. Flame* 188 (2018) 129–141.
- [235] L. Ruwe, L. Cai, K. Moshhammer, N. Hansen, H. Pitsch, K. Kohse-Höinghaus, *Combust. Flame* 206 (2019) 411–423.
- [236] L. Ruwe, K. Moshhammer, N. Hansen, K. Kohse-Höinghaus, *Phys. Chem. Chem. Phys.* 20 (2018) 10780–10795.
- [237] L. Ruwe, K. Moshhammer, N. Hansen, K. Kohse-Höinghaus, *Combust. Flame* 175 (2017) 34–46.
- [238] L. León, L. Ruwe, K. Moshhammer, et al., *Combust. Flame* 208 (2019) 182–197.
- [239] C. Irimiea, A. Faccinnetto, X. Mercier, et al., *Carbon* 144 (2019) 815–830.
- [240] S.A. Skeen, H.A. Michelsen, K.R. Wilson, D.M. Popolan, A. Violi, N. Hansen, *J. Aerosol Sci.* 58 (2013) 86–102.
- [241] A. Faccinnetto, C. Focsa, P. Desgroux, M. Ziskind, *Environ. Sci. Technol.* 49 (2015) 10510–10520.
- [242] T. Mouton, X. Mercier, P. Desgroux, *Appl. Phys. B* 122:123 (2016) 1–13.
- [243] J.H. Miller, *Proc. Combust. Inst.* 30 (2005) 1381–1388.
- [244] R.L. Vander Wal, A.J. Tomasek, *Combust. Flame* 136 (2004) 129–140.
- [245] R.L. Vander Wal, C.J. Mueller, *Energy Fuels* 20 (2006) 2364–2369.
- [246] R.L. Vander Wal, V.M. Bryg, M.D. Hays, *Aerosol Sci.* 41 (2010) 108–117.
- [247] K. Yehliu, R.L. Vander Wal, O. Armas, A.L. Boehman, *Combust. Flame* 159 (2012) 3597–3606.
- [248] T.S. Totton, D. Chakrabarti, A.J. Misquitta, M. Sander, D.J. Wales, M. Kraft, *Combust. Flame* 157 (2010) 909–914.
- [249] H. Jander, C. Borchers, H. Böhm, A. Emelianov, C. Schulz, *Carbon* 150 (2019) 244–258.
- [250] A. Giordana, A. Maranzana, G. Tonachini, *J. Phys. Chem. A* 115 (2011) 17237–17251.
- [251] H. Bladh, N.-E. Olofsson, T. Mouton, et al., *Proc. Combust. Inst.* 35 (2015) 1843–1850.
- [252] C. Betranccourt, F. Liu, P. Desgroux, et al., *Aerosol Sci. Technol.* 51 (2017) 916–935.
- [253] F.J. Bauer, K.J. Daun, F.J.T. Huber, S. Will, *Appl. Phys. B* 125:109 (2019) 1–15.
- [254] B.D. Adamson, S.A. Skeen, M. Ahmed, N. Hansen, *J. Phys. Chem. A* 122 (2018) 9338–9349.
- [255] M. Schenk, S. Lieb, H. Vieker, et al., *ChemPhysChem* 14 (2013) 3248–3254.
- [256] F. Schulz, M. Commodo, K. Kaiser, et al., *Proc. Combust. Inst.* 37 (2019) 885–892.
- [257] M. Commodo, K. Kaiser, G. De Falco, et al., *Combust. Flame* 205 (2019) 154–164.
- [258] B. Apicella, P. Prè, M. Alfè, et al., *Proc. Combust. Inst.* 35 (2015) 1895–1902.
- [259] C. Saggese, A. Cuoci, A. Frassoldati, et al., *Combust. Flame* 167 (2016) 184–197.
- [260] C. Saggese, A.V. Singh, X. Xue, et al., *Fuel* 235 (2019) 350–362.
- [261] H.J. Curran, *Proc. Combust. Inst.* 37 (2019) 57–81.
- [262] J.A. Miller, M.J. Pilling, J. Troe, *Proc. Combust. Inst.* 30 (2005) 43–88.
- [263] S.J. Klippenstein, *Proc. Combust. Inst.* 36 (2017) 77–111.
- [264] A.A. Konnov, *Combust. Flame* 203 (2019) 14–22.
- [265] T. Lu, C.K. Law, *Prog. Energy Combust. Sci.* 35 (2009) 192–215.
- [266] T. Faravelli, F. Manenti, E. Ranzi (Eds.), *Computer-Aided Chemical Engineering*, 45, Elsevier, 2019, eBook ISBN: 9780444640888, 1034 pp.
- [267] P. Glarborg, *Computer-Aided Chemical Engineering*, 45, Elsevier, 2019, pp. 603–745. eBook ISBN: 9780444640888.
- [268] P. Glarborg, J.A. Miller, B. Ruscic, S.J. Klippenstein, *Prog. Energy Combust. Sci.* 67 (2018) 31–68.
- [269] A. Frassoldati, T. Faravelli, E. Ranzi, *Int. J. Hydrogen Energy* 31 (2006) 2310–2328.
- [270] F. Buda, R. Bounaceur, V. Warth, P.A. Glaude, R. Fournet, F. Battin-Leclerc, *Combust. Flame* 142 (2005) 170–186.
- [271] G. Blanquart, P. Pepiot-Desjardins, H. Pitsch, *Combust. Flame* 156 (2009) 588–607.
- [272] C.K. Westbrook, W.J. Pitz, O. Herbinet, H.J. Curran, E.J. Silke, *Combust. Flame* 156 (2009) 181–199.
- [273] S.M. Sarathy, C.K. Westbrook, M. Mehl, et al., *Combust. Flame* 158 (2011) 2338–2357.
- [274] J.Y.W. Lai, K.C. Lin, A. Violi, *Prog. Energy Combust. Sci.* 37 (2011) 1–14.
- [275] L. Coniglio, H. Bennadji, P.A. Glaude, O. Herbinet, F. Billaud, *Prog. Energy Combust. Sci.* 39 (2013) 340–382.
- [276] O. Herbinet, W.J. Pitz, C.K. Westbrook, *Combust. Flame* 157 (2010) 893–908.
- [277] R. Xu, H. Wang, *Proc. Combust. Inst.* 37 (2019) 613–620.
- [278] H. Wang, R. Xu, K. Wang, et al., *Combust. Flame* 193 (2018) 502–519.
- [279] R. Xu, K. Wang, S. Banerjee, et al., *Combust. Flame* 193 (2018) 520–537.
- [280] P.T. Lynch, T.P. Troy, M. Ahmed, R.S. Tranter, *Anal. Chem.* 87 (2015) 2345–2352.
- [281] N. Hansen, R.S. Tranter, J.B. Randazzo, J.P.A. Lockhart, A.L. Kastengren, *Proc. Combust. Inst.* 37 (2019) 1401–1408.
- [282] N. Hansen, R.S. Tranter, K. Moshhammer, et al., *Combust. Flame* 181 (2017) 214–224.
- [283] U. Struckmeier, P. Obwald, T. Kasper, et al., *Z. Phys. Chem.* 223 (2009) 503–537.
- [284] V. Gururajan, F.N. Egolfopoulos, K. Kohse-Höinghaus, *Proc. Combust. Inst.* 35 (2015) 821–829.
- [285] L. Deng, A. Kempf, O. Hasemann, O.P. Korobeinichev, I. Wlokas, *Combust. Flame* 162 (2015) 1737–1747.
- [286] D. Krüger, P. Obwald, M. Köhler, P. Hemberger, T. Bierkandt, T. Kasper, *Proc. Combust. Inst.* 37 (2019) 1563–1570.
- [287] X. Zhang, Y. Zhang, T. Li, et al., *Combust. Flame* 204 (2019) 260–267.
- [288] N. Hansen, J. Wullenkord, D.A. Obenchain, I. Graf, K. Kohse-Höinghaus, J.-U. Grabow, *RSC Adv.* 7 (2017) 37867–37872.

- [289] J. Pieper, S. Schmitt, C. Hemken, et al., *Z. Phys. Chem.* 232 (2018) 153–187.
- [290] C. Huang, B. Yang, F. Zhang, *J. Chem. Phys.* 150 (2019) 164305.
- [291] C. Bahrini, P. Morajkar, C. Schoemaeker, et al., *Phys. Chem. Chem. Phys.* 15 (2013) 19686–19698.
- [292] N.L. Le Tan, M. Djehiche, C.D. Jain, P. Dagaut, G. Dayma, *Fuel* 158 (2015) 248–252.
- [293] P. Oßwald, H. Güldenber, K. Kohse-Höinghaus, B. Yang, T. Yuan, F. Qi, *Combust. Flame* 158 (2011) 2–15.
- [294] N. Hansen, X. He, R. Griggs, K. Moshhammer, *Proc. Combust. Inst.* 37 (2019) 743–750.
- [295] N. Atef, G. Kukkadapu, S.Y. Mohamed, et al., *Combust. Flame* 178 (2017) 111–134.
- [296] H.J. Curran, P. Gaffuri, W.J. Pitz, C.K. Westbrook, *Combust. Flame* 129 (2002) 253–280.
- [297] H.J. Curran, P. Gaffuri, W.J. Pitz, C.K. Westbrook, *Combust. Flame* 114 (1998) 149–177.
- [298] K. Zhang, C. Banyon, H. Bugler, et al., *Combust. Flame* 172 (2016) 116–135.
- [299] K. Narayanaswamy, P. Pepiot, H. Pitsch, *Combust. Flame* 161 (2014) 866–884.
- [300] C. Saggese, A. Frassoldati, A. Cuoci, T. Faravelli, E. Ranzi, *Combust. Flame* 160 (2013) 1168–1190.
- [301] K. Narayanaswamy, G. Blanquart, H. Pitsch, *Combust. Flame* 157 (2010) 1879–1898.
- [302] L. Cai, H. Pitsch, *Combust. Flame* 162 (2015) 1623–1637.
- [303] W.K. Metcalfe, S.M. Burke, S.S. Ahmed, H.J. Curran, *Int. J. Chem. Kinet.* 45 (2013) 638–675.
- [304] S.M. Sarathy, S. Vranckx, K. Yasunaga, et al., *Combust. Flame* 159 (2012) 2028–2055.
- [305] K.A. Heufer, S.M. Sarathy, H.J. Curran, A.C. Davis, C.K. Westbrook, W.J. Pitz, *Energy Fuels* 26 (2012) 6678–6685.
- [306] M. Köhler, T. Kathrotia, P. Oßwald, M.L. Fischer-Tammer, K. Moshhammer, U. Riedel, *Combust. Flame* 162 (2015) 3197–3209.
- [307] L. Cai, Y. Uygun, C. Toghé, et al., *Proc. Combust. Inst.* 35 (2015) 419–427.
- [308] B. Heuser, P. Mauermann, R. Wankhade, F. Kremer, S. Pischinger, *Int. J. Engine Res.* 16 (2015) 627–638.
- [309] B. Kerschgens, L. Cai, H. Pitsch, B. Heuser, S. Pischinger, *Combust. Flame* 163 (2016) 66–78.
- [310] L. Cai, A. Sudholt, D.J. Lee, et al., *Combust. Flame* 161 (2014) 798–809.
- [311] Y. Sakai, J. Herzler, M. Werler, C. Schulz, M. Fikri, *Proc. Combust. Inst.* 36 (2017) 195–202.
- [312] F. Hoppe, U. Burke, M. Thewes, A. Heufer, F. Kremer, S. Pischinger, *Fuel* 167 (2016) 106–117.
- [313] K.P. Somers, J.M. Simmie, W.K. Metcalfe, H.J. Curran, *Phys. Chem. Chem. Phys.* 16 (2014) 5349–5367.
- [314] L.-S. Tran, Z. Wang, H.-H. Carstensen, C. Hemken, F. Battin-Leclerc, K. Kohse-Höinghaus, *Combust. Flame* 181 (2017) 251–269.
- [315] D. Felsmann, H. Zhao, Q. Wang, et al., *Proc. Combust. Inst.* 36 (2017) 543–551.
- [316] Y.L. Wang, D.J. Lee, C.K. Westbrook, F.N. Egolopoulos, T.T. Tsotsis, *Combust. Flame* 161 (2014) 810–817.
- [317] W. Sun, B. Yang, N. Hansen, et al., *Combust. Flame* 164 (2016) 224–238.
- [318] U. Burke, K.P. Somers, P. O’Toole, et al., *Combust. Flame* 162 (2015) 315–330.
- [319] H. Jin, J. Pieper, C. Hemken, E. Brüner, L. Ruwe, K. Kohse-Höinghaus, *Combust. Flame* 193 (2018) 36–53.
- [320] L.-S. Tran, J. Pieper, M. Zeng, et al., *Combust. Flame* 175 (2017) 47–59.
- [321] M. Salamanca, J. Wullenkord, I. Graf, S. Schmitt, L. Ruwe, K. Kohse-Höinghaus, *Proc. Combust. Inst.* 37 (2019) 1725–1732.
- [322] Z. Tian, Y. Li, L. Zhang, P. Glarborg, F. Qi, *Combust. Flame* 156 (2009) 1413–1426.
- [323] Y. Song, H. Hashemi, J.M. Christensen, C. Zou, P. Marshall, P. Glarborg, *Fuel* 181 (2016) 358–365.
- [324] A. Lucassen, K. Zhang, J. Warkentin, et al., *Combust. Flame* 159 (2012) 2254–2279.
- [325] E. Ranzi, A. Frassoldati, R. Grana, et al., *Prog. Energy Combust. Sci.* 38 (2012) 468–501.
- [326] C. Saggese, A. Frassoldati, A. Cuoci, T. Faravelli, E. Ranzi, *Proc. Combust. Inst.* 34 (2013) 427–434.
- [327] P. Pepiot, L. Cai, H. Pitsch, *Computer-Aided Chemical Engineering*, 45, Elsevier, 2019, pp. 799–827. eBook ISBN: 9780444640888.
- [328] A. Stagni, A. Cuoci, A. Frassoldati, T. Faravelli, E. Ranzi, *Ind. Eng. Chem. Res.* 53 (2014) 9004–9016.
- [329] K. Wang, A.M. Dean, *Computer-Aided Chemical Engineering*, 45, Elsevier, 2019, pp. 203–257. eBook ISBN: 9780444640888.
- [330] L. Cai, H. Pitsch, *Combust. Flame* 161 (2014) 405–415.
- [331] P. Pepiot-Desjardins, H. Pitsch, R. Malhotra, S.R. Kirby, A.L. Boehman, *Combust. Flame* 154 (2008) 191–205.
- [332] K. Narayanaswamy, H. Pitsch, P. Pepiot, *Combust. Flame* 165 (2016) 288–309.
- [333] W.H. Green, *Computer-Aided Chemical Engineering*, 45, Elsevier, 2019, pp. 259–294. eBook ISBN: 9780444640888.
- [334] C.W. Gao, J.W. Allen, W.H. Green, R.H. West, *Comput. Phys. Commun.* 203 (2016) 212–225.
- [335] R. Van de Vijver, B.R. Devocht, K.M. Van Geem, J.W. Thybaut, G.B. Marin, *Curr. Opin. Chem. Eng.* 13 (2016) 142–149.
- [336] N.M. Vandewiele, K.M. Van Geem, M.-F. Reyniers, G.B. Marin, *Chem. Eng. J.* 207–208 (2012) 526–538.
- [337] M. Keçeli, S.N. Elliott, Y.-P. Li, et al., *Proc. Combust. Inst.* 37 (2019) 363–371.
- [338] S.J. Klippenstein, L.B. Harding, B. Ruscic, *J. Phys. Chem. A* 121 (2017) 6580–6602.
- [339] K. Han, W.H. Green, R.H. West, *Comput. Chem. Eng.* 100 (2017) 1–8.
- [340] R. Van de Vijver, K.M. Van Geem, G.B. Marin, *Proc. Combust. Inst.* 37 (2019) 283–290.
- [341] M.J. Pilling, *Science* 346 (2014) 1183–1184.
- [342] A.W. Jasper, K.M. Pelzer, J.A. Miller, E. Kamarchik, L.B. Harding, S.J. Klippenstein, *Science* 346 (2014) 1212–1215.
- [343] K. Hoyermann, F. Mauß, M. Olzmann, O. Welz, T. Zeuch, *Phys. Chem. Chem. Phys.* 19 (2017) 18128–18146.
- [344] D.R. Glowacki, C.-H. Liang, C. Morley, M.J. Pilling, S.H. Robertson, *J. Phys. Chem. A* 116 (2012) 9545–9560.
- [345] T. Lu, C.K. Law, *Proc. Combust. Inst.* 30 (2005) 1333–1341.

- [346] P. Pepiot-Desjardins, H. Pitsch, *Combust. Flame* 154 (2008) 67–81.
- [347] A. Stagni, A. Frassoldati, A. Cuoci, T. Faravelli, E. Ranzi, *Combust. Flame* 163 (2016) 382–393.
- [348] L. Cai, H. Pitsch, S.Y. Mohamed, et al., *Combust. Flame* 173 (2016) 468–482.
- [349] E. Ranzi, A. Frassoldati, A. Stagni, M. Pelucchi, A. Cuoci, T. Faravelli, *Int. J. Chem. Kinet.* 46 (2014) 512–542.
- [350] Y. Chang, M. Jia, Y. Li, et al., *Proc. Combust. Inst.* 35 (2015) 3037–3044.
- [351] S. Ren, Z. Wang, B. Li, H. Liu, J. Wang, *Fuel* 238 (2019) 208–224.
- [352] L. Bates, D. Bradley, I. Gorbatenko, A.S. Tomlin, *Combust. Flame* 185 (2017) 105–116.
- [353] H. Wang, *Computer-Aided Chemical Engineering*, 45, Elsevier, 2019, pp. 723–762. eBook ISBN: 9780444640888.
- [354] A.S. Tomlin, *Proc. Combust. Sci.* 34 (2013) 159–176.
- [355] H. Wang, D.A. Sheen, *Prog. Energy Combust. Sci.* 47 (2015) 1–31.
- [356] É. Valkó, T. Varga, A.S. Tomlin, Á. Busai, T. Turányi, *J. Math. Chem.* 56 (2018) 864–889.
- [357] É. Valkó, T. Varga, A.S. Tomlin, T. Turányi, *Proc. Combust. Inst.* 36 (2017) 681–689.
- [358] F. vom Lehn, L. Cai, H. Pitsch, *Proc. Combust. Inst.* 37 (2019) 771–779.
- [359] T. Nagy, T. Turányi, *Reliab. Eng. Syst. Safe.* 107 (2012) 29–34.
- [360] T. Varga, T. Nagy, C. Olm, et al., *Proc. Combust. Inst.* 35 (2015) 589–596.
- [361] Y. Tao, G.P. Smith, H. Wang, *Combust. Flame* 195 (2018) 18–29.
- [362] C. Olm, T. Varga, É. Valkó, H.J. Curran, T. Turányi, *Combust. Flame* 186 (2017) 45–64.
- [363] R.J. Shannon, A.S. Tomlin, S.H. Robertson, M.A. Blitz, M.J. Pilling, P.W. Seakins, *J. Phys. Chem. A* 119 (2015) 7430–7438.
- [364] W. Sun, J. Wang, C. Huang, N. Hansen, B. Yang, *Combust. Flame* 205 (2019) 11–21.
- [365] S. Li, B. Yang, F. Qi, *Combust. Flame* 168 (2016) 53–64.
- [366] R. Ranade, S. Alqahtani, A. Farooq, T. Echehki, *Fuel* 241 (2019) 625–636.
- [367] W. Ji, J. Wang, O. Zahm, et al., *Combust. Flame* 190 (2018) 146–157.
- [368] S. Li, T. Tao, J. Wang, B. Yang, C.K. Law, F. Qi, *Proc. Combust. Inst.* 36 (2017) 709–716.
- [369] M.S. Bernardi, M. Pelucchi, A. Stagni, et al., *Combust. Flame* 168 (2016) 186–203.
- [370] M. Pelucchi, U. Burke, L. Cai, et al. Towards a common C0-C2 mechanism: a critical evaluation of rate constants for syngas combustion kinetics, *Proceedings of the 1st International Conference on Smart Energy Carriers*, Naples, Italy, Jan. 21–23, 2019, paper ICSEC – IV-4.
- [371] J.N. Crowley, M. Ammann, R.A. Cox, et al., *Atmos. Chem. Phys.* 10 (2010) 9059–9223.
- [372] M. Haghightalari, J. Hachmann, *Curr. Opin. Chem. Eng.* 23 (2019) 51–57.
- [373] B.S. Haynes, *Proc. Combust. Inst.* 37 (2019) 1–32.
- [374] C.A. Taatjes, O. Welz, A.J. Eskola, et al., *Science* 340 (2013) 177–180.
- [375] F. Mühlberger, R. Zimmermann, A. Kettrup, *Anal. Chem.* 73 (2001) 3590–3604.
- [376] P. Fjodorow, S. Löhden, O. Hellmig, C. Schulz, V.M. Baev, *Opt. Express* 27 (2019) 11122–11136.
- [377] G. Coskun, M. Jonsson, J. Bood, et al., *Combust. Flame* (2015) 3131–3139.
- [378] L.A. Bahr, P. Fendt, Y. Pang, et al., *Opt. Lett.* 43 (2018) 4477–4480.
- [379] L.A. Bahr, T. Dousset, S. Will, A.S. Braeuer, *J. Aerosol Sci.* 126 (2018) 143–151.
- [380] M. Simeni Simeni, E. Baratte, Y.-C. Hung, K. Frederickson, I.V. Adamovich, *Proc. Combust. Inst.* 37 (2019) 1497–1504.
- [381] D.G. Park, S.H. Chung, M.S. Cha, *Combust. Flame* 198 (2018) 240–248.
- [382] A. Jocher, H. Pitsch, T. Gomez, G. Legros, *Proc. Combust. Inst.* 35 (2015) 889–895.
- [383] A. Starikovskiy, N. Aleksandrov, *Prog. Energy Combust. Sci.* 39 (2013) 61–110.
- [384] Y. Ju, W. Sun, *Prog. Energy Combust. Sci.* 48 (2015) 21–83.
- [385] G. Vanhove, M.-A. Boumehdi, S. Shcherbanev, Y. Fenard, P. Desgroux, S.M. Starikovskaia, *Proc. Combust. Inst.* 36 (2017) 4137–4143.
- [386] Y. Ju, J.K. Lefkowitz, C.B. Reuter, et al., *Plasma Chem. Plasma Process* 36 (2016) 85–105.
- [387] A. Rouso, X. Mao, Q. Chen, Y. Ju, *Proc. Combust. Inst.* 37 (2019) 5595–5603.
- [388] R. Zhang, H. Liao, J. Yang, X. Fan, B. Yang, *Proc. Combust. Inst.* 37 (2019) 5577–5586.
- [389] R.B. Miles, J.B. Michael, C.M. Limbach, et al., *Phil. Trans. R. Soc. A* 373 (2015) 20140338.
- [390] S. Wang, J. Yu, W. Cheng, et al., *Chem. Phys. Lett.* 730 (2019) 399–406.
- [391] F. Kunze, S. Kuns, M. Spree, et al., *Powder Technol.* 342 (2019) 880–886.
- [392] R. Snoeckx, W. Wang, X. Zhang, M.S. Cha, A. Bogaerts, *Sci. Rep.* (2018) 1–7 (2018) 8:15929, doi:10.1038/s41598-018-34359-x.
- [393] M.B. Toftegaard, J. Brix, P.A. Jensen, P. Glarborg, A.D. Jensen, *Prog. Energy Combust. Sci.* 36 (2010) 581–625.
- [394] M. Baroncelli, D. Felsmann, N. Hansen, H. Pitsch, *Combust. Flame* 204 (2019) 320–330.
- [395] D. Felsmann, M. Baroncelli, J. Beeckmann, H. Pitsch, *Proc. Combust. Inst.* 37 (2019) 2801–2808.
- [396] J. Köser, T. Li, N. Vorobiev, A. Dreizler, M. Schiemann, B. Böhm, *Proc. Combust. Inst.* 37 (2019) 2893–2900.
- [397] G.L. Tufano, O.T. Stein, A. Kronenburg, et al., *Fuel* 240 (2019) 75–83.
- [398] Z. Zhou, C. Liu, X. Chen, et al., *J. Anal. Appl. Pyrolysis* 137 (2019) 285–292.
- [399] R. Sur, K. Sun, J.B. Jeffries, J.G. Socha, R.K. Hanson, *Fuel* 150 (2015) 102–111.
- [400] T. Li, Ø. Skreiberg, T. Løvås, P. Glarborg, *Fuel* 254 (2019) 115569.
- [401] S. Hameed, A. Sharma, V. Pareek, H. Wu, Y. Yu, *Biomass Bioenergy* 123 (2019) 104–122.
- [402] S. Wang, G. Dai, H. Yang, Z. Luo, *Prog. Energy Combust. Sci.* 62 (2017) 33–86.
- [403] P.R. Westmoreland, *Curr. Opin. Chem. Eng.* 23 (2019) 123–129.
- [404] V.S. Sikarwar, M. Zhao, P.S. Fennell, N. Shah, E.J. Anthony, *Prog. Energy Combust. Sci.* 61 (2017) 189–248.
- [405] N. Dahmen, E. Henrich, E. Dinjus, F. Weirich, *Energy Sustain. Soc.* 2:3 (2012) 1–44.
- [406] P. Azadi, O.R. Inderwildi, R. Farnood, D.A. King, *Renew. Sustain. Energy Rev.* 21 (2013) 506–523.

- [407] W.-C. Wang, L. Tao, *Renew. Sustain. Energy Rev.* 53 (2016) 801–822.
- [408] Z. Zhou, X. Chen, H. Ma, C. Liu, C. Zhou, F. Qi, *Fuel* 235 (2019) 962–971.
- [409] I. Delidovich, R. Palkovits, *ChemSusChem* 9 (2016) 547–561.
- [410] I. Delidovich, K. Leonhard, R. Palkovits, *Energy Environ. Sci.* 7 (2014) 2803–2830.
- [411] J. Mantzaras, *Prog. Energy Combust. Sci.* 70 (2019) 169–211.
- [412] A. Zellner, R. Suntz, O. Deutschmann, *Angew. Chem. Int. Ed.* 54 (2015) 2653–2655.
- [413] A.M. Beale, F. Gao, I. Lezcano-Gonzalez, C.H.F. Peden, J. Szanyi, *Chem. Soc. Rev.* 44 (2015) 7371–7405.
- [414] B. Torkashvand, L. Maier, M. Hettel, T. Schedlbauer, J.-D. Grunwaldt, O. Deutschmann, *Chem. Eng Sci.* 195 (2019) 841–850.
- [415] D. Fino, S. Bensaid, M. Piumetti, N. Russo, *Appl. Catal. A: Gen.* 509 (2016) 75–96.
- [416] R. Ramdas, E. Nowicka, R. Jenkins, D. Sellick, C. Davies, S. Golunski, *Appl. Catal. B: Environ.* 176–177 (2015) 436–443.
- [417] H. Stotz, L. Maier, A. Boubnov, A.T. Gremminger, J.-D. Grunwaldt, O. Deutschmann, *J. Catal.* 370 (2019) 152–175.
- [418] R. Sui, J. Mantzaras, R. Bombach, *Proc. Combust. Inst.* 36 (2017) 4313–4320.
- [419] B.O. Arani, J. Mantzaras, C.E. Frouzakis, K. Boulouchos, *Combust. Flame* 198 (2018) 320–333.
- [420] Y. Wang, H. Zeng, A. Banerjee, Y. Shi, O. Deutschmann, N. Cai, *Energy Fuels* 30 (2016) 7778–7785.
- [421] D. Kaczmarek, B. Atakan, T. Kasper, *Combust. Flame* 205 (2019) 345–357.
- [422] Y.X. Yin, B. Yang, H. Wang, S.L. Anderson, C.K. Law, *Proc. Combust. Inst.* 35 (2015) 2233–2240.
- [423] J.N. Bär, C. Antinori, L. Maier, O. Deutschmann, *Catalysts* 6 (2016) 207, doi:10.3390/catal6120207.
- [424] M.S. Kamal, S.A. Razzak, M.M. Hossain, *Atmos. Environ.* 140 (2016) 117–134.
- [425] H. Xu, N. Yan, Z. Qu, et al., *Environ. Sci. Technol.* 51 (2017) 8879–8892.
- [426] Z. Zhou, X. Chen, Y. Wang, et al., *Bioresour. Technol.* 275 (2019) 130–137.
- [427] F. Jiao, J. Li, X. Pan, et al., *Science* 351 (2016) 1065–1068.
- [428] P. Hemberger, V.B.F. Custodis, A. Bodi, T. Gerber, J.A. van Bokhoven, *Nat. Commun.* (2017) 1–9 8:15946, doi:10.1038/ncomms15946.
- [429] G. Zichitella, M. Scharfe, B. Puértolas, et al., *Angew. Chem. Int. Ed.* 58 (2019) 5877–5881.
- [430] Y. Liu, F.M. Kirchberger, S. Müller, et al., *Nat. Commun.* (2019) 1–9 (2019) 10:1462, doi:10.1038/s41467-019-09449-7.
- [431] U. Olsbye, S. Svelle, M. Bjørgen, et al., *Angew. Chem. Int. Ed.* 51 (2012) 5810–5831.
- [432] K. Hemelsoet, J. Van der Mynsbrugge, K. De Wispelaere, M. Waroquier, V. Van Speybroeck, *ChemPhysChem* 14 (2013) 1526–1545.
- [433] A.D. Chowdhury, K. Houben, G.T. Whiting, et al., *Angew. Chem. Int. Ed.* 55 (2016) 15840–15845.
- [434] P. Tian, Y. Wei, M. Ye, Z. Liu, *ACS Catal.* 5 (2015) 1922–1938.
- [435] J.-L. Liu, R. Snoeeks, M.S. Cha, *J. Phys. D: Appl. Phys.* 51 (2018) 385201.
- [436] L.A. Schulz, L.S.C. Kahle, K. Herrera Delgado, et al., *Appl. Catal. A: Gen.* 504 (2015) 599–607.
- [437] B. Wolk, I. Ekoto, W.F. Northrop, K. Moshhammer, N. Hansen, *Fuel* 185 (2016) 348–361.
- [438] L. Tartakovsky, M. Sheintuch, *Prog. Energy Combust. Sci.* 67 (2018) 88–114.
- [439] L. Maier, M. Hartmann, S. Tischer, O. Deutschmann, *Combust. Flame* 158 (2011) 796–808.
- [440] T.M. Gür, *Prog. Energy Combust. Sci.* 54 (2016) 1–64.
- [441] J.D. Kirtley, M.B. Pomfret, D.A. Steinhurst, J.C. Owrutsky, R.A. Walker, *J. Phys. Chem. C* 119 (2015) 12781–12791.
- [442] Y. Wang, A. Banerjee, L. Wehrle, Y. Shi, N. Brandon, O. Deutschmann, *Energy Convers. Manag.* 196 (2019) 484–496.
- [443] V. Menon, Q. Fu, V.M. Janardhanan, O. Deutschmann, *J. Power Sources* 274 (2015) 768–781.
- [444] K. Banke, R. Hegner, D. Schröder, C. Schulz, B. Atakan, S.A. Kaiser, *Fuel* 243 (2019) 97–103.
- [445] R. Hegner, B. Atakan, *Int. J. Hydrogen Energy* 42 (2017) 1287–1297.
- [446] A. Saylam, B. Atakan, S. Kaiser, *Combust. Theory Model.* 23 (2019) 1119–1133.
- [447] S. Wiemann, R. Hegner, B. Atakan, C. Schulz, S.A. Kaiser, *Fuel* 215 (2018) 40–45.
- [448] X. Zhang, Q. Che, X. Cui, et al., *Bioresour. Technol.* 254 (2018) 130–138.
- [449] A.A. Kaniyal, P.J. van Eyk, G.J. Nathan, P.J. Ashman, J.J. Pincus, *Energy Fuels* 27 (2013) 3538–3555.
- [450] G.J. Nathan, M. Jafarian, B.B. Dally, et al., *Prog. Energy Combust. Sci.* 64 (2018) 4–28.
- [451] M. Romero, A. Steinfeld, *Energy Environ. Sci.* 5 (2012) 9234–9245.
- [452] M.F. Kuehnle, E. Reisner, *Angew. Chem. Int. Ed.* 57 (2018) 3290–3296.
- [453] L. Kong, S.M. Sen, C.A. Henao, J.A. Dumesic, C.T. Maravelias, *Comput. Chem. Eng.* 91 (2016) 68–84.
- [454] A.F. Ghoniem, Z. Zhao, G. Dimitrakopoulos, *Proc. Combust. Inst.* 37 (2019) 33–56.
- [455] M. Ditaranto, J. Bakken, *Int. J. Greenh. Gas Control* 83 (2019) 166–175.
- [456] P. Bains, P. Psarras, J. Wilcox, *Prog. Energy Combust. Sci.* 63 (2017) 146–172.
- [457] T. Kuramochi, A. Ramirez, W. Turkenburg, A. Faaij, *Prog. Energy Combust. Sci.* 38 (2012) 87–112.
- [458] J. Koornneef, A. Ramirez, W. Turkenburg, A. Faaij, *Prog. Energy Combust. Sci.* 38 (2012) 62–86.
- [459] G. Fontaras, N.-G. Zacharof, B. Ciuffo, *Prog. Energy Combust. Sci.* 60 (2017) 97–131.
- [460] T. Takeshita, *Int. J. Environ. Res. Public Health* 8 (2011) 3032–3062.
- [461] V. Franco, M. Kousoulidou, M. Muntean, L. Ntziachristos, S. Hausberger, P. Dilara, *Atmos. Environ.* 70 (2013) 84–97.
- [462] H. Ma, F. Balthasar, N. Tait, X. Riera-Palou, A. Harrison, *Energy Policy* 44 (2012) 160–173.
- [463] U. Hahn, A.J.L. Harris, A. Corner, *Top. Cogn. Sci.* 8 (2016) 180–195.



- [464] M. Frenklach, *Proc. Combust. Inst.* 31 (2007) 125–140.
- [465] A. Cuoci, A. Frassoldati, T. Faravelli, E. Ranzi, *Comput. Phys. Commun.* 192 (2015) 237–264.
- [466] L. Pulga, G.M. Bianchi, S. Falfari, C. Forte, *Combust. Flame* 216 (2020) 72–81.
- [467] J. Xing, K. Luo, H. Pitsch, et al., *Proc. Combust. Inst.* 37 (2019) 2943–2950.
- [468] H. Gossler, L. Maier, S. Angeli, S. Tischer, O. Deutschmann, *Phys. Chem. Chem. Phys.* 20 (2018) 10857–10876.
- [469] F. Farazi, J. Ackroyd, S. Mosbach, et al., *J. Chem. Inf. Model.* 60 (2020) 108–120.
- [470] H. Gao, T.J. Struble, C.W. Coley, Y. Wang, W.H. Green, K.F. Jensen, *ACS Cent. Sci.* 4 (2018) 1465–1476.
- [471] A. Menon, N.B. Krdzavac, M. Kraft, *Curr. Opin. Chem. Eng.* 26 (2019) 33–37.
- [472] A. Eibeck, M.Q. Lim, M. Kraft, *Comput. Chem. Eng.* 131 (2019) 106586.
- [473] O. Inderwildi, C. Zhang, X. Wang, M. Kraft, *Energy Environ. Sci.* 13 (2020) 744–771.
- [474] Z. Abdin, A. Zafaranloo, A. Rafiee, W. Mérida, W. Lipiński, K.R. Khalilpour, *Renew. Sustain. Energy Rev.* 120 (2020) 109620.
- [475] J. Mantzaras, *Advances in Chemical Engineering* 45, Elsevier, 2014, pp. 97–157. ISBN: 978-0-12-800422-7.
- [476] F. Yan, L. Xu, Y. Wang, *Renew. Sustain. Energy Rev.* 82 (2018) 1457–1488.
- [477] F. Dawood, M. Anda, G.M. Shafiqullah, *Int. J. Hydrogen Energy* 45 (2020) 3847–3869.
- [478] K. Wittich, M. Krämer, N. Bottke, S.A. Schunk, *ChemCatChem* 12 (2020) 2130–2147.
- [479] A. Buttler, H. Spliethoff, *Renew. Sustain. Energy Rev.* 82 (2018) 2440–2454.
- [480] S. Weidner, M. Faltenbacher, I. François, D. Thomas, J.B. Skúlason, C. Maggi, *Int. J. Hydrogen Energy* 43 (2018) 15625–15638.
- [481] T. da Silva Veras, T.S. Mozer, D. da Costa Rubim Messeder dos Santos, A. da Silva César, *Int. J. Hydrogen Energy* 42 (2017) 2018–2033.
- [482] P. Nikolaidis, A. Poullikkas, *Renew. Sustain. Energy Rev.* 67 (2017) 597–611.
- [483] S. Arrhenius, *Lond. Edinb. Phil. Mag. Ser. 5* (41) (1896) 237–276.
- [484] J. v. Neumann, *World Scientific Series in 20th Century Mathematics*, 1, World Scientific Publishing Co. Pte. Ltd., Singapore, 1995, pp. 658–673. and his related article of the same title in *Fortune Magazine*, June 1955, reprinted from archives in *Fortune* on Jan 13, 2013; available online at <https://fortune.com/2013/01/13/can-we-survive-technology/>.